

**MULTI-TRACER GEOCHEMICAL INVESTIGATION OF LAMINATED
DIATOMACEOUS SEDIMENTS: MIOCENE MONTEREY FORMATION
AND HOLOCENE MARINE ENVIRONMENTS
(SAANICH INLET AND SANTA BARBARA BASIN)**

by

KRISTEN M. JOHNSON

B.Sc., Trinity College, Hartford, Connecticut, 1995

A THESIS SUBMITTED IN PARTIAL FULFILLMENT OF THE REQUIREMENTS
FOR THE DEGREE OF MASTER OF SCIENCE

in

THE FACULTY OF GRADUATE STUDIES
(Department of Earth and Ocean Sciences)

We accept this thesis as conforming to the required standard

THE UNIVERSITY OF BRITISH COLUMBIA

March, 1998

© Kristen M. Johnson, 1998

In presenting this thesis in partial fulfilment of the requirements for an advanced degree at the University of British Columbia, I agree that the Library shall make it freely available for reference and study. I further agree that permission for extensive copying of this thesis for scholarly purposes may be granted by the head of my department or by his or her representatives. It is understood that copying or publication of this thesis for financial gain shall not be allowed without my written permission.

Department of Earth and Ocean Sciences

The University of British Columbia
Vancouver, Canada

Date 31 March, 1998

ABSTRACT

Organic-rich hemipelagic sediments possessing millimetre-scale laminae of alternating biosiliceous and lithogenic material from Saanich Inlet, British Columbia, the Monterey Formation, California, and Santa Barbara Basin, California were studied to interpret the paleo-environmental controls on sediment composition and fabric and to determine if the sedimentary processes recorded in the laminated sediments can be linked to distinct trends in biogeochemical cycling of opal and carbon. To accomplish this, individual laminae and groups of laminae extracted from ODP cores and outcrop samples were analyzed using a multi-tracer geochemical approach.

Total organic carbon, opal, C/N ratios, stable carbon isotopes of organic matter, Rock-Eval pyrolysis and major and minor element analyses were performed. Saanich Inlet (SI) sediments (n=82) have 52 to 84% detritus, 15 to 45% opal and one to two percent organic carbon. Stable carbon isotopes and C/N ratios indicate a marine source of the organic matter present in the sediments. Monterey Formation (MF) samples (n=22) have six to 41% detritus, 28 to 87% opal, one to five percent organic carbon, and kerogen types, C/N ratios, and carbon isotopes suggestive of a marine organic matter source. Santa Barbara Basin (SBB) samples (n=42) have 59 to 90% detritus, six to 34% opal, three to 22% calcite, and one to five percent organic carbon. SI and SBB have similar bulk compositions with the exception of the presence of calcite in SBB samples. MF sediments differ from those of SI and SBB primarily in the significantly lower detrital and higher opal contents, suggesting that SI and SBB are not appropriate modern analogs for the MF.

Subannual/seasonal changes in the fluxes of opal and lithogenic detritus are responsible for the formation of the laminated sediment fabric; biogenic laminae form as a result of prolific diatom growth and sedimentation whereas detrital laminae form during periods of higher relative detrital flux. Seasonal variability influences the deposition of opal and detritus, producing different lamination styles which were characterized according to a new classification scheme that facilitates core description and clarifies interpretation of the various mechanisms of deposition.

In the Monterey Formation, opal and TOC are negatively correlated, implying that the

coupling of opal and organic matter created in the surface ocean by diatom productivity is not preserved in the sediments. The observed relationship is attributed to dilution of organic matter by large quantities of opal or the respiration and/or redistribution of organic matter during diagenesis and/or weathering. In Saanich Inlet sediments, there is a strong positive correlation between opal and organic matter. However, linking trends in opal and organic carbon export to specific laminae is problematic, and is complicated by possible sampling error.

Future studies would benefit by the selection of an on-land site which is known to have experienced no weathering, complete sedimentological and paleontological characterization of a measured section prior to geochemical sampling, and the retrieval of large enough samples so that multiple analyses can be performed on individual laminae.

TABLE OF CONTENTS

ABSTRACT.	ii
Table of Contents.	iv
List of Tables.	vi
List of Figures.	vii
1. INTRODUCTION.	1
2. ENVIRONMENTAL SETTINGS.	3
2.1 Saanich Inlet	3
2.2 Monterey Formation	3
2.3 Santa Barbara Basin	9
3. METHODS	11
3.1 Sample collection	11
3.2 X-radiography	15
3.3 Sub-sampling	15
3.4 Geochemistry	17
4. RESULTS	19
4.1 Bulk sediment composition	19
4.2 Lamina classification	23
4.3 Sediment composition reflected in x-radiographs	30
4.4 Geochemical proxies of organic matter source	33
4.5 Distribution of organic matter	36
5. DISCUSSION	40
5.1 Comparison of bulk sediment compositions	40
5.2 Sediment fabric	40
5.3 Carbon and opal cycling recorded in sediments	54
5.3.1 Sources of organic matter	54
5.3.2 Settling and sedimentation	61
5.3.3 Shallow burial diagenesis	69

5.3.4 Unroofing71
6. CLOSING STATEMENTS	72
6.1 Summary and conclusions72
6.2 Suggestions for future work	73
REFERENCES75
APPENDIX I. Saanich Inlet and Monterey Formation x-radiograph prints	83
APPENDIX II. Saanich Inlet and Monterey Formation sub-sample descriptions89
APPENDIX III. Analytical methods	93
APPENDIX IV. Geochemical data from SI, MF, and SBB96

LIST OF TABLES

Table 1. Bulk sediment composition of the Monterey Formation, Saanich Inlet, and the Santa Barbara Basin	20
Table 2. Geochemical proxies of organic matter source.	34
APPENDIX II	
Table II-1. Descriptions of Saanich Inlet ODP samples	89
Table II-2. Descriptions of Monterey Formation samples	92
APPENDIX IV	
Table IV-1. Geochemistry of Saanich Inlet samples: TOC, opal, C/N, $\delta^{13}\text{C}$	96
Table IV-2. Geochemistry of Monterey Formation samples: TOC, opal, C/N, $\delta^{13}\text{C}$	98
Table IV-3. Geochemistry of Santa Barbara Basin samples: TOC, opal, calcite, C/N	99
Table IV-4. Major element abundances of Saanich Inlet samples.	101
Table IV-5. Major element abundances of Monterey Formation samples.	102
Table IV-6. Major element abundances of Santa Barbara Basin samples.	103
Table IV-7. Minor element abundances of Saanich Inlet samples.	104
Table IV-8. Minor element abundances of Santa Barbara Basin samples.	105
Table IV-9. Rock-Eval data from Monterey Formation samples.	106

LIST OF FIGURES

Figure 1. Location map: Saanich Inlet	4
Figure 2. On-shore distribution of Monterey Formation	5
Figure 3. Location map: Lompoc, Celite diatomite quarry, Santa Barbara County, California	7
Figure 4. Paleogeography of central and southern California during Miocene	8
Figure 5. Location map: Santa Barbara Basin	10
Figure 6. Location map: ODP drill sites in Saanich Inlet	12
Figure 7. Outcrop exposure of Monterey Formation in Celite quarry	13
Figure 8. Stratigraphic column of described Monterey Formation section in Celite quarry	14
Figure 9. Flowchart depicting analytical methodology for Monterey Formation samples	16
Figure 10. Comparison of analytical methods used to determine % opal and TOC	21
Figure 11. Saanich Inlet major element/Al relationships	22
Figure 12. Monterey Formation major element/Al relationships	24
Figure 13. Monterey Formation Ca, Mg, and P contents	25
Figure 14. Santa Barbara Basin Ca, Mg, and P contents	26
Figure 15. Classification of lamination styles	27
Figure 16. Lamination styles in Monterey Formation outcrop photographs	29
Figure 17. Geochemical data versus visually-determined lamina composition	31
Figure 18. Mud laminae and amalgamated opal laminae in Saanich Inlet x-radiographs	32
Figure 19. Modified van Krevelen diagram for Monterey Formation samples	37
Figure 20. Distribution of TOC with respect to opal and detritus	38
Figure 21. Sediment traps in Saanich Inlet	42
Figure 22. Opal fluxes to shallow and deep sediment traps	44
Figure 23. Discharge rates of the Cowichan and Fraser Rivers	45
Figure 24. Detrital fluxes to shallow sediment traps	46
Figure 25. Detrital fluxes to shallow and deep sediment traps	47

Figure 26. Monthly detrital fluxesto deep sediment traps 48

Figure 27. Opal and detrital fluxes to deep sediment traps 49

Figure 28. Annual variability in opal flux and its influence on lamina style 52

Figure 29. Annual variability in detrital flux and its influence on lamina style 53

Figure 30. Accumulation rates of opal and organic carbon in shallow sediment traps 56

Figure 31. Monterey Formation C/N ratios and $\delta^{13}\text{C}$ values 58

Figure 32. Comparison of C/N ratios in shallow and deep sediment traps 60

Figure 33. Monterey Formation TOC versus S2 62

Figure 34. Monterey Formation opal and TOC content versus Ti/Al ratio 64

Figure 35. Saanich Inlet Ti/Al ratios versus opal and TOC content 65

Figure 36. Monterey Formation opal values versus C/N ratios, $\delta^{13}\text{C}$ values, and hydrogen index . 68

1. INTRODUCTION

Finely-laminated, biosiliceous sediments provide a high-resolution record of the processes that govern opal and organic carbon export, deposition, and burial. The controls on the distribution of opal and organic carbon in sediments have been studied at decimetre to metre scales in outcrops and well-based studies resulting in the interpretations of differences between laminated and non-laminated intervals (e.g. Govean and Garrison, 1981; Kennett and Ingram, 1995; Behl and Kennett, 1996). However, there is just as much, if not more information to be obtained by studying variations *within* the laminated intervals (Brodie and Kemp, 1994; Grimm et al., 1996; Kemp, 1996).

This study examines laminated, biosiliceous sediments from two locations in detail: Saanich Inlet, British Columbia, where laminated, biosiliceous, organic-rich sediments have been deposited and preserved throughout the Holocene, and the Monterey Formation of California; a Miocene sedimentary deposit containing a finely-laminated biosiliceous unit. Analytical results from Santa Barbara Basin samples are also briefly considered. A multi-tracer geochemical approach was utilized to explore and address the following topics:

- (1) To better understand the formation of the important source- and reservoir-rocks of the Monterey Formation, modern environments thought to be similar to the Miocene conditions of deposition have been used as analogs (Soutar et al., 1981; Donegan and Schrader, 1981). In this study, bulk sediment compositions of the laminated hemipelagites in Saanich Inlet, Santa Barbara Basin, and the Monterey Formation will be investigated to assess the general suitability of Saanich Inlet and Santa Barbara Basin as modern comparisons for the Monterey Formation.
- (2) Sediment composition and fabric are directly influenced by sedimentary processes. A new classification scheme is developed which characterizes lamina styles based on visually-defined physical expressions of discrete laminae. This method of characterization and classification aims to explore the linkages between sediment composition, fabric, and process.
- (3) In regions where diatoms contribute to primary productivity, a direct coupling between opal and organic carbon exists in the surface waters. The survival of this coupling through settling,

sedimentation, burial, diagenesis, and weathering is explored by analyzing the distributions of opal and organic matter in the three environments.

2. ENVIRONMENTAL SETTINGS

2.1 Saanich Inlet

Saanich Inlet is located on the southeast portion of Vancouver Island in British Columbia, 25 km north of Victoria (Figure 1). It is a 26 km long, single basin fjord with widths varying from 0.4 to 7.6 km, and reaches a maximum depth of 240 metres. A shallow sill (~80 m) at the mouth separates the inlet from Haro Strait and open water. Fresh water enters the inlet at the mouth, sourced predominantly from the Cowichan and Fraser Rivers. The deeper waters of the inlet are anoxic nearly year-round due to the sill which restricts circulation within the inlet and also because of the high levels of primary productivity. The sedimentation rate in Saanich Inlet is high (4-6 mm/year, Gucluer and Gross, 1964; 100-250 mg/cm²/yr, Francois, 1988) and is dominated by pulsed inputs of biogenic opal and terrigenous detritus. These materials accumulate on the inlet floor as discrete laminae. The low-oxygen setting is prohibitive to benthic fauna, enabling the preservation of the finely-laminated sediment fabric (Bornhold et al., 1997).

Phytoplankton productivity in Saanich Inlet is dominated by diatom taxa. Diatoms bloom in response to increased sunlight in the early spring (~March). Depletion of nutrients leads to the fallout of the bloom, but the continuation of diatom populations throughout the summer is spurred by the release of recycled nutrients generated by heterotrophic grazing, by the influx of nutrient-rich waters over the sill during neap tides, and by the upwelling of sub-surface waters in July and August. In the fall, light levels decrease, restricting diatom growth, and opal fluxes are minimal by September or October (Sancetta and Calvert, 1988; Collins, 1997; Stucchi and Whitney, 1997).

2.2 Monterey Formation

The Miocene Monterey Formation is present throughout much of California (Figure 2), and at many locations consists of three main facies: a lower calcareous facies, a transitional phosphatic facies, and an upper siliceous facies. The lithologic sequence of the Monterey Formation (MF) has been attributed to broad-scale changes in the global climatic and oceanographic regime including

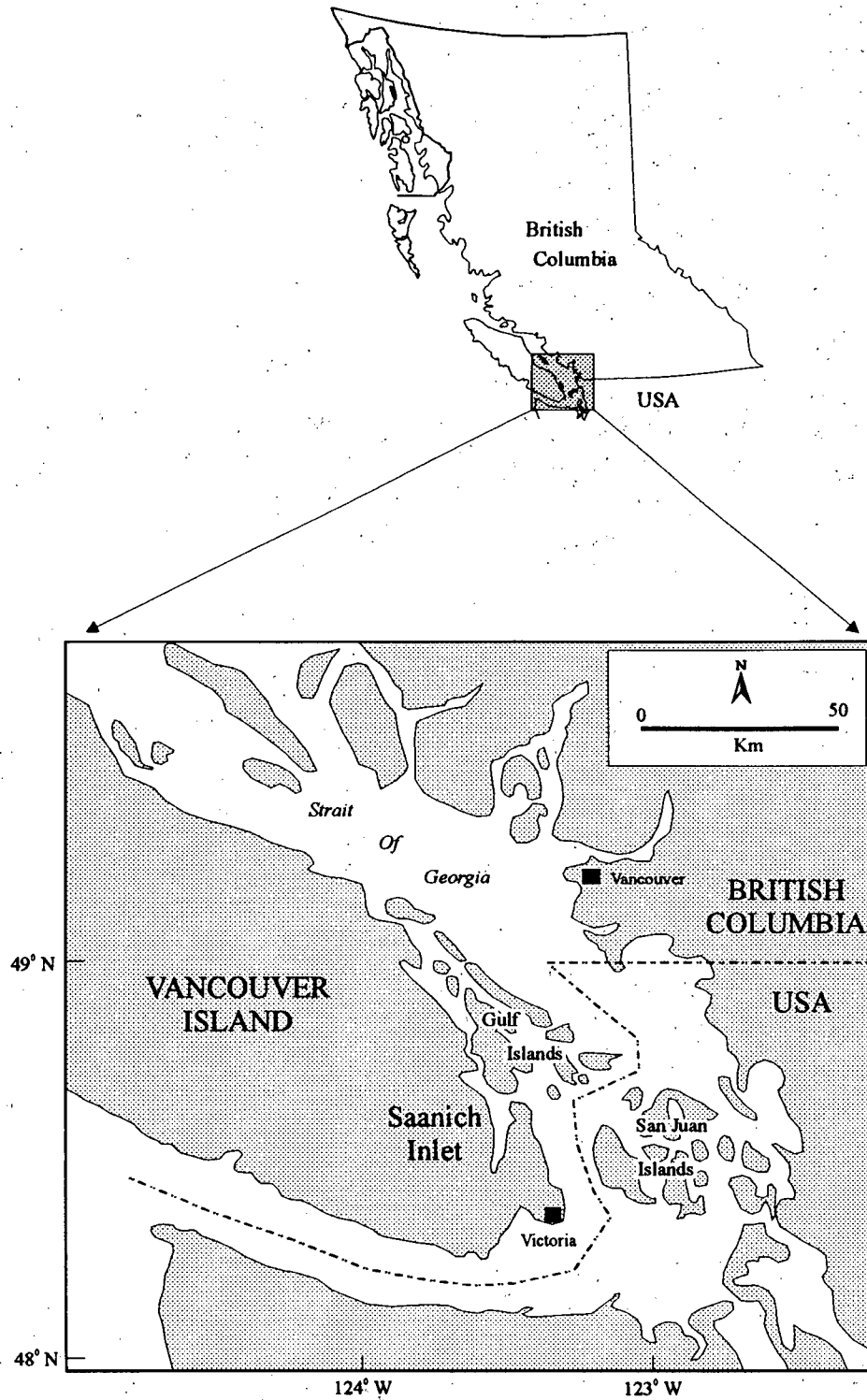


Figure 1. Locality map of Saanich Inlet; situated on the southern portion of Vancouver Island, north of Victoria.



Figure 2. Map of California showing on-shore distribution of Monterey Formation (hatched areas). From Obradovich and Naeser, 1981.

global cooling, intensified wind strengths, and increased upwelling (Ingle, 1981a; Barron and Baldauf, 1989, White et al., 1992). Proposed environments for the deposition of this layered sequence have included steep-sided, fault-bounded basins, basin slopes, and the continental shelf/slope region, similar to the present day California Borderland basins and the Guaymas Basin and slope (Pisciotta and Garrison, 1981; Govean and Garrison, 1981).

A developing view on the depositional environment of the MF is described in Isaacs (in press). This model proposes deposition at upper middle bathyal depths on low-gradient slopes of broad depressions along an open continental margin in which a dynamic prograding margin controls and determines the depositional facies via shoaling and shoring. Local topography influenced the manifestation of the MF throughout California as the distribution of facies and thicknesses of units vary regionally.

Isaacs' model of MF deposition refutes the previously-held notion that primary productivity was very high during the late Miocene. She assessed accumulation rates of phosphate, organic carbon, and silica, along with diatom assemblages and suggests that throughout much of the Miocene, productivity off California was only moderate compared to the known high productivity regions of modern times (e.g. Peru and the Gulf of California) with high levels of productivity occurring only in very localized regions. One of those regions is the Lompoc area in Santa Barbara County (Figure 3). At this location during the late Miocene, silica accumulation rates were relatively high ($>10 \text{ mg/cm}^2/\text{year}$; Barron, 1975) and diatom floras—including bloom and mat assemblages—indicate high productivity (Chang, 1998b), attributable to the upwelling of subsurface water near a regional shoal (~150-500 m; Figure 4).

The Monterey Formation is an economically-important deposit in California. It is the source and reservoir for vast quantities of oil, both on-shore and off. Also, deposits of very pure diatomite in the upper siliceous facies are mined as "diatomaceous earth"; the Celite quarry (formerly Johns Mannville) is one of the largest diatomite quarries in the world.

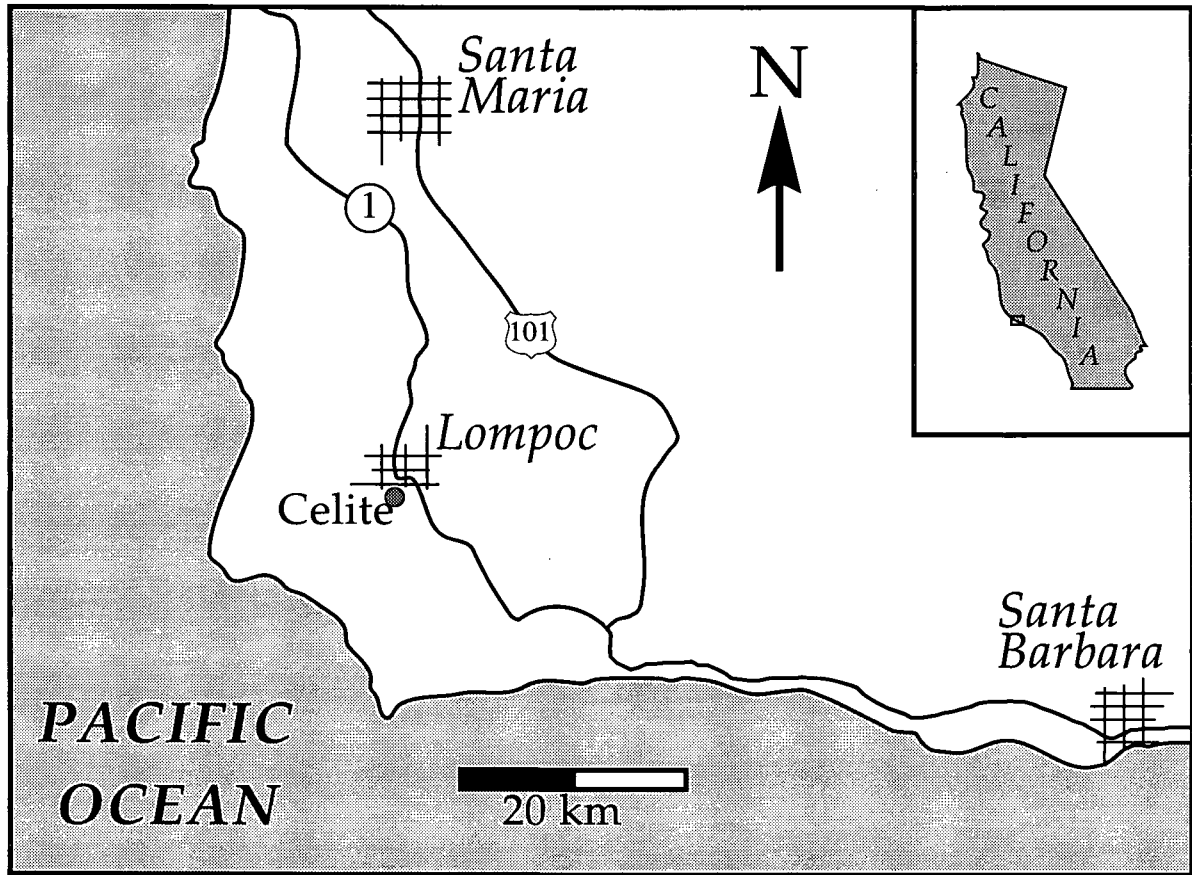


Figure 3. Locations of the city of Lompoc and the Celite diatomite quarry in Santa Barbara County, California. From Grimm and Orange, 1996.

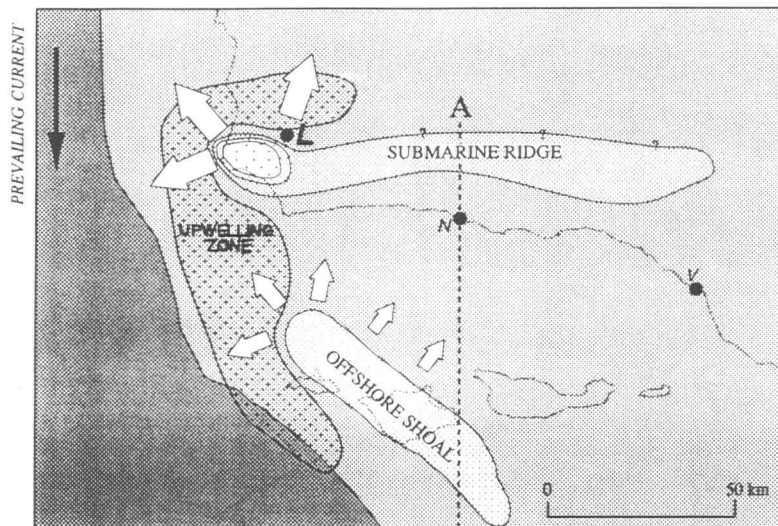
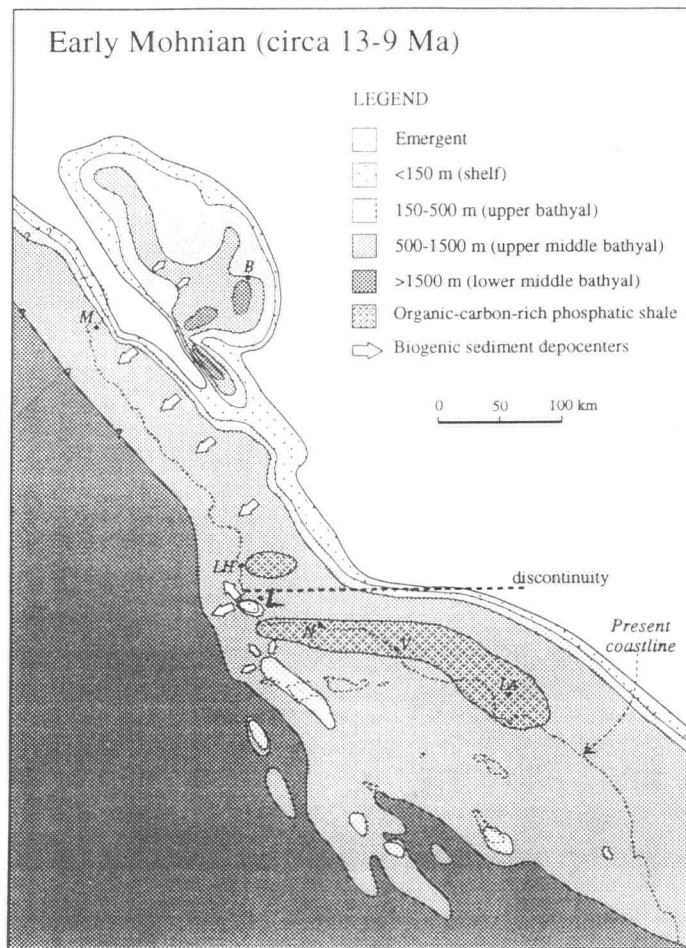


Figure 4. Paleogeography of central and southern California during the Miocene. L=Lompoc. From Isaacs, in press.

2.3 Santa Barbara Basin

The Santa Barbara Basin is a 600-metre-deep basin located in the California Borderland (Figure 5). The basin is bordered by the California mainland to the north, the Channel Islands to the south, and is silled to the east and the west at 230 and 475 metres, respectively. Basin waters below sill depth are anoxic due to the low oxygen content of the Pacific Intermediate Water mass which feeds the basin, the oxygen minimum zone present along the coast of California, and high levels of primary productivity.

The sedimentation rate in the basin is high (120 cm/1000 years; Kennett et al., 1994) and is dominated by detritus and biogenic silica. The sediment supply in the Santa Barbara Basin is seasonal; runoff from the Ventura and Santa Clara Rivers and rainstorms during the winter and early spring deliver siliciclastic materials to the basin whereas planktonic phytodetritus, generated from diatoms, radiolarians, and foraminifers is deposited in the late spring, summer, and fall (Kennett, Baldauf, et al., 1994). This seasonal deposition results in the formation of laminae which are preserved as varves due to the low-oxygen content of the bottom waters (Grimm et al., 1996).

The predominance of a laminated fabric in diatomaceous/terrigenous couplets in the Santa Barbara Basin and in Saanich Inlet has lead many workers to suggest such environments as modern analogs for the Miocene Monterey Formation (e.g. Soutar et al., 1981). Comparison of bulk compositions of these deposits in this report and coupled sedimentological and paleontological investigations (Chang, 1998a,b) permit assessment of this common comparison.

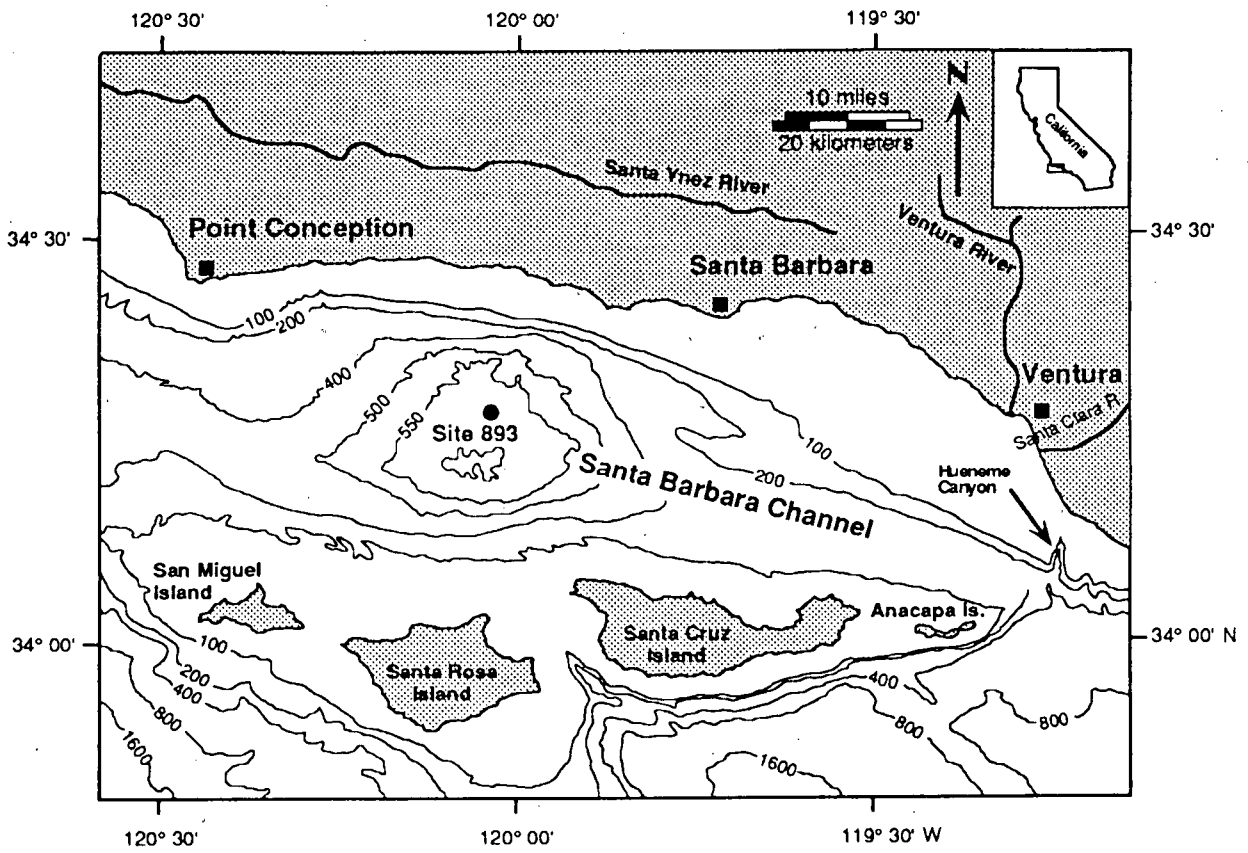


Figure 5. Location of Santa Barbara Basin showing ODP site 893. From Kennet et al., 1994.

3. METHODS

3.1 Sample collection

Saanich Inlet

Samples were retrieved from two sites, 1033 and 1034, of Leg 169S of the Ocean Drilling Program (ODP) in Saanich Inlet, British Columbia (Figure 6). The holes were drilled in the central portion of the basin, in water depths of 200 and 238 metres, with maximum penetration to 118.2 metres below the sea floor (Bornhold et al., 1997).

Selected sections of the cores were collected with a "cookie-cutter" apparatus described by Schimmelmann et al. (1990; cf. Grimm et al., 1996), resulting in slabs 20 cm long, 1 cm wide, and of variable depth; a total of 30 slabs were collected. These sections were wrapped in plastic wrap and refrigerated.

Monterey Formation

Field work was done at the Celite diatomite quarry in Lompoc, California. Pit 35 of the quarry was selected as the location for the study; its low topographic position was desirable since the dark olive color of the sediments at this location suggested that they had experienced less intense weathering compared to other localities in the quarry where the diatomites are bright white.

Two surfaces (the main traverse and bench two) were planed with a bulldozer, smoothed with a front-end loader, and further cleaned with sharpened hoes. Bench two had a thickness of 18 metres and was stratigraphically lower than the main traverse which was 41 metres thick, and stratigraphically continuous with bench two. Beds dip 45° to the north, and therefore the sediment fabric is exposed on the horizontally planed surface (Figure 7). This transect was measured, divided into 19 units based on relative opal and mud content, described, and photographed. Samples representative of various depositional styles (well-laminated, burrowed, opal-rich, etc.) were selected from the units, and 23 blocks ranging up to 110 x 20 x 15 cm were removed from the traverse with a gas-powered concrete saw and chisels (Figure 8). These blocks were placed on masonite boards,

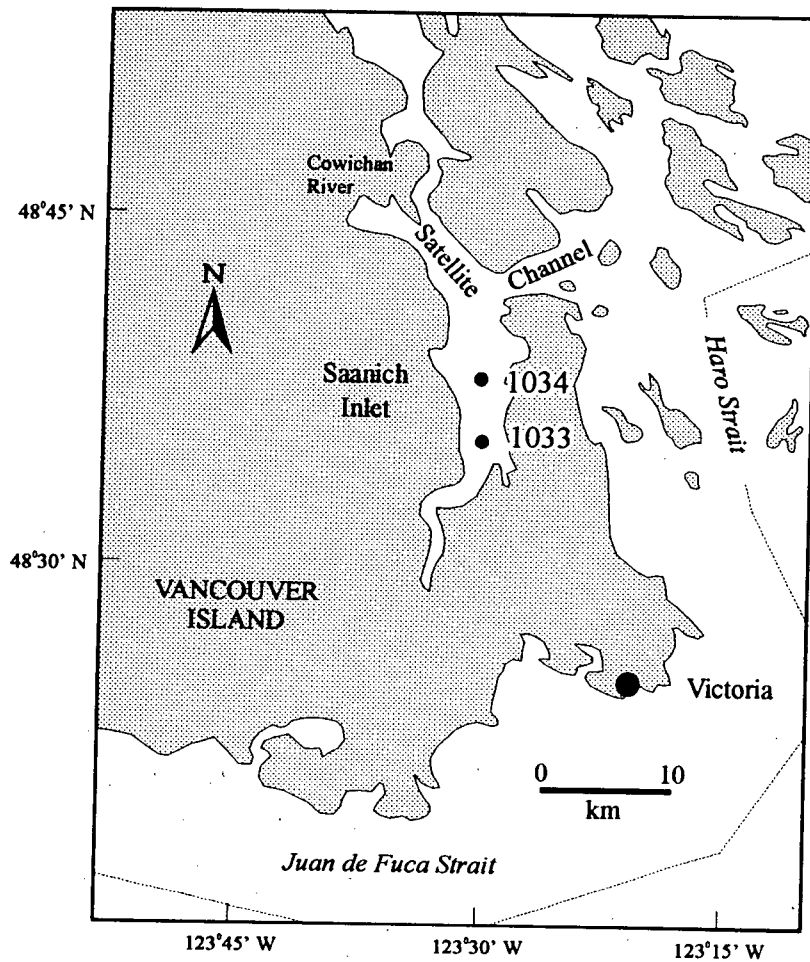


Figure 6. Location of ODP drill sites in Saanich Inlet. Site 1033 was drilled in 200 metres water depth and site 1034 in 238 metres.

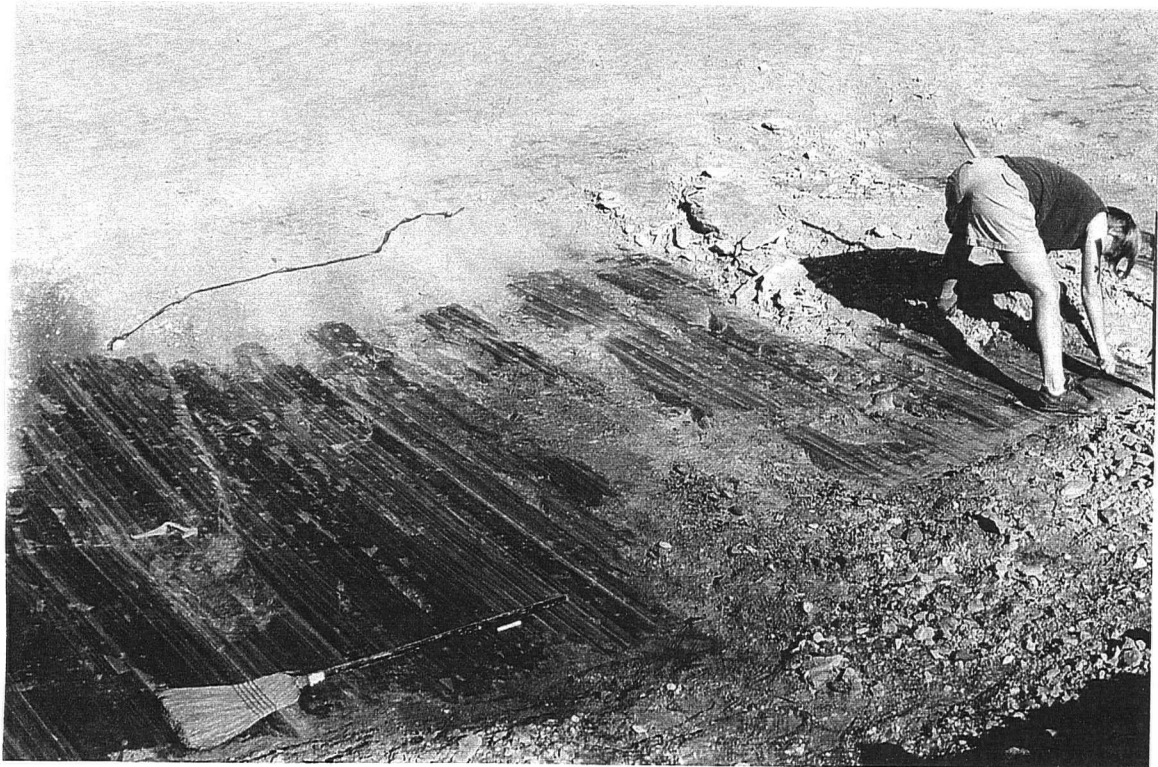
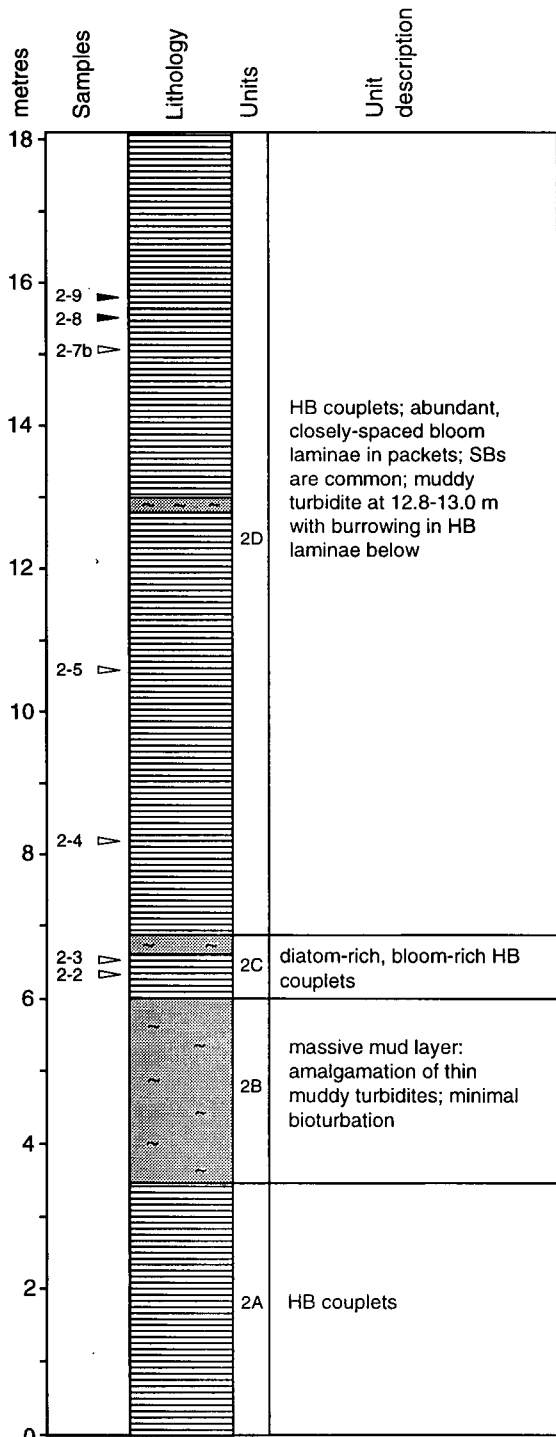
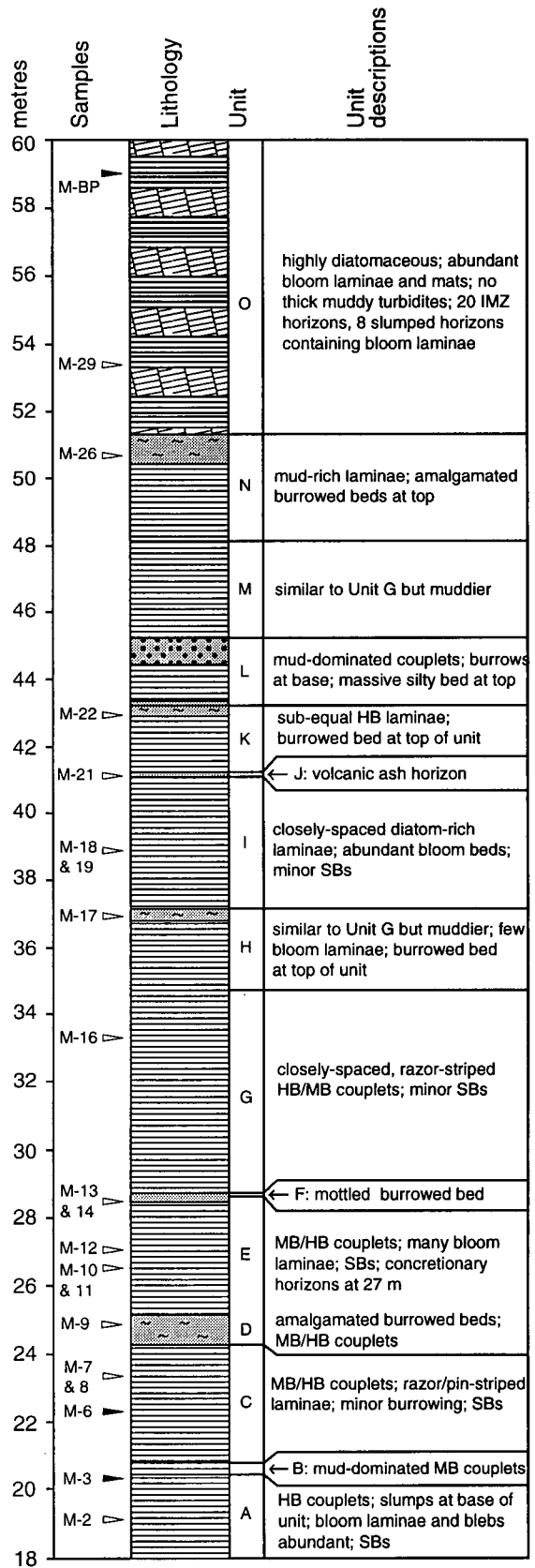


Figure 7. Outcrop exposure of Monterey Formation in Celite quarry. Exposure had been cleared with a bulldozer and smoothed with sharpened hoes. Note exposure of laminae on horizontal surface (beds dipping 45° N).

Figure 8. Stratigraphic column of Monterey Formation section in the Celite quarry. Section was divided into units based on general sedimentological features, and from those units, representative samples were chosen and extracted. HB, MB, LB=high-, moderate-, and low-bimodality; SB="speckled bed" (a type of gravity flow); IMZ=intrastratal microfractured zones. From Chang, 1997.

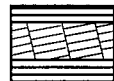


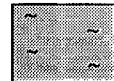
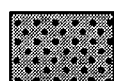
BENCH 2



MAIN TRAVERSE

- ▽ Samples collected, slabbed & x-rayed
- ▶ Samples analysed in detail for this study

-  Laminated diatomite
-  Laminated diatomite with IMZ horizon

-  Mud
-  Mud with burrows
-  Silt

wrapped with plastic wrap, aluminum foil, packing tape, and bubble wrap, and were transported to the lab.

The large sample blocks were sub-sectioned with a bandsaw perpendicular to bedding. Three slabs with a thickness of one centimetre, and one with a thickness of two centimetres were made for subsampling and the analyses described below (Figure 9).

3.2 X-radiography

One-centimetre thick sediment slabs from Saanich Inlet and the Monterey Formation were imaged via x-radiography performed at the Vancouver Hospital at the University of British Columbia. The images were produced with a CGR 300-T mammography x-ray machine running at 26Kv. Saanich Inlet slabs were exposed at 25 milliamperes/second (mAs), mud-rich slabs from the Monterey Formation were exposed at 50 mAs, and opal-rich MF slabs were exposed at 25 mAs.

X-radiography has become a standard procedure for analyzing laminated sediments due to its ability to image the original sediment fabric (e.g. Schimmelmann et al., 1990; Grimm et al., 1996). Mammography is superior to standard x-radiography for imaging laminated sediments because the collimated beam produces a higher-resolution image (Collins, 1997; Algeo et al., 1994); the mammography unit at the Vancouver Hospital produces an image with 131 line pairs per millimetre (a measurement of spatial resolution), whereas standard x-radiography produces only 7 line pairs per millimetre (S. Deering, UBC Hospital, personal communication).

X-radiographs reveal variations in the bulk densities of the laminae in a sediment slab as shades of grey. Porous laminae are more transparent to the impinging x-rays, resulting in increased exposure of the negative compared to less porous laminae. Contact prints developed from the exposed negative depict porous laminae as lighter in color. Conversely, dense, detrital-rich laminae permit lower saturation of the x-ray film and therefore produce a darker lamina on a contact print.

3.3 Sub-sampling

Based on the quality of the x-radiograph print and on the variety of lamination styles evident,

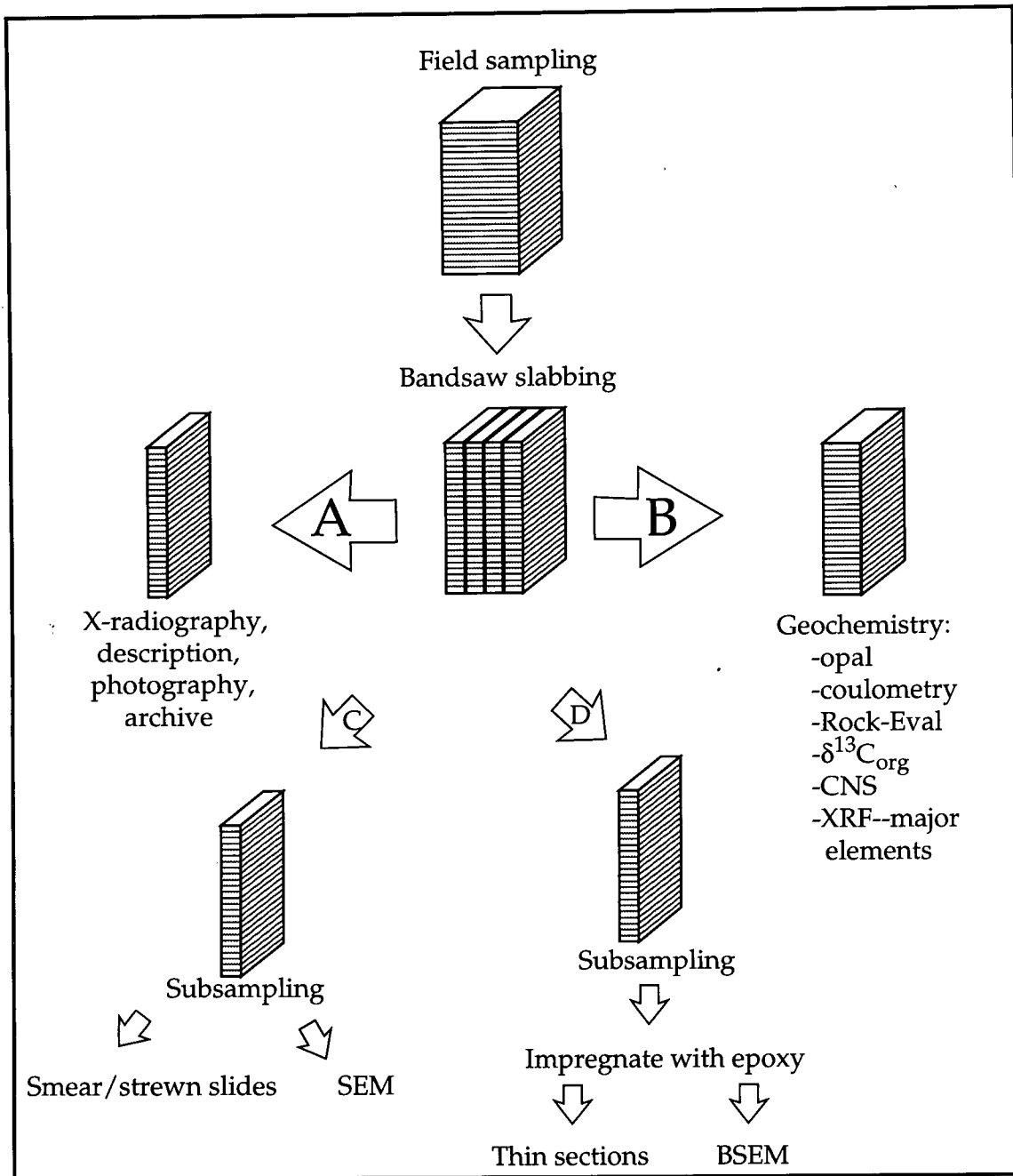


Figure 9. Flowchart depicting analytical methodology for Monterey Formation samples. Slabs A and B pertain to the current study, while results from slabs C and D were reported in Chang, 1997.

eight of the 30 Saanich slabs (A3, F, I, M, N, P, Q, S), and five of the 23 Monterey slabs (2-8, 2-9, M-3, M-6, M-BP) were selected for subsampling for optical microscopy and geochemical analyses. Ideally, individual laminae were to be subsampled. In the MF sediments, extraction of discrete laminae was an arduous process due to the very thin laminae and the brittle nature of the rock. Saanich Inlet sediments are easier to subsample—the sediments are soft and uncompacted. However, restricted sample volumes did not permit the extraction of adequate amounts for multi-tracer analyses. Because of these difficulties, distinct intervals and groups of laminae were sampled; sampling intervals ranged from individual laminae (sub-millimetre scale) to several centimetres of sediment. The locations of these samples were selected and delineated on the x-radiograph contact prints.

Saanich sample slabs were removed from refrigeration, unwrapped, and the intervals selected for subsampling were designated on the x-ray contact print. Guided by these prints, subsamples were extracted with a scalpel and placed into labelled vials. The resulting 82 samples were freeze-dried and subsequently pulverized with a glass rod. The Monterey Formation slabs were similarly sub-sampled, resulting in 22 discrete samples. See Appendix I for location of all samples on x-radiographs, and Appendix II for sample descriptions.

Forty-two samples were selected from ODP Leg 146, Site 893, from the collection of Kurt Grimm. Samples had previously been described, x-rayed, and subsampled, similar to the processes used in the Monterey Formation and Saanich Inlet samples.

3.4 Geochemistry

Geochemical analyses were performed at the University of British Columbia. Detailed analytical methods are listed in Appendix III.

All Saanich, Monterey, and Santa Barbara Basin samples were analyzed for weight percent opal using a method modified from Mortlock and Froelich (1989) involving the extraction of biosilica with sodium carbonate and its subsequent measurement via molybdate-blue spectrophotometry.

Monterey Formation samples were analyzed for total carbon, nitrogen and sulfur, whereas the Saanich Inlet and Santa Barbara Basin samples were analyzed only for carbon and nitrogen. This

analysis was performed on a Carlo Erba NA-1500 analyzer following the method described by Verardo et al. (1990).

The carbonate content of the Monterey formation and Santa Barbara Basin samples was determined via coulometric titration following a method similar to Engleman et al. (1985).

Twenty of the Monterey Formation samples (limited sample prohibited isotopic analysis of two samples) and all the Saanich Inlet samples were analyzed for stable carbon isotopes of organic matter following methods similar to Pedersen et al. (1991) and Reineking et al. (1993). All Saanich Inlet samples were also analyzed for stable nitrogen isotopes following Farrell et al. (1995) and Reineking et al. (1993).

Major element abundances were determined for 19 Monterey Formation samples, 15 Saanich Inlet samples, and 11 Santa Barbara Basin samples. Minor elements were analyzed for in 15 Saanich Inlet samples and 15 Santa Barbara Basin samples. These were determined via x-ray fluorescence (XRF) spectrometry, following a method similar to that of Calvert (1990). Elements analyzed for include: majors--Al, Ca, Fe, K, Mg, Mn, Na, P, Si, Ti; minors--V, Cr, Mn, Co, Ni, Cu, Zn, As, Rb, Sr, Y, Zr, Nb, Ba, Pb.

Rock-Eval pyrolysis was performed on 20 of the Monterey samples following standard procedures outlined in Espitalié et al. (1977) and Peters (1986).

4. RESULTS

4.1 Bulk sediment composition

The bulk compositions of the samples from Saanich Inlet (SI), the Monterey Formation (MF), and Santa Barbara Basin (SBB) are shown in Table 1. Total organic carbon (TOC) of MF samples was measured with two methods: (1) via Rock-Eval pyrolysis; and (2) by subtracting carbonate carbon (determined via coulometry) from total carbon (determined via CNS analysis). The close agreement of these two methods is shown in Figure 10a. Weight percent opal was also determined with two methodologies in MF samples. The first is the method of Mortlock and Froelich (1989) involving extraction of opal with sodium carbonate. Opaline silica is measured in this method and weight percent opal is calculated by multiplying the silica percent by 2.4. The second method calculates opal based on XRF major element abundances (Isaacs et al., 1983); $\% \text{ opal} = \text{SiO}_2 - (3.5 \times \text{Al}_2\text{O}_3)$. The results from these two methods are compared in Figure 10b. The data from the extraction method of opal determination and total carbon minus carbonate carbon for TOC will be used in the following discussions.

Saanich Inlet samples are dominated by detritus and opal, with organic matter having a smaller contribution. Coulometry was not performed on the SI samples in this study; however, Sancetta and Calvert (1988) report negligible carbonate content in collected sediment trap material and Collins (1997) similarly reports less than 0.2% carbonate carbon in cored samples. Figure 11 shows the major element abundances of SI samples. The ratios of Fe, K, and Ti to Al can all be defined by a single regression passing near the origin, indicating that these elements are confined to the detrital fraction. The Fe and Ti contents are similar to the World Shale Average (WSA; Wedepohl, 1969) whereas the K content is significantly lower. The Ca/Al ratio can also be defined by a single regression, with the exception of sample F5, which has a higher Ca content than the other samples. Sample F5 also has a higher P content, perhaps indicating the presence of apatite in that sample. Ca/Al and K/Al ratios lower in SI sediments compared to the WSA are most likely the result of higher relative amounts of clay minerals (muscovite/illite) and lesser amounts of feldspars compared

	MF n=22	SI n=82	SBB n=42
TOC weight %	1.4 - 4.5 x=3.0	1.1 - 2.4 x=1.6	1.2 - 4.7 x=1.9
OPAL weight %	28.4 - 87.1 x=55.5	14.5 - 44.9 x=28.6	5.6 - 34.4 x=13.1
CARBONATES weight %	0.1 - 14.5 x=2.8 (dolomite)	negligible	2.8 - 22.1 x=6.5 (calcite)
DETRITUS weight %	6.3 - 40.5 x=23.1	51.5 - 83.7 x=68.9	59.0 - 89.6 x=77.5

Table 1. Bulk sediment composition of the Monterey Formation (MF), Saanich Inlet (SI), and the Santa Barbara Basin (SBB).

Opal = $2.4 \times \%Siopal$ (Mortlock and Froelich, 1989).

Dolomite (MF) = $[MgO - (0.11 \times Al_2O_3)]/0.219$ (Isaacs et al., 1983).

Calcite (SBB) = $8.33 \times \text{weight \% inorganic carbon determined via coulometry}$.

Detritus (MF) = $Al_2O_3 \times 5.6$ (Isaacs et al., 1983).

Detritus (SI and SBB) estimated to be everything other than opal, carbonates, and organic matter (TOC $\times 2.5$).

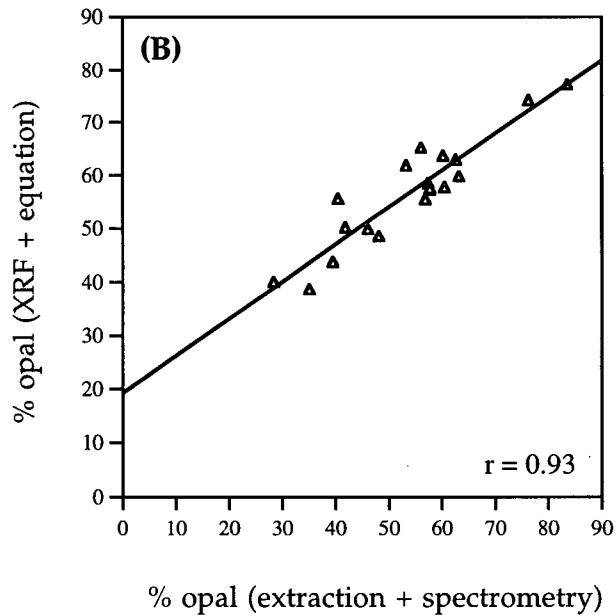
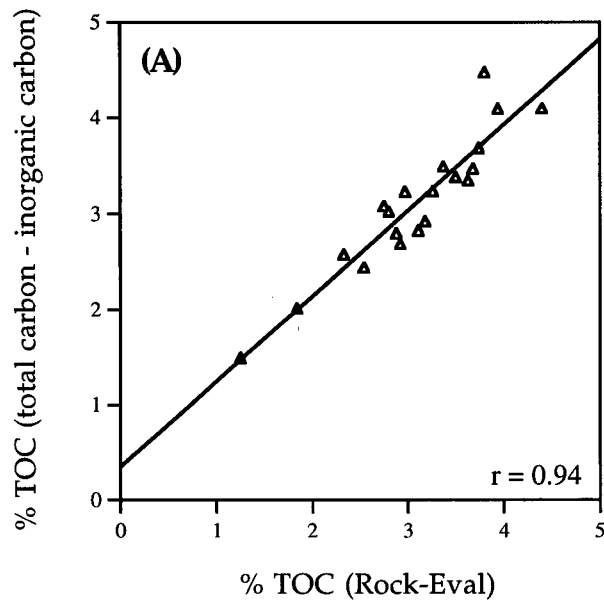


Figure 10. Comparison of methods used to determine % TOC and % opal. (A) TOC determination via Rock-Eval pyrolysis compared with calculating TOC by subtracting inorganic carbon (via coulometry) from total carbon (via CNS elemental analysis). (B) Opal determination via extraction of biosilica and measurement via spectrometry (Mortlock and Froelich, 1989) compared with calculation of opal content using equation of Isaacs et al. (1983) based on XRF data.

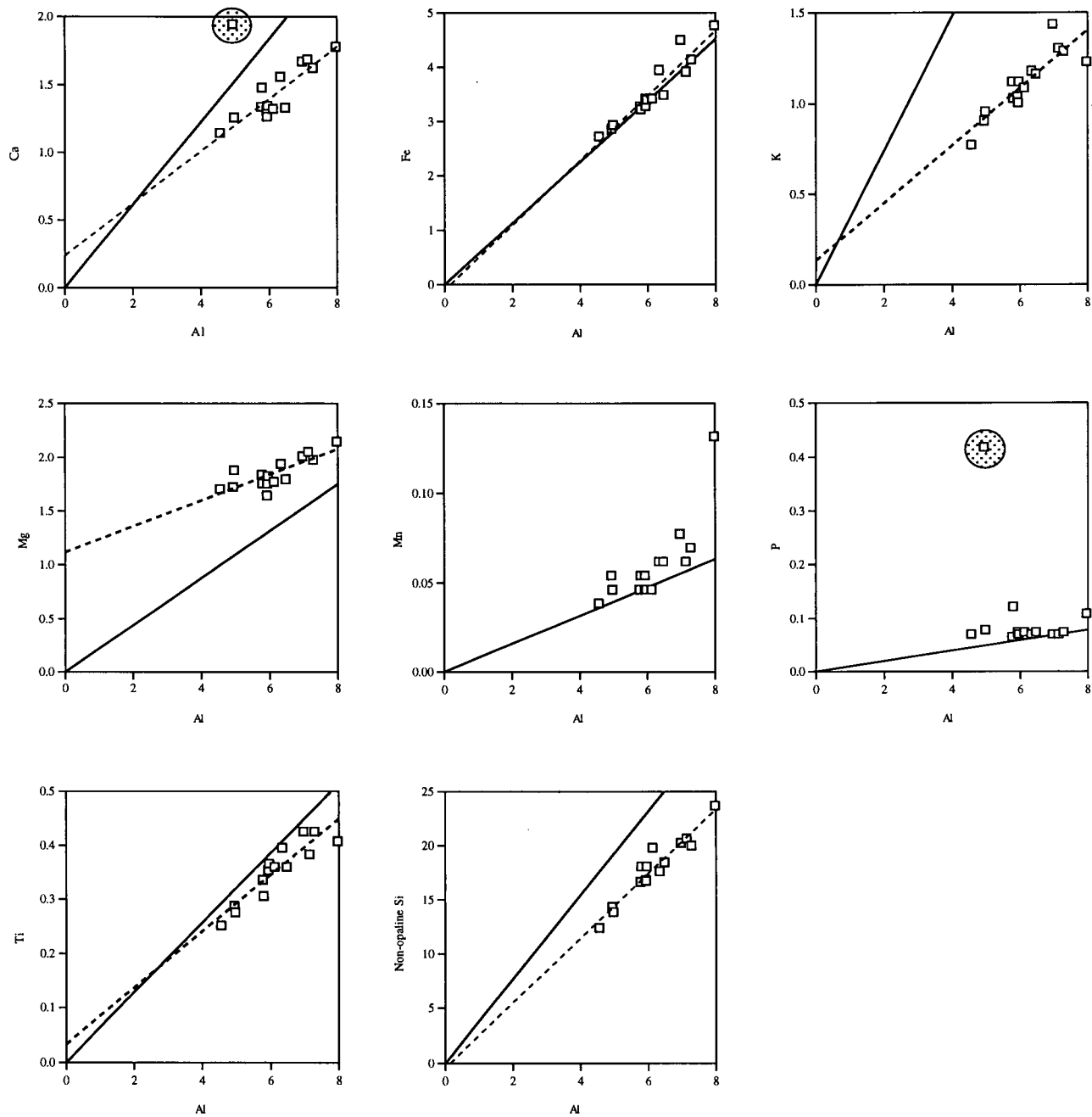


Figure 11. SI major element/Al relationships. Solid line is the WSA regression (Wedepohl, 1969); broken line is the regression for the SI data. Single linear regressions passing near the origin indicate contribution of that element by lithogenic materials (no biogenic or hydrogenous inputs). Highlighted sample in Ca/Al and P/Al most likely contains apatite. The Mg/Al plot shows that Mg has a significant contribution from sources other than lithogenic detritus.

to the WSA, as well as a high plagioclase feldspar/K-feldspar ratio in Saanich Inlet. The first of these explanations is supported by Francois (1987) who found larger relative clay contents in the central basin of SI. The latter reflects the mineralogy and lithology of the region (Francois, 1987).

Monterey Formation sediments are similarly dominated by opal, detritus, and organic matter, with these three components responsible for greater than 70% by weight of all samples. The detritus present in the MF samples is very similar to the WSA as evidenced by the correlation of Fe, K, Ti, and Si to Al ratios to the WSA regression (Figure 12). In addition to opal, detritus, and organic matter, there are smaller amounts of dolomite and apatite. The presence of these minerals can be detected in the plots of Ca, Mg, P, and Al (Figure 13) and their quantitative contribution may be calculated by equations developed by Isaacs et al. (1983). Six samples have >2% dolomite (see Table 1 caption for equation), and three have >7% dolomite, whereas six samples have >0.6% apatite ($\% \text{ apatite} = [\text{P}_2\text{O}_5 - (0.032 \times \text{Al}_2\text{O}_3)]/0.424$).

Santa Barbara Basin sediments are different from SI and MF in that they have a significant carbonate component in addition to detritus, opal, and organic matter. Apatite is also likely present in these samples as shown in Figure 14.

4.2 Lamina classification

X-radiograph prints of SI and MF samples reveal highly variable laminated fabrics (see Appendix I). To communicate and categorize the various laminae expressions, a classification scheme was developed and five major categories were delineated: domination, bimodality, thickness, spacing, and cyclicity (Figure 15; cf. Chang, 1997). The laminae were classified primarily using x-radiograph contact prints, but scraped sediment slabs were referred to if the x-radiographs were unclear.

Bimodality as a lamina descriptor was introduced by Grimm et al. (1996). Bimodality values are assigned by determining the relative contrast in grey scale of adjacent laminae on an x-radiograph print. A large contrast between adjacent laminae is termed "high bimodality" (HB), small contrast in grey scale of adjacent laminae would be labeled "low bimodality" (LB), and intermediate contrasts are

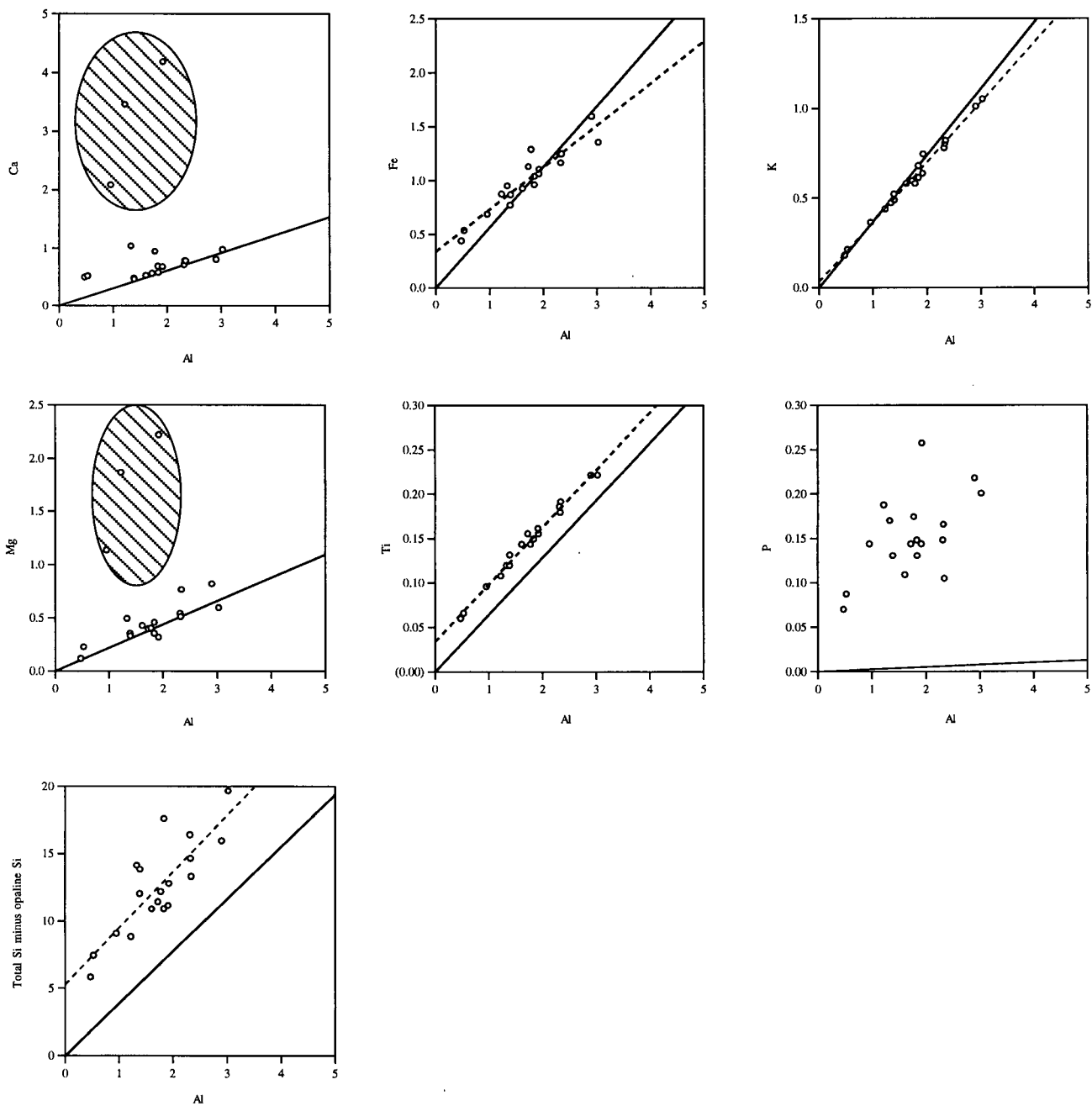


Figure 12. MF major element/Al relationships. Regressions are as described in Figure 11. Ca and Mg have a lithogenic source (solid line) as well as some other source (hatched area). P is enriched in MF samples relative to the WSA and shows no linear relationship with Al, suggesting input from a non-lithogenic source.

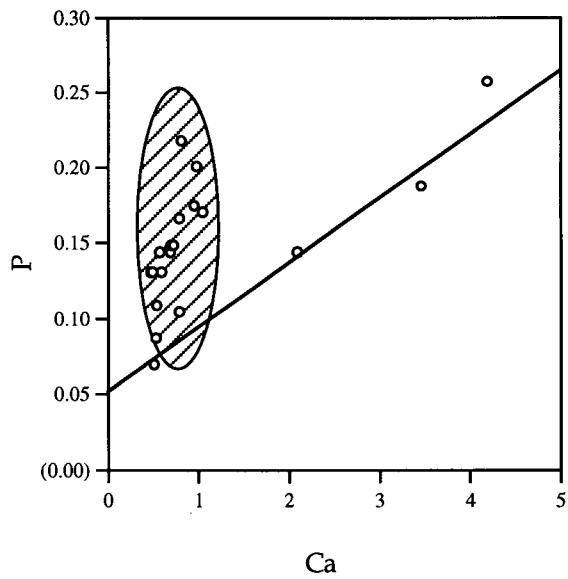
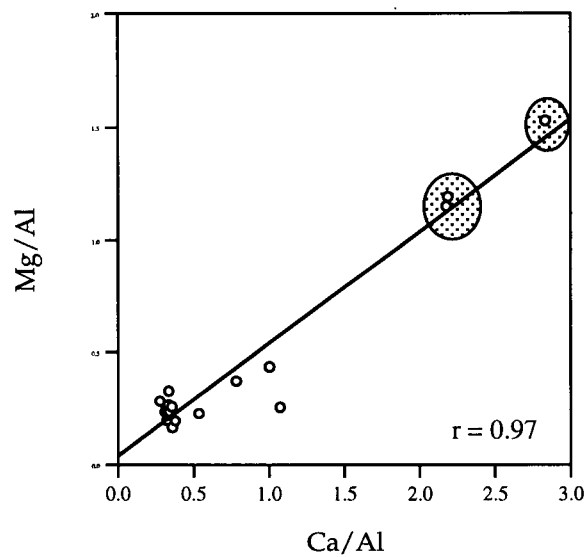


Figure 13. MF Ca, Mg, and P contents. Linear relationship of Ca/Al and Mg/Al suggests the presence of dolomite, with high concentrations in three samples (highlighted). The two trends evident in the Ca/P plot suggest the presence of apatite (solid regression) as well as some other source for P (hatched area), most likely organic matter.

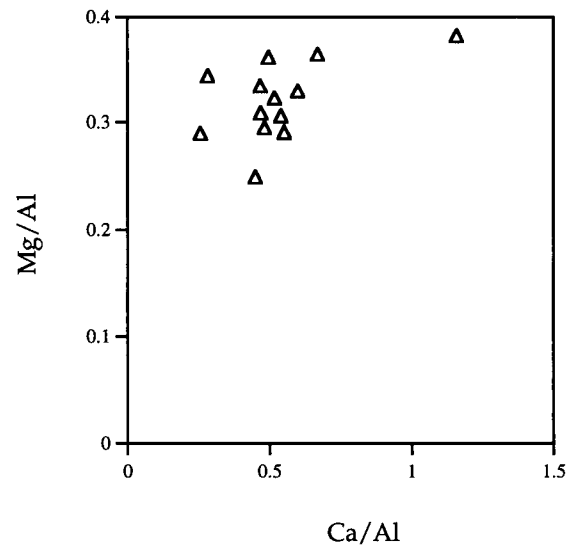
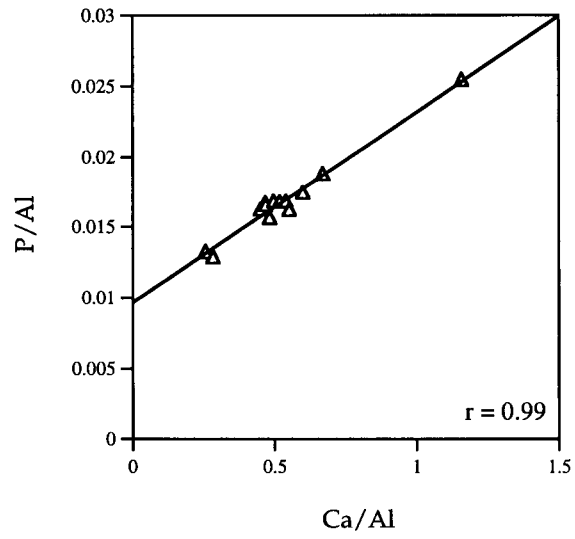


Figure 14. SBB Ca, Mg, and P relationships showing presence of apatite (correlation of Ca/Al and P/Al), but not dolomite (lack of correlation between Ca and Mg).

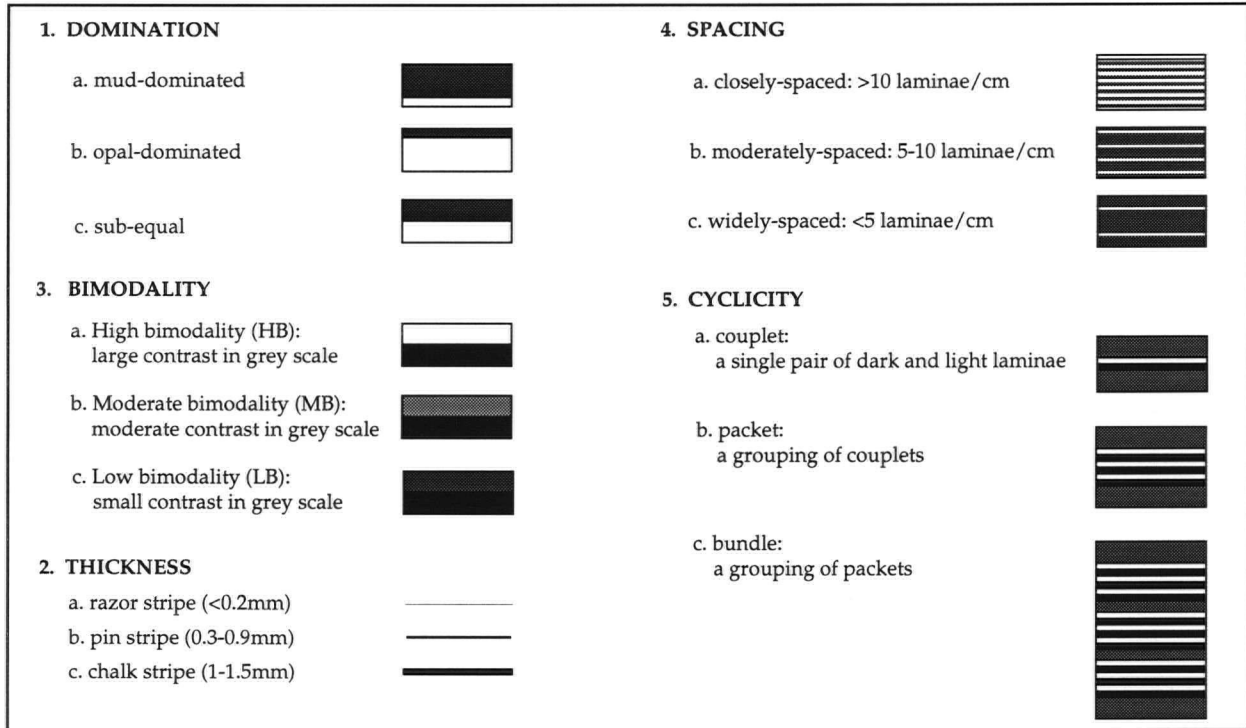


Figure 15. Classification of lamination styles. White, black, and grey represent very opal-rich, very mud-rich, and mixed opal/mud laminae, respectively.

delineated as "moderate bimodality" (MB).

Domination is a parameter describing the relative contributions made by opal and detritus to a sample. In a couplet (one dark lamina, one light lamina), if the biosiliceous lamina is at least 50% thicker than the adjacent detrital lamina, that sample is labeled opal-dominated. Conversely, if the detrital lamina is at least 50% thicker than the biosiliceous lamina, that couplet is described as mud-dominated. If the two laminae have approximately the same thickness, it is described as sub-equal.

Thickness is a simple parameter used to describe how thick diatomaceous or detrital laminae are. The terms razor, pin, and chalk stripes are used to describe laminae less than 0.2 mm, 0.3 to 0.9 mm, and 1.0 to 1.5 mm thick, respectively.

The *spacing* classification is used to describe how close together diatomaceous laminae are in the sample and is directly influenced by lamina thickness. Closely-spaced, moderately-spaced, and widely-spaced laminae are the terms used to describe greater than 10 laminae/cm, 5 to 10 laminae/cm, and less than 5 laminae/cm respectively.

Cyclicity describes the grouping of laminae. Two laminae (one dark and one light) are termed a couplet, a group of couplets is a packet, and a group of packets is a bundle. These groupings of couplets are commonly cyclic on several scales, ranging from centimetres to decimetres to tens of metres (Pisciotta and Garrison, 1981).

An additional lamina descriptor evolved during the classification of the Saanich Inlet samples. Closely-spaced, razor-striped, opal-rich laminae are common in the SI sediment slabs. These laminae are termed "amalgamated opal laminae" based on the observation that several discrete blooms may occur each year (Parsons et al., 1983; Whitney, 1995). Electron micrographs of SI sediments show these amalgamated blooms (Grimm, unpublished data), and similar laminae are evident in electron micrographs in the Santa Barbara Basin (Grimm et al., 1996).

Examples of these parameters as they are expressed in the sediments are shown in Figure 16. The Monterey samples have relatively thinner laminae than the Saanich samples (generally <1 mm in MF and 3-5 mm in SI), most likely due to sediment compaction. Another difference between the Monterey and Saanich laminae is the presence of bright white laminae (see Appendix I); this

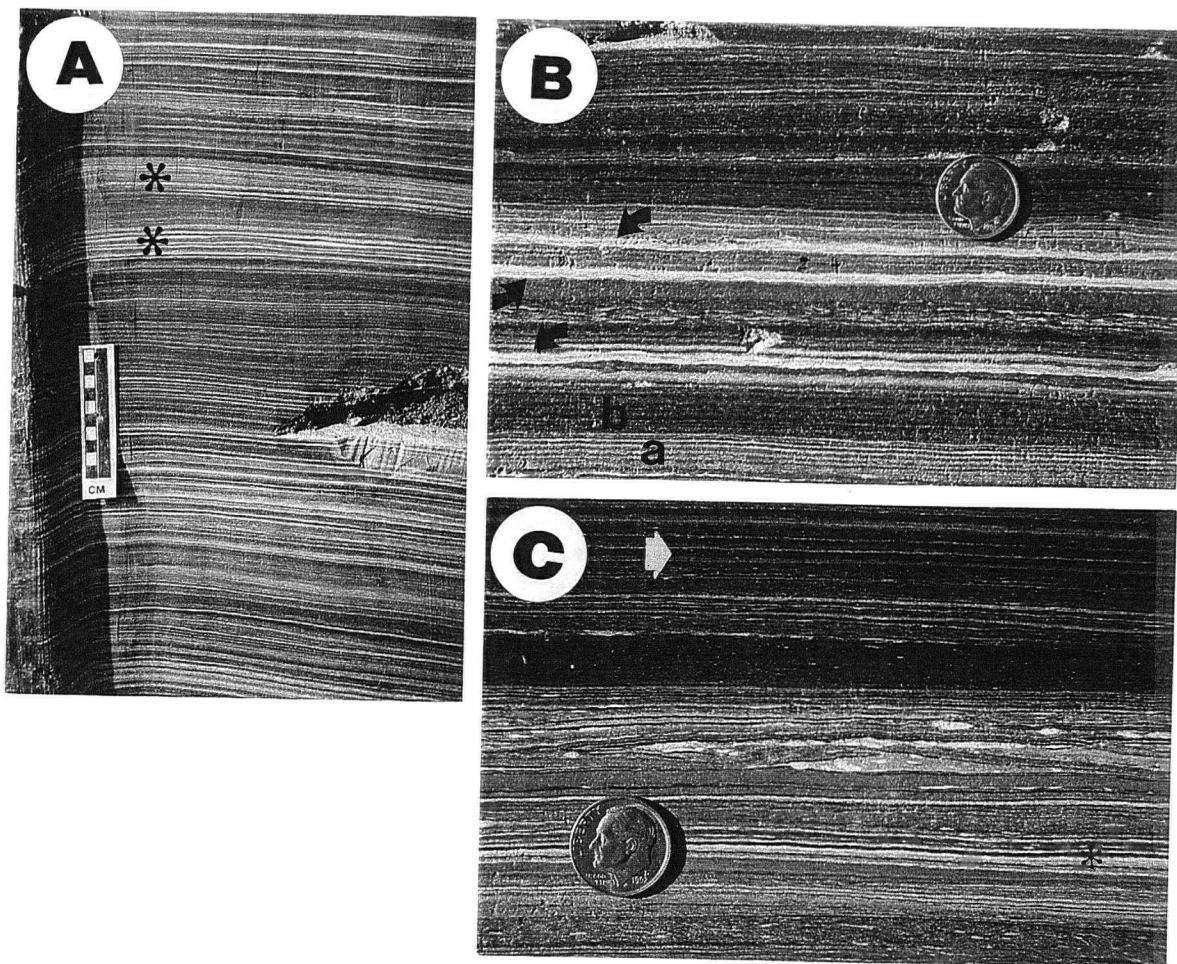


Figure 16. Outcrop photographs of MF displaying various lamination styles. (A) Two packets of sub-equal, closely-spaced, pinstripes (asterisk). (B) Three thick, chalk-striped opal laminae (arrows); moderate-bimodality, sub-equal, pinstripes (a); low-bimodality, mud-dominated pinstripes (b). (C) High bimodality couplet (asterisk); low-bimodality, mud-dominated, moderately-spaced laminae (white arrow).

produces generally higher bimodality couplets in Monterey samples and is likely responsible for the nearly pure diatomite of some MF laminae (cf. Table 1).

4.3 Sediment composition reflected in x-radiographs

X-radiographs record variations in bulk density which are directly related to sediment composition. Opal-rich laminae are less dense than detritus-rich laminae due to the relative larger size and irregular shape, and the porous nature of diatom frustules, both of which favor open packing (Schimmelmann et al., 1990; Lange and Schimmelmann, 1995). Because of this relationship, the relative composition of individual laminae is qualitatively discernible on x-radiograph prints; lighter laminae are less dense, and hence more opal-rich, whereas the darker laminae are more dense, and hence more mud-rich (e.g. Grimm et al., 1996).

Visually-assigned qualitative estimates of sample composition (opal-dominated, sub-equal, and mud-dominated) are plotted versus the quantitative opal and detrital content (Figure 17). MF samples described as opal-dominated cluster at higher measured amounts of opal and lower detritus percentages relative to those samples described as mud-dominated, and the sub-equal samples are intermediate. There is overlap between these classifications which is especially apparent in Figure 17b. This overlap is most likely the result of the assignment of the domination parameter which superimposes a tripartite classification scheme on sediments that record a continuum in bulk composition from mud-rich to opal-rich.

The Saanich Inlet samples do not show similar trends; opal-dominated, sub-equal, and mud-dominated samples all have a wide range of opal values. If an opal content of 30% is assigned as the limit separating mud-dominated from opal-dominated, two groups of samples emerge as problematic: individual mud laminae and amalgamated opal laminae.

These types of laminae are shown in Figure 18. Mud laminae range in thickness from 1.5 mm to 5 mm, appear black on the x-radiograph print, and have lighter-colored laminae above and below. Amalgamated opal laminae are thin, closely-spaced, light-colored laminae separated by darker laminae.

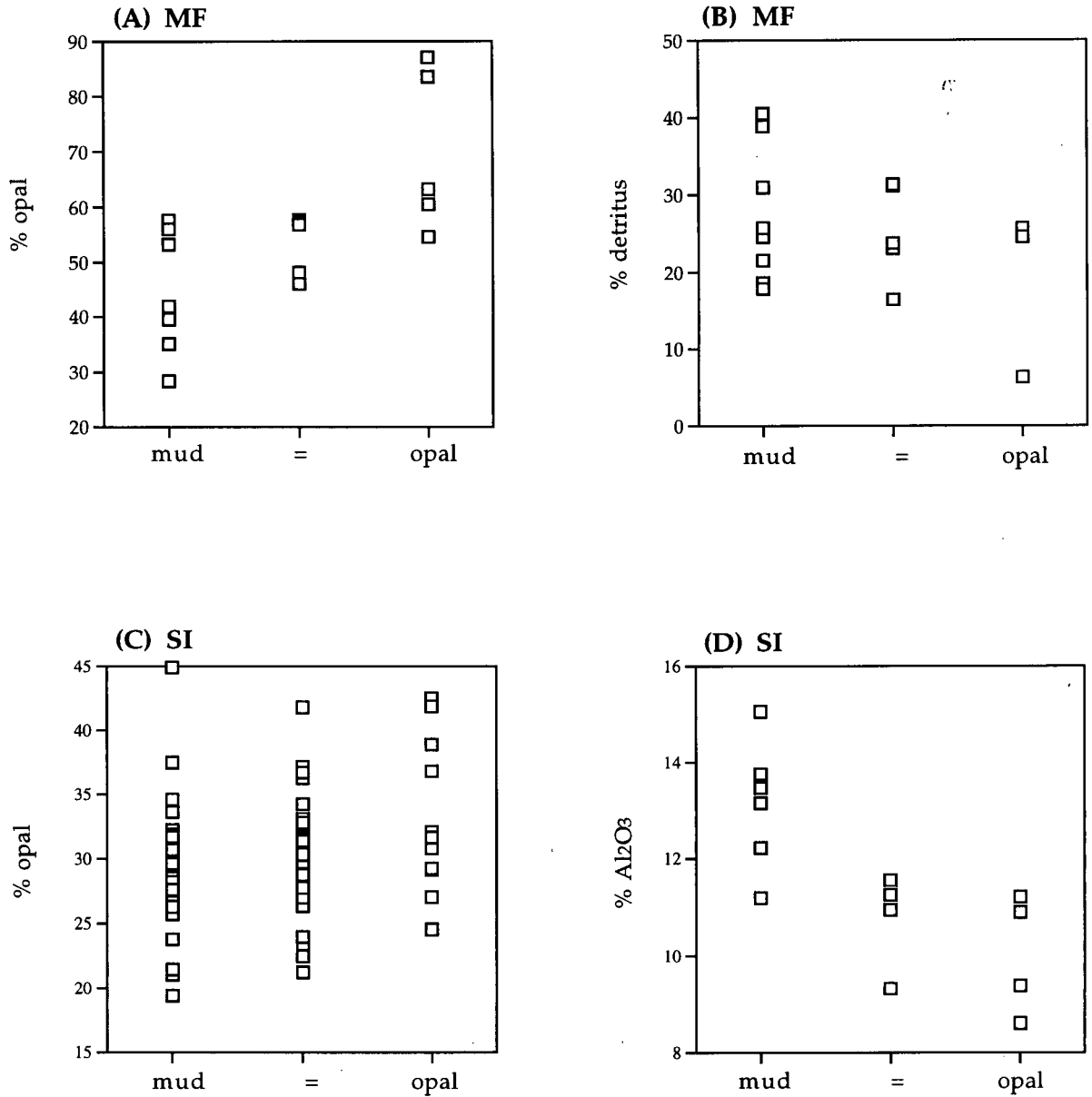


Figure 17. Quantitative geochemical data versus qualitative visually-determined domination. (A) MF domination versus opal content; note mud-dominated samples have <60% opal whereas opal-dominated have >55%; (B) MF domination versus detritus; trend not as clear as in (A); (C) SI domination versus opal; note enormous scatter; (D) SI domination versus Al content (proxy of detritus); less scatter, but fewer samples analyzed.

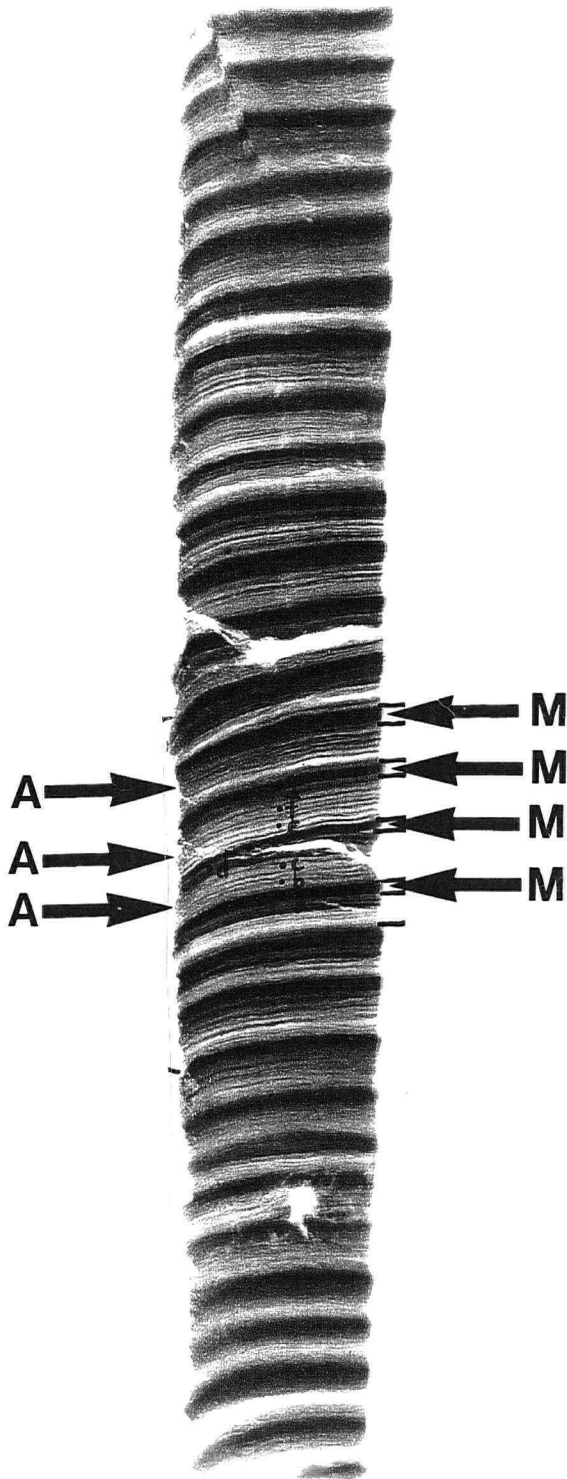


Figure 18. X-radiograph print of Saanich sample Q; examples of "mud laminae" and "amalgamated opal laminae" indicated with M and A respectively.

These samples are enigmatic; the geochemical data and the x-radiograph prints do not corroborate. An error in subsampling could be responsible for these puzzling results; imprecise extraction of laminae (i.e. contaminating an opal-rich lamina with the sediment of the enclosing mud-rich laminae) could render the geochemical results impossible to interpret accurately on a lamina-scale. Another possible explanation could involve poor understanding of the composition and nature of some laminae; perhaps some dark-colored, high-density laminae contain very closely packed, highly fragmented diatom frustules that are relatively more opaque to impinging x-rays whereas the amalgamated opal laminae may possess a lower bulk density, and hence higher x-ray transparency due to more loosely arranged sediment. Future investigations may benefit from the coupling of SEM analyses and geochemical subsampling that are focused on resolving this problem.

4.4 Geochemical proxies of organic matter source

Distinct geochemical signatures of organic matter enable the determination of the sources of these materials: C/N ratios, stable carbon isotopes of organic matter, and kerogen type. Results from Saanich Inlet and Monterey Formation samples are shown in Table 2.

C/N ratios

The weight ratio of organic carbon to total nitrogen can be diagnostic of a particular source of organic matter due to the various chemical compositions of organisms. Protein-rich marine organisms have lower relative C/N ratios compared to carbohydrate-rich terrigenous organic matter; typically, marine sedimentary OM has ratios between five and 13 (Müller, 1977) and terrigenous OM has ratios greater than 20 (Emerson and Hedges, 1988). Saanich Inlet C/N values (mean=7.2; range=6.1-8.7) suggest a marine source for the sedimentary organic matter whereas the Monterey Formation data are intermediate between marine and terrigenous (mean=15.0; range=13.0-16.2), suggesting a mixture of OM sources.

	MF	SI
C/N	13.1 - 16.2 x=15.0	6.1 - 8.9 x=7.2
δ¹³C (‰)	-21.4 - -20.1 x= -20.6	-22.2 - -20.9 x= -21.6
OI (mg CO ₂ /g C _{org})	28 - 63 x=39	-
HI (mg hydrocarbon/g C _{org})	273 - 429 x=338	-

Table 2. Geochemical proxies of organic matter source: C_{org}/N_{total} weight ratios, δ¹³C isotopic ratios of organic matter, and the oxygen and hydrogen indices (OI and HI) can be used collectively to infer the marine or terrigenous source of organic material in sediments.

Stable carbon isotopes of organic matter

The source of sedimentary organic matter can also be assessed using carbon isotopes of organic matter due to the distinct isotopic signatures of marine and land plants. These differences are the combined result of the sources of carbon used in photosynthesis and the kinetic fractionations involved in the fixation of carbon. These differences are expressed as $\delta^{13}\text{C}_{\text{org}}$ —the measurement of the relative amounts of carbon-12 and 13 in a sample¹.

Land plants use atmospheric CO_2 with a $\delta^{13}\text{C}$ of -7.8‰ (Keeling, 1993), whereas marine plants use molecular CO_2 or bicarbonate with a $\delta^{13}\text{C}$ of 0‰ (Kroopnick, 1985). Kinetic fractionation occurring during the photosynthetic fixation of carbon produces $\delta^{13}\text{C}$ of terrestrial C_3 plants between -26 and -28‰ ; in low- to mid-latitude marine phytoplankton, $\delta^{13}\text{C}$ values typically range between -18 to -22‰ (Deines, 1980; Fontugne and Duplessy, 1981; Rau et al., 1989; Freeman and Hayes, 1992). These distinctive values of marine and terrigenous organic matter allow for the determination of organic matter source. $\delta^{13}\text{C}$ values of SI (mean= -21.6‰ ; range= -22.2 to -20.9‰) and MF (mean= -20.6‰ ; range= -21.4 to -20.1‰) suggest a marine source.

Kerogen type

Variations in the type of organic matter (e.g. algae vs. bacteria vs. fir tree), the depositional environment (e.g. lake vs. river; anoxic vs. oxic), and the diagenetic history of an organic-rich sedimentary rock unit affect the elemental composition of the kerogens present in that rock, producing distinct and diagnostic ratios of hydrogen, carbon, and oxygen. The ratios of H/C and O/C can be plotted on a van Krevelen diagram, and the location of the data points indicates the source and/or environment of the original organic matter and its stage on an evolutionary pathway (Tissot and Welte, 1984).

Rock-Eval pyrolysis of whole rock samples allows for a similar determination of kerogen type. Rock-Eval does not directly determine the elemental compositions of carbon, oxygen, and

¹ $\delta^{13}\text{C} = \left(\frac{^{13}\text{C}/^{12}\text{C}_{\text{sample}}}{^{13}\text{C}/^{12}\text{C}_{\text{reference}}} - 1 \right) \times 1000$ and is expressed as parts per thousand (permil, ‰); $\delta^{13}\text{C}$ is relative to a belemnite of the Pee Dee Formation (PDB).

hydrogen, but measures pyrolyzates evolved from the heating of the rock. The pyrogram displays three peaks: S1, S2, and S3. The S1 peak is the amount of hydrocarbons thermally distilled from the rock, expressed as mg HC/g rock, and is proportional to the OM that is soluble in organic solvents. The S2 and S3 peaks are the amounts of hydrocarbons (and hydrocarbon-like substances) and CO₂ generated from the pyrolysis of kerogen (OM that is not soluble in organic solvents, acids, and bases) in the rock. These parameters can be combined and expressed as a hydrogen index (HI) equal to $(S2 \times 100)/\text{TOC}$ and an oxygen index (OI) equal to $(S3 \times 100) / \text{TOC}$. These two indices are comparable to the H/C and O/C ratios of the van Krevelen diagram, and can be plotted similarly (Espitalié et al., 1977).

The modified van Krevelen diagram for the Monterey Formation, shown in Figure 19, depicts a cluster of points between the curves of the type II and III paths, indicating organic matter sourced from phytoplankton, zooplankton, bacteria and terrestrial plants.

4.5 Distribution of organic matter

Figure 20 shows the relationships of organic carbon, opal, and detritus (or aluminum content) for Saanich Inlet, Monterey Formation, and Santa Barbara Basin samples. In Saanich Inlet, there is a positive linear association of total organic carbon (TOC) with opal ($r=0.72$) and a negative association with detritus ($r=-0.85$). The distribution of TOC in the Monterey samples is opposite that of Saanich; the OM is associated with the detrital component ($r=0.79$), not opal ($r= -0.87$). In Santa Barbara Basin samples, there is no clear association of these three components.

These various trends are counterintuitive. All three are hemipelagic deposits, in which opal and terrigenous detritus are the predominant components. All record significant diatom productivity and have preserved opal-rich and detritus-rich laminae. The close association of organic carbon with opal seen in Saanich Inlet samples is expected; the growth of diatoms involves the production of both opal and organic carbon and the concurrent settling and deposition of these materials results in laminae rich in both. Using similar reasoning, this same association might also be expected in the Monterey Formation samples as well as the Santa Barbara Basin samples. The dynamics controlling

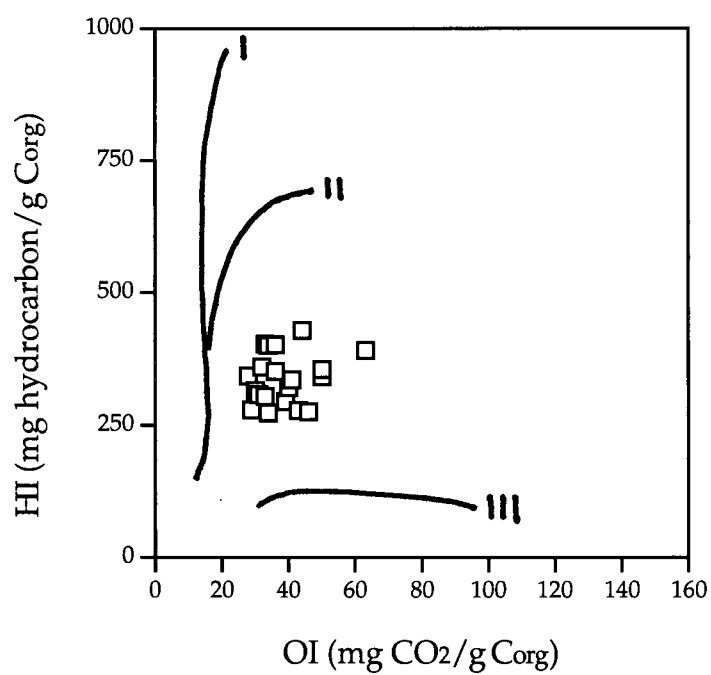


Figure 19. Modified van Krevelen diagram for MF samples. $OI = S3 \times 100/TOC$; $HI = S2 \times 100/TOC$. Data points cluster between the type II and type III kerogen pathways, suggesting a mixture of organic matter sourced from phytoplankton, bacteria, zooplankton, and higher land plants.

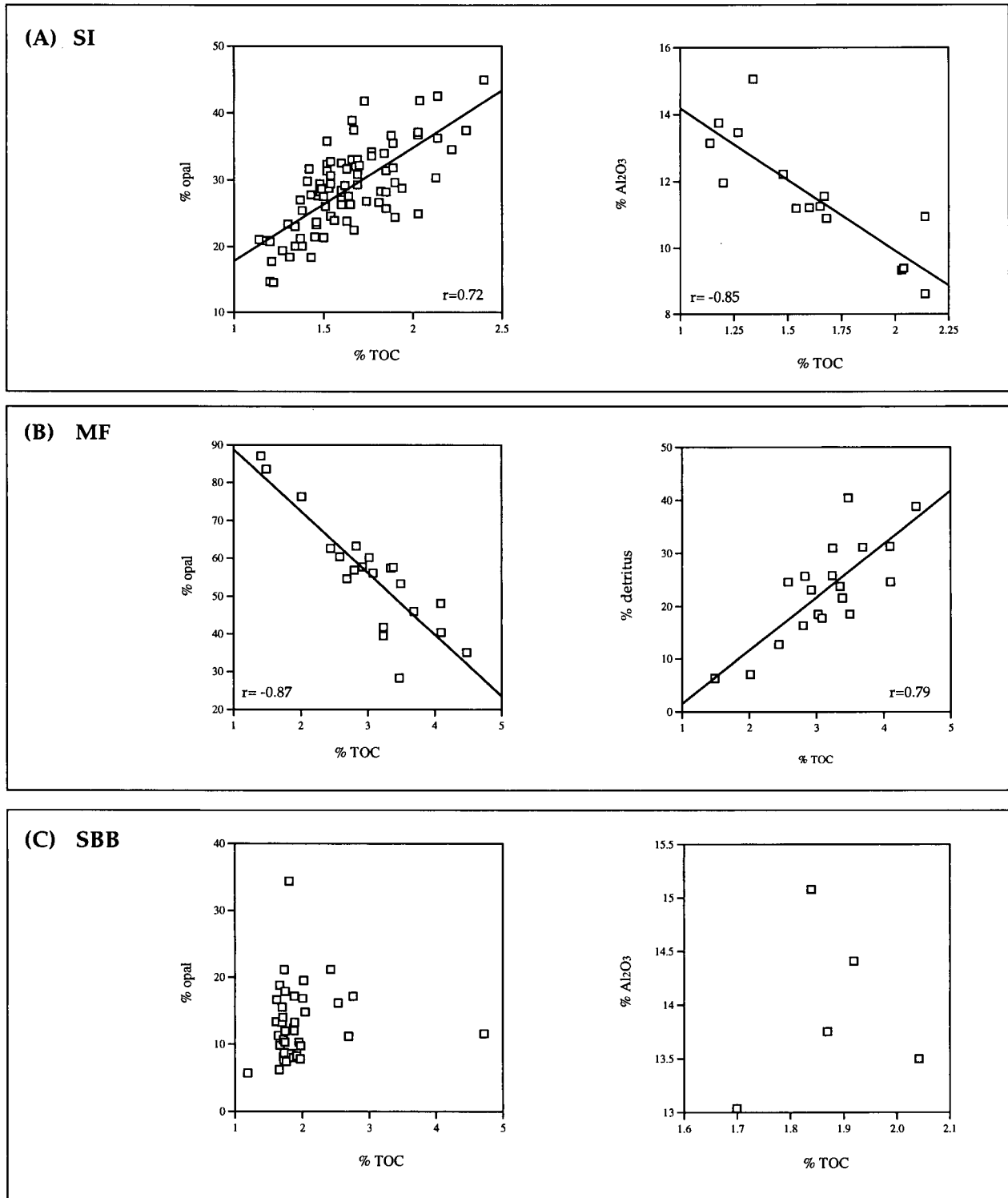


Figure 20. Associations of TOC with respect to opal and lithogenic detritus (or Al) in (A) Saanich Inlet; (B) Monterey Formation; (C) Santa Barbara Basin. Note opposite distributions of TOC in SI and MF and the lack off any association in SBB samples.

and influencing the distribution of organic matter in these three environments must be different and warrant further discussion.

5. DISCUSSION

5.1 Bulk sediment composition—comparison of MF, SI, and SBB

Sediments of Saanich Inlet and Santa Barbara Basin have very similar bulk compositions; organic matter, opal, and detrital contents overlap. One difference, however, is the appreciable carbonate in SBB; calcareous nannofossils are present in many SBB smear slides, whereas they are absent in SI samples (Grimm, unpublished data). The similar detrital content of SI and SBB is interesting, considering that SI is a small basin surrounded by land in a high rainfall area whereas SBB is isolated from the arid coastline of California. This surprising similarity in detrital content, despite contrasting environments, highlights the primary importance of point sources of detrital sediment in governing the bulk composition of hemipelagites.

Comparison of bulk composition of Monterey Formation sediments versus Saanich Inlet and Santa Barbara Basin sediments reveals three main differences: (1) MF samples contain significant localized dolomite; (2) average TOC is higher in MF samples, although the ranges overlap; (3) the detrital content is significantly lower in MF sediments. The lower detrital content of MF samples is a key contrast; it suggests an arid climate for the MF and/or a more outboard position compared to SI and SBB and is also the factor that permitted the formation of economically-viable diatomite. This final contrast suggests that SI and SBB are not appropriate analogs for the upper siliceous facies of the MF near Lompoc. Perhaps if the Fraser River were re-routed, so that its discharge did not reach SI, then SI could produce more pure diatomites like those found in Lompoc.

5.2 Sediment fabric

Sediments in Saanich Inlet and the Monterey Formation contain sedimentary fabrics which range along a continuum from distinctly laminated to non-laminated. The well-laminated sections contain alternating light-dark laminae arranged as couplets, packets, or bundles, whereas the non-laminated intervals are characteristically muddy and are attributable to bioturbation, gravity-flow redeposition, and/or soft-sediment failure and erosive reworking (Chang, 1998a). The composition

and the processes responsible for lamina formation will be investigated and discussed in the following section.

Formation of laminae

In the Monterey Formation, x-radiographs and geochemical data suggest that the laminated fabric is the result of varying relative contributions of opal and detritus. The alternation of light-colored, less dense, opal-rich laminae and darker-colored, more dense, mud-rich laminae produces the observed fabric. The Saanich samples are more problematic to interpret; the lamina-scale geochemical data and x-radiographs do not endorse the alternation of opal and detritus deposition as the mechanism for the formation of the laminated fabric, as the light-colored laminae on x-radiograph prints were not consistently enriched in opal. Previous work done in Saanich Inlet however, does suggest that laminae are formed due to the alternating deposition of opal and detritus (e.g. Gross et al., 1963; Sancetta and Calvert, 1988; Collins, 1997), and therefore, the problematic results of this investigation are attributed to sampling errors.

The formation of biogenic and detrital laminae in coastal regions is most commonly propelled by the seasonal responses of primary productivity and runoff (Sancetta, 1996). This has been shown to be the driving mechanism of lamina formation in the Santa Barbara Basin (e.g. Bull and Kemp, 1996; Schimmelmann and Lange, 1996) and in the Gulf of California (Thunell et al., 1994).

In Saanich Inlet, seasonal control on sedimentation can be investigated with sediment traps. Traps were deployed in SI in 1984 (by S. Calvert, M. Soon, and) at two sites to assess sedimentation rates (Figure 21a). The trap experiment apparatus consisted of collection containers moored at three different depths at each site (Figure 21b). Trapped materials were collected approximately each month for six years and geochemical analyses (including weight percents and accumulation rates of total mass, opal, and organic carbon) were performed on the collected trap material (unpublished data supplied by D. Timothy, UBC).

The seasonal response of primary productivity is evidenced by the opal flux. The curve of opal mass accumulation rate distinctly and repeatedly peaks in spring/summer in the shallow traps,

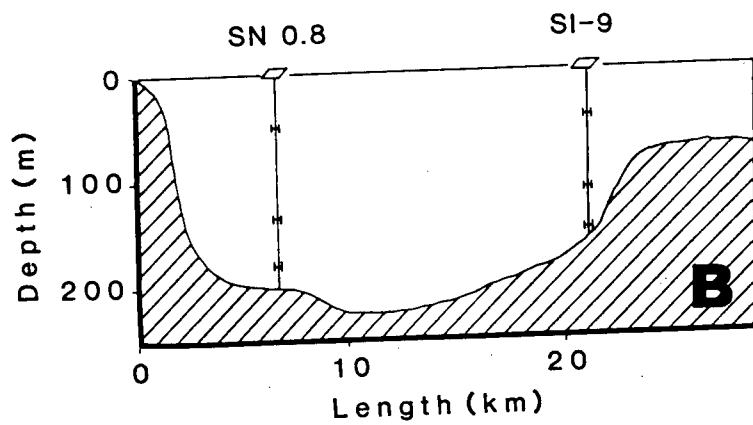
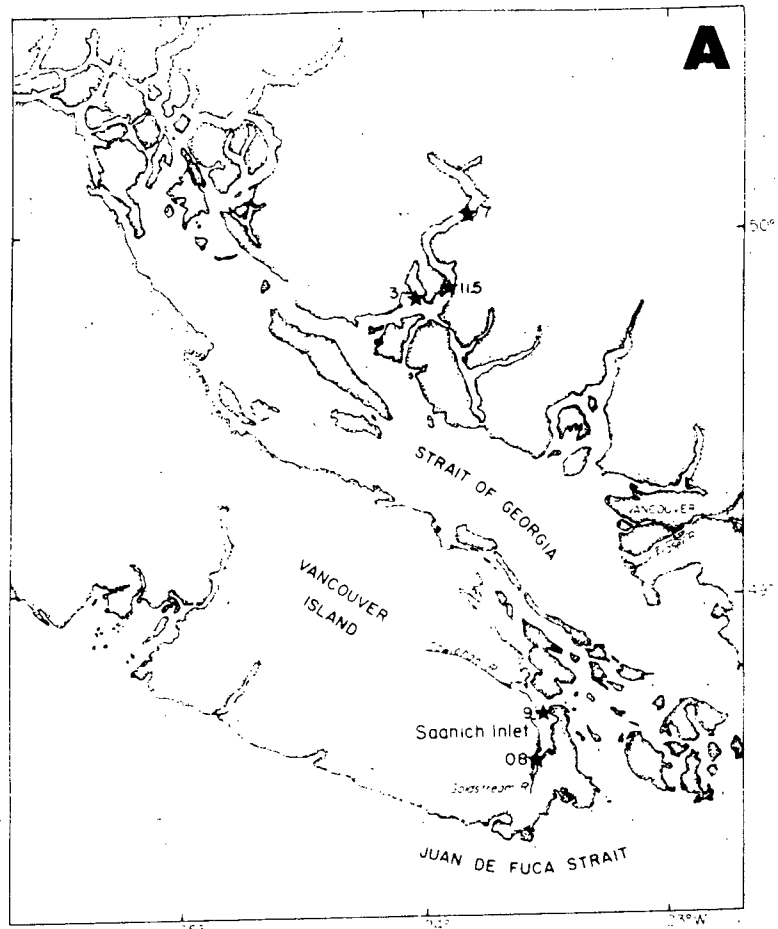


Figure 21. Sediment traps in Saanich Inlet: (A) Locations of sediment trap moorings, SN0.8 and SI9 (From Sancetta, 1989); (B) Set-up of trapping containers at three different depths at each site. At SN0.8, traps at 50 m, 135 m, and 180 m; at SI9, traps at 45 m, 115 m, and 150 m. (From Francois, 1987)

indicating increased productivity during this time (Figure 22). The trend is carried to the deepest traps, suggesting that this pulsed opal productivity generated in the euphotic zone is efficiently transferred to the inlet floor where it is deposited as an opal-rich lamina between March and October (cf. Grimm et al., 1997).

The seasonal response of runoff and its control on the formation of the laminated fabric is less clear. Prominent sources of lithogenic detritus to Saanich Inlet are the sediment loads carried by the Cowichan and Fraser Rivers. These rivers have peak discharges November through April, and May to August respectively (Environment Canada; Figure 23). The detrital flux at the shallow traps shows an irregular pulsed pattern; however, peaks generally occur in the warmer months, reflecting the Fraser River discharge (Figure 24).

In contrast to the parallel patterns of opal flux observed at shallow and deep traps, the profiles of detrital flux at these depths are very different (Figure 25; cf. Figure 22). The detrital flux is greater at depth compared to the shallow trap at both sites and the deep flux pattern is characterized by large spikes that are neither coincident nor systematically in phase with the flux at the shallow traps. This profile suggests that the detrital flux at depth is influenced by laterally advected and/or resuspended material.

The material collected at the deepest trap at each site is most representative of the sediment that is ultimately deposited, and therefore it is this flux that needs to be examined to assess seasonal control on the deposition of detrital laminae. At SN0.8, the detrital flux at 180 metres is typically greatest October through May whereas at SI9, the detrital flux at 150 metres is greatest in July and August (Figure 26). The non-coincidence of peak detrital flux to the deep traps, as well as the lack of correlation to peak fluvial discharge events, suggests local, not regional, control on the deposition of detritus in Saanich Inlet.

A plot showing both opal and detrital fluxes to the deepest traps (Figure 27) best illustrates the timing of deposition of opal and detritus in Saanich Inlet. At SN0.8, it appears that the most opal-rich laminae are deposited in the spring and summer, coincident with increased diatom productivity, and the most mud-rich laminae in the fall and winter. However, the detrital flux is greater than the

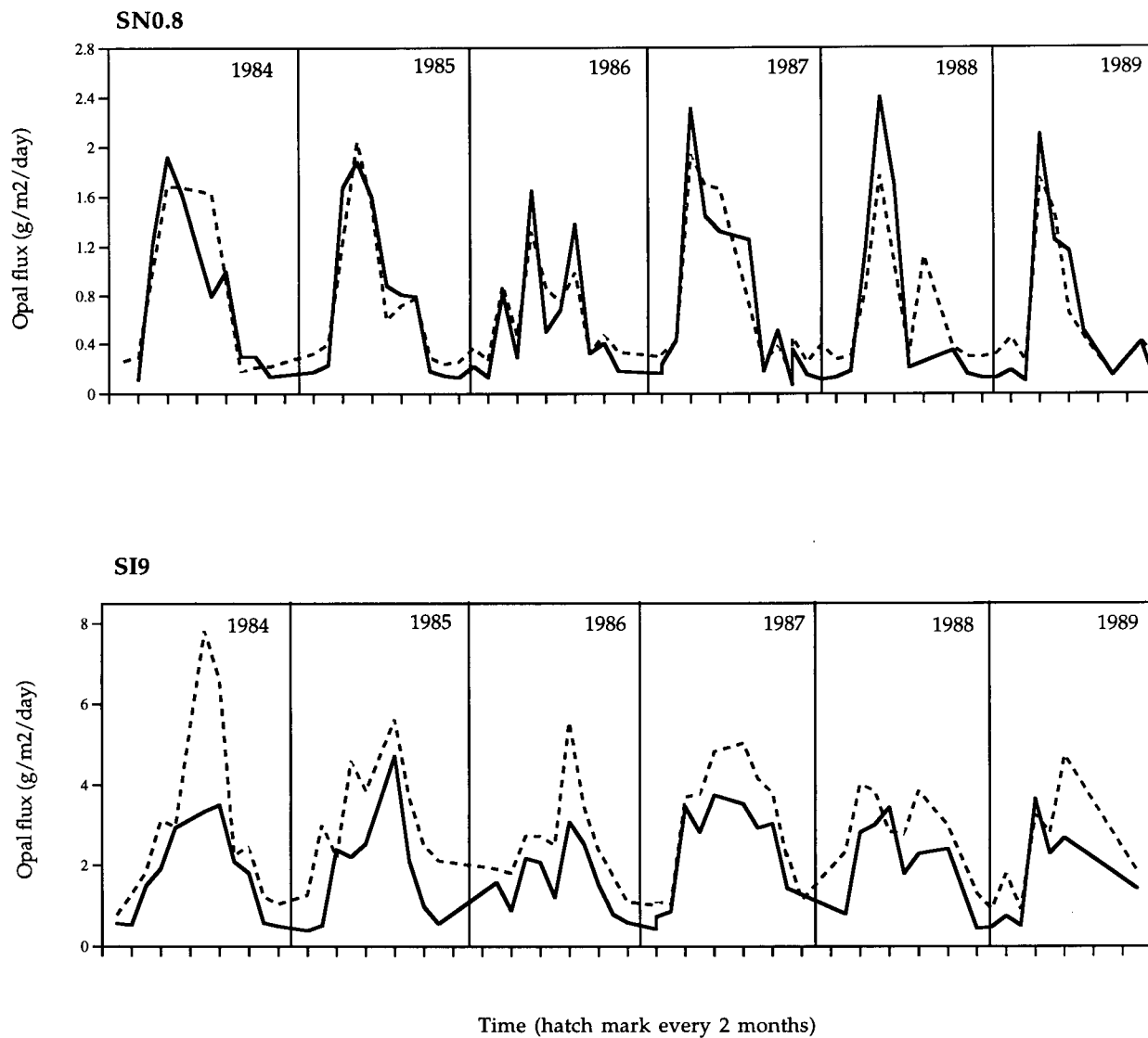


Figure 22. Opal flux at SN0.8 and SI9. Solid line is the flux at the shallow trap, broken line is the flux at the deep trap. Note excellent correlation in quantity and timing of opal flux at two depths at SN0.8 indicating rapid and efficient transport of opal through the water column. At SI9, opal flux is greater at depth; this trend is attributed to lateral advection and/or resuspension near the sill.

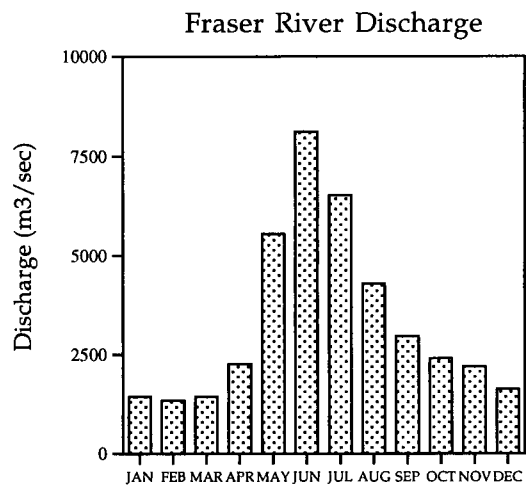
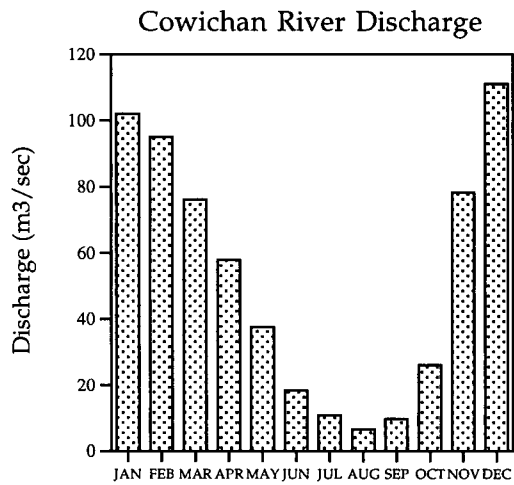


Figure 23. Average monthly discharge rates (m³/sec) for the Cowichan and Fraser Rivers (Environment Canada). Cowichan River rates were measured near Duncan and were averaged over 29 years. Fraser River rates were measured at Mission and were averaged over 24 years. Note much larger discharge rate of the Fraser.

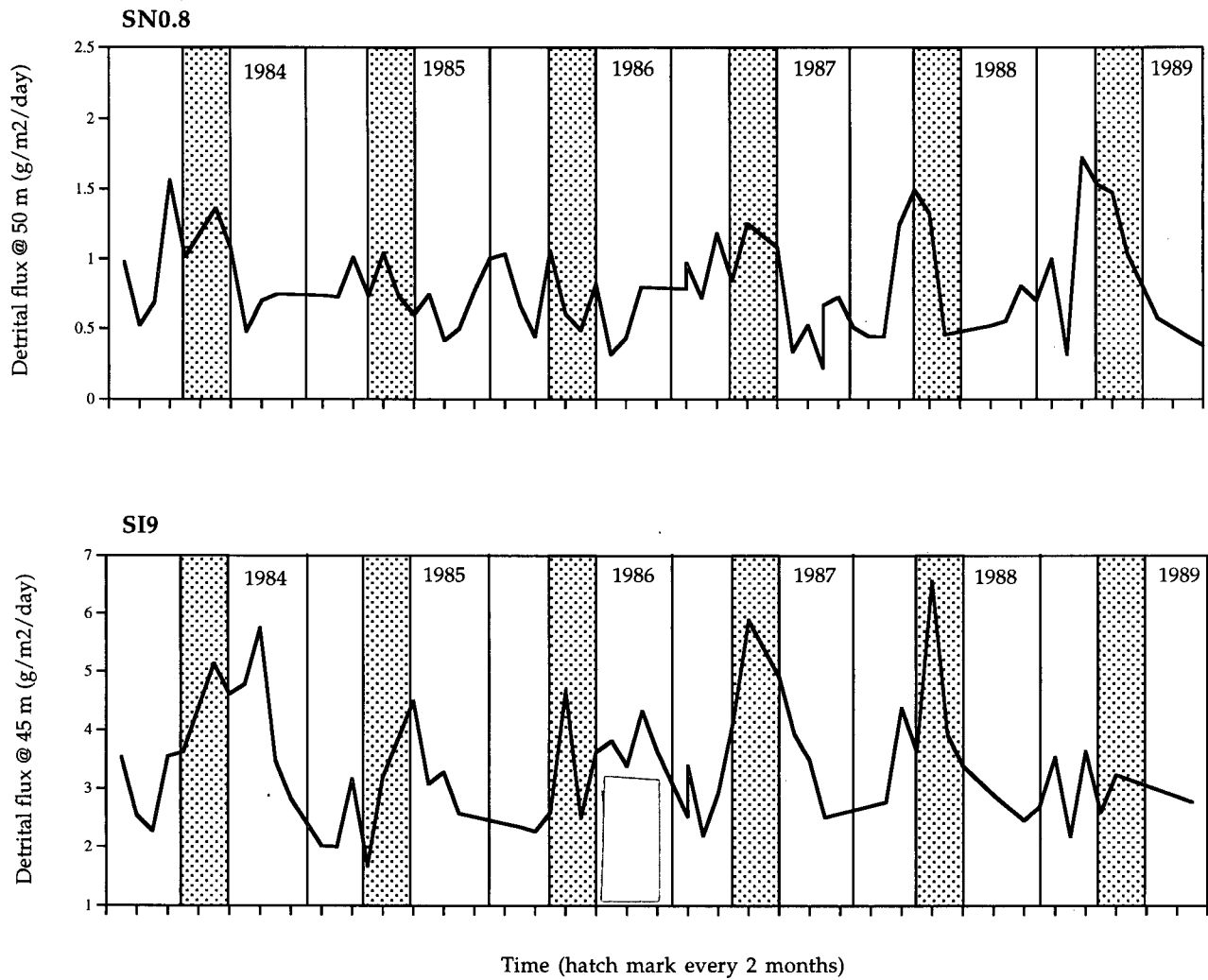


Figure 24. Detrital fluxes at shallow traps at SN0.8 and SI9. Fluxes are generally greater during the warmer months, often coinciding with peak Fraser discharge (represented by stippled regions).

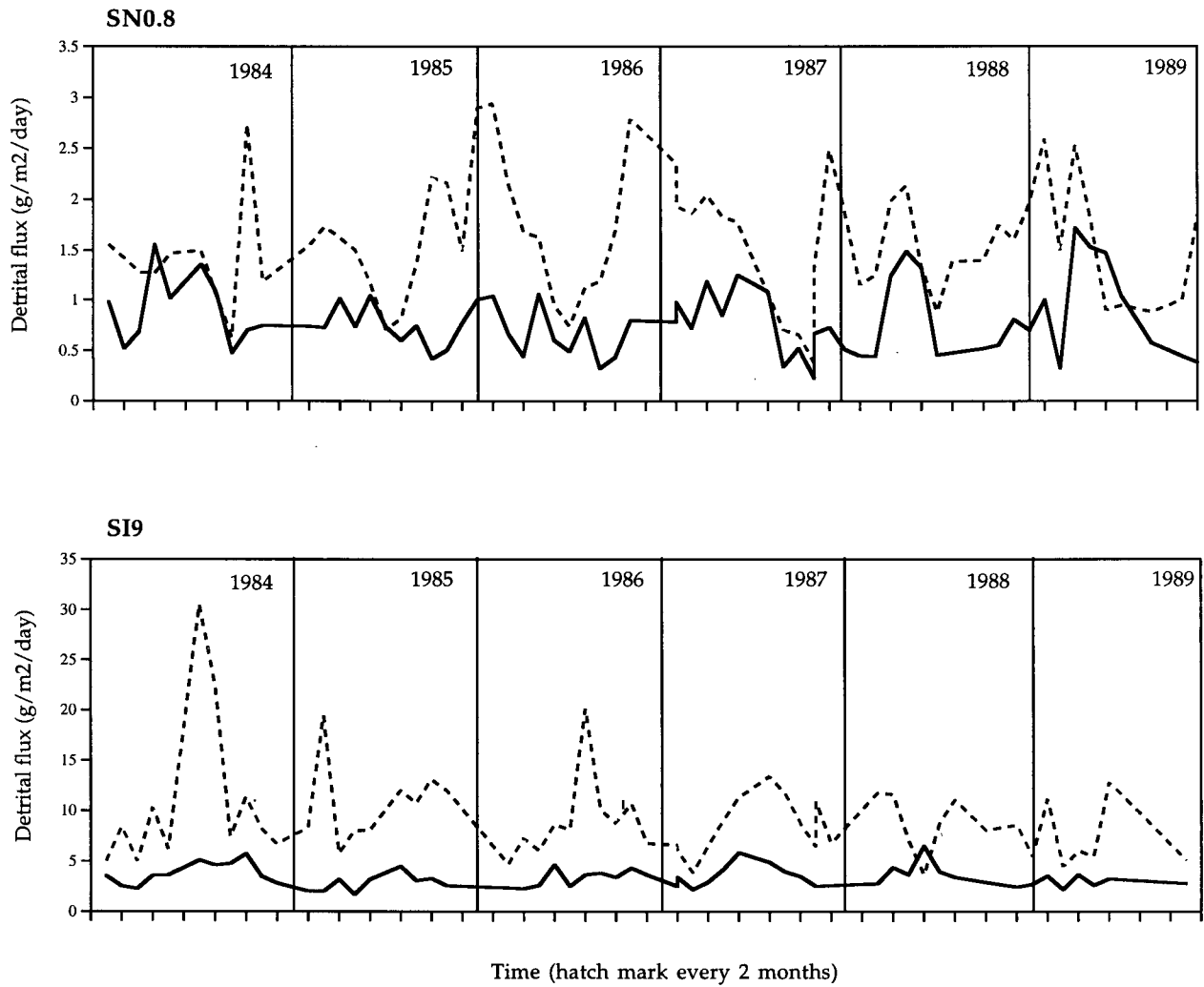


Figure 25. Comparison of detrital fluxes at shallow (solid) and deep (broken) traps at SN0.8 and SI9. Note much larger flux at the deeper trap compared to the shallow trap, especially at SI9. This increase is attributed to laterally advected and/or resuspended sediments.

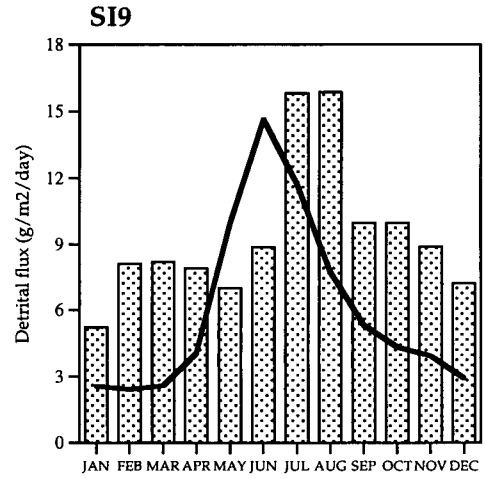
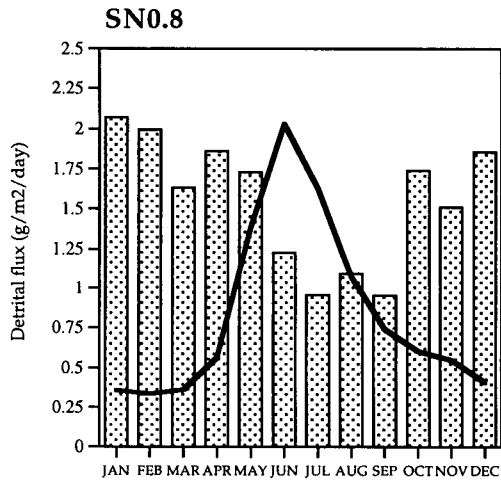


Figure 26. Average monthly detrital fluxes to the deepest traps at SN0.8 and SI9 compared with Fraser River discharge (solid line). Large detrital fluxes in July and August at SI9 are most likely due to large spikes in 1984 and 1986 (see Figure 25). Note that the deep detrital flux does not coincide with peak fluvial discharge.

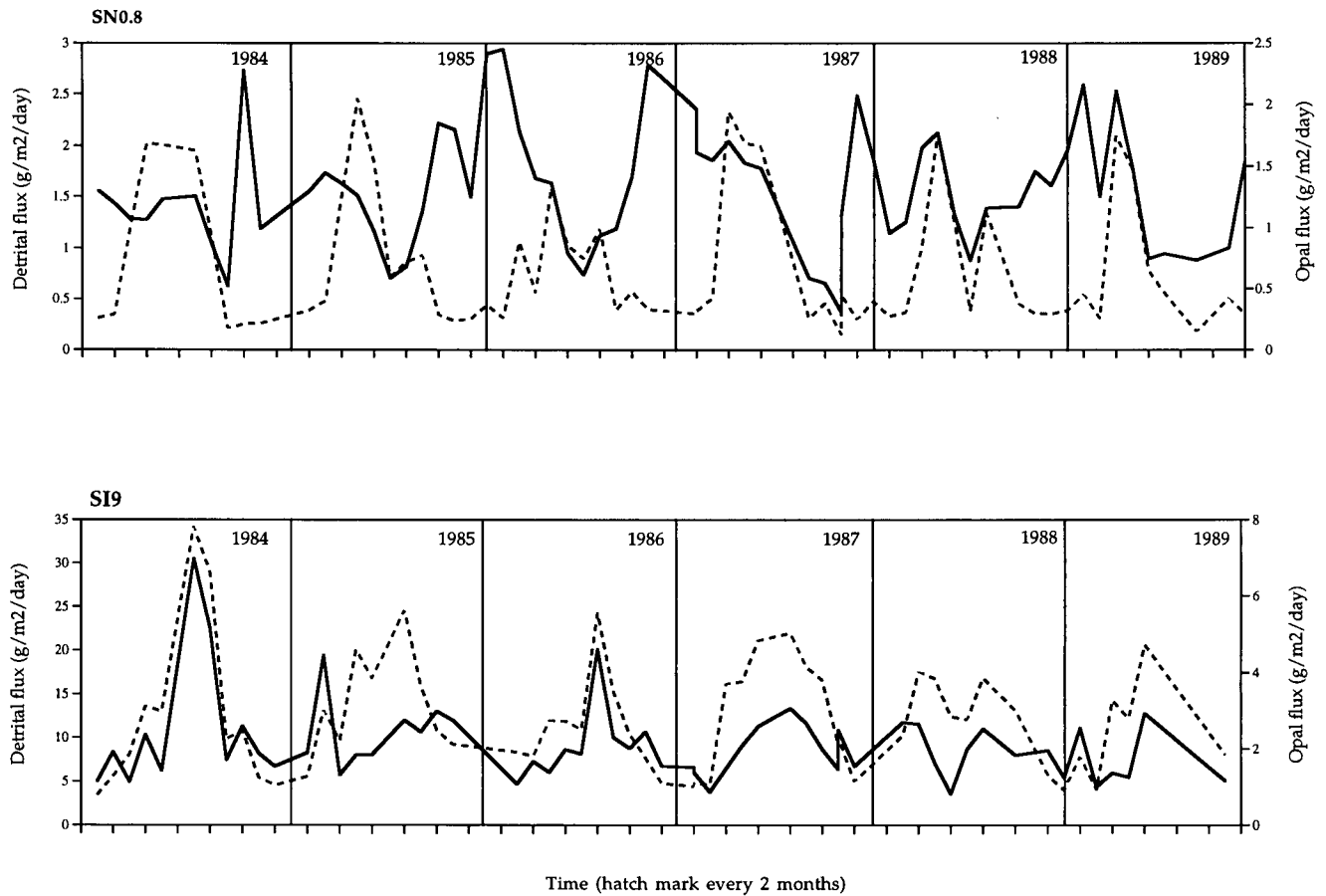


Figure 27. Deep fluxes of detritus (solid) and opal (broken) at SN0.8 and SI9. The curves of SN0.8 suggest that deposition of opal and detritus is seasonal, with opal deposition occurring in the spring and summer and detrital deposition in the fall and winter. The fluxes of opal and detritus at SI9 are nearly in phase, making it difficult to understand the method of lamina formation beneath this trap.

opal flux year-round and shows less seasonal regularity than the opal flux. Therefore, the laminated fabric beneath SN0.8 most likely forms in response to a seasonally-controlled strong pulse of opal deposition, superimposed on year-round delivery of detritus (cf. Calvert, 1966). At SI9, the opal and detrital fluxes at the 150 metre trap are nearly in phase and it is therefore difficult to interpret the method of lamina formation beneath this trap.

In the Monterey Formation, the seasonal control on lamina formation can be inferred by analogy to similar depositional environments. The present day Guaymas Basin and slope and the Peru margin are the most appropriate analogs (Soutar et al., 1981; Donegan and Schrader, 1981) and in both regions, laminated diatomaceous sediments are deposited and preserved in response to seasonal signals. Upwelling of nutrient-rich water spurs diatom growth, and their sedimentation produces an opal-rich lamina. The presence of diverse diatom blooms and mat floras in the MF opal-rich laminae supports this hypothesis of seasonal nutrient pulses, diatom blooms and rapid sedimentation (Chang, 1998b). The decrease in primary productivity after nutrient exhaustion along with an increase in allochthonous material (supplied by fluvial or eolian processes) results in the deposition of detrital-rich laminae in the Guaymas Basin and on the Peru margin (Thunell et al., 1994; Brodie and Kemp, 1994). By analogy, the laminated biosiliceous/detrital sediments of the Miocene Monterey Formation can be attributed to the seasonal waxing and waning of the diatom population due to pulsed upwelling coupled with the seasonal delivery of detritus.

Lamina types

The classification of lamination styles (see Figure 15) was developed for the recognition of various sedimentary dynamics as they are reflected in the sedimentary fabric. Variations in parameters affecting either the opal or detrital flux will be manifested in the sedimentary record as a change in lamina style. This approach is similar to that of Kemp (1990), where different lamina styles determined from BSEM images were related to distinct paleoceanographic events.

Domination may record the most prominent "season" of the year. In opal-dominated couplets, the diatomaceous lamina is thicker than the detrital lamina, possibly indicating a more

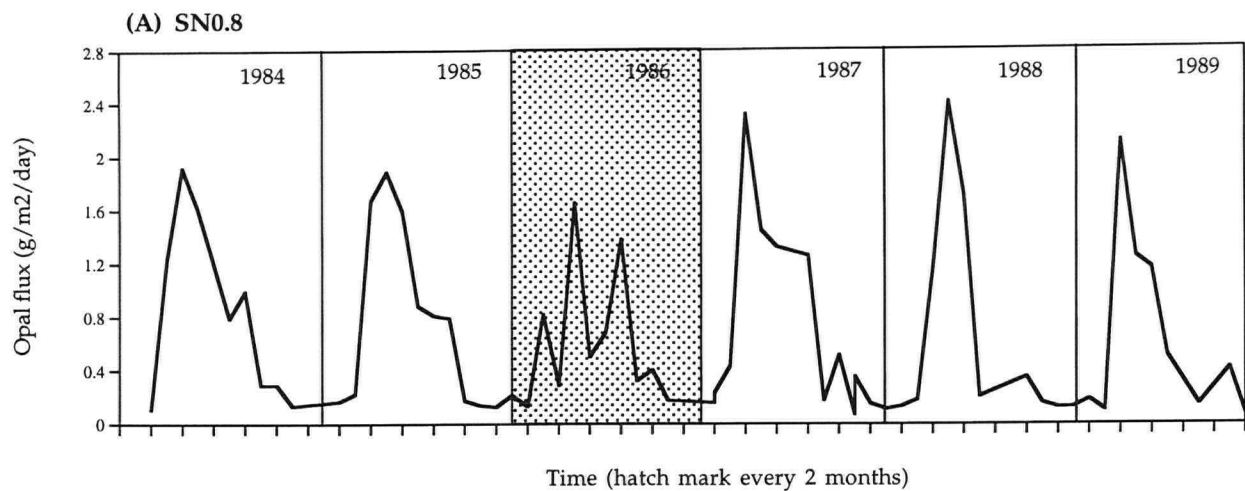
productive spring and summer than that of a sub-equal or mud-dominated couplet.

Lamina thickness can be used to assess the length or intensity of the productive or runoff season. If productivity were higher than average, and opal was efficiently transferred from the surface waters to the sediments, a thicker opal-rich lamina would result. If the winter season was wetter, longer, or had more high discharge events, the mud-rich laminae would be thicker. Additionally, thick laminae can result from the absence of deposition one year; a thick mud lamina may result from the absence of the production and/or preservation of a diatom population.

Lamina spacing may also be an indicator of annual variability. If multiple discrete blooms occurred during the productive season, thin, closely-spaced opal-rich laminae may result (as in the amalgamated opal laminae of SI). If productivity was absent one year (or if the phytodetritus was not preserved), opal-rich laminae might be spaced further apart.

Examples of this variability can be observed in the sediment trap data of Saanich Inlet. In 1986, there are three distinct spikes in the opal flux at SN0.8 (Figure 28a). These peaks may represent three separate diatom bloom events occurring that spring and summer and the sediment record may record these events as three thin, closely-spaced, opal-rich laminae ("amalgamated opal laminae"; Figure 28b). Another example is presented in the detrital flux at SI9; in July and August of 1984, there is a large spike in detrital flux at the deep trap (Figure 29). The lamina formed in response to this large resuspension event may be thicker than the lamina formed in 1988. This event would also increase the spacing of the adjacent opal-rich laminae.

Differences in lamination style in sediments from Saanich Inlet and the Monterey Formation are attributed to variations in the fundamental driving mechanisms of lamina formation. In general, the detrital flux in Saanich Inlet has a significant year-round background component with larger seasonal pulses. This may account for the absence of high bimodality couplets in Saanich Inlet sediments, and it certainly contributed to its bulk detrital enrichment in comparison with the Monterey Formation. One may suggest that near Lompoc in the late Miocene, there was a distinct season of fluvial discharge and detrital sediment supply which did not overlap the season of diatom production and sedimentation, resulting in purer diatomaceous laminae and therefore, higher



(B)

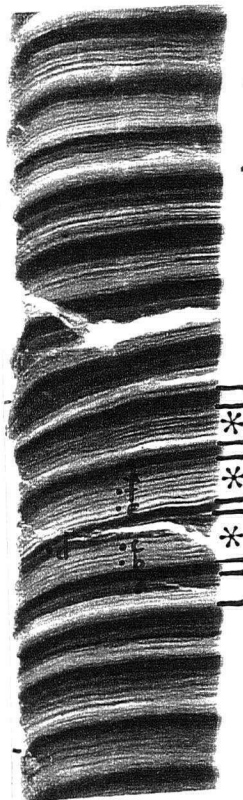


Figure 28. Annual variability and its influence on lamina style. (A) Opal flux at shallow trap at SN0.8. Note three spikes in opal flux in the spring/summer of 1986 (stippled region). These spikes, representing pulsed diatom productivity, may be responsible for the formation of amalgamated opal laminae seen in (B).

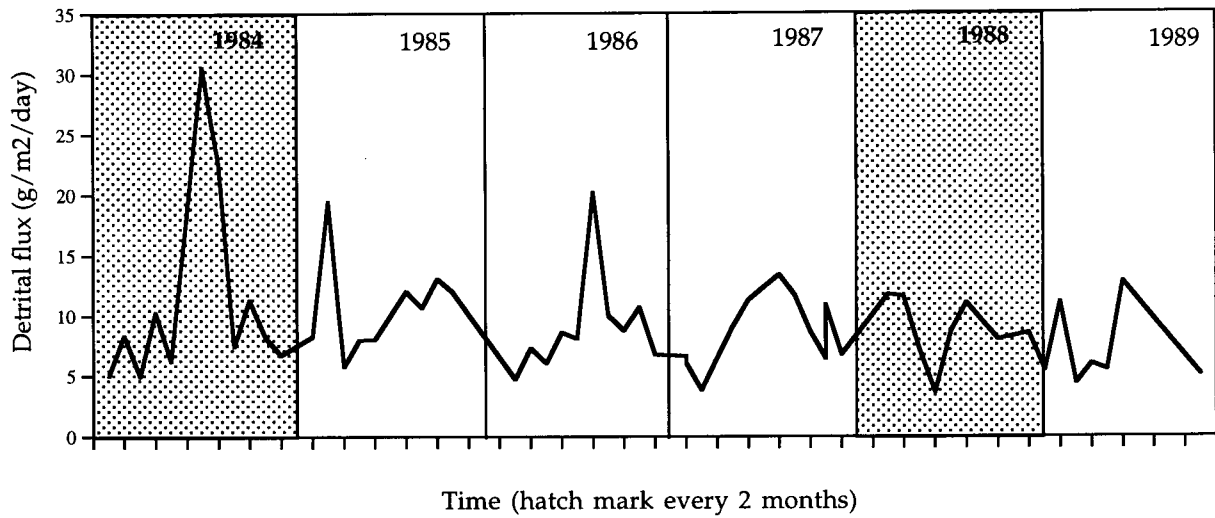


Figure 29. Detrital flux at the deep trap at SI9. Note large spike in flux in 1984, and absence of large increase in detrital flux in 1988. These differences may result in very different lamina expressions. For example, a thicker mud-rich lamina may have been deposited in 1984 relative to the lamina deposited in 1988.

bimodality. Quantifying the relationship of relative seasonality in bimodal laminites is a high priority for future research.

5.3 Carbon and opal cycling recorded in sediments

There is a paradoxical distribution of organic matter in the three settings studied here; Saanich Inlet sediments record highest organic carbon contents in opal-rich laminae and intervals, whereas highest amounts of organic carbon in the Monterey Formation sediments are found in the most detrital-rich and opal-lean laminae and intervals. Santa Barbara Basin sediments have no clear association of organic carbon with opal or detritus. These relationships are counterintuitive and warrant further exploration, particularly the opposite OM distributions in SI and MF sediments.

There is no clear resolution of this problem which is a standing issue in many research laboratories. The discussion that follows moves through alternate hypotheses to explain the organic carbon distributions and associations in Saanich Inlet and the Monterey Formation. The source of the organic matter and processes occurring during settling and sedimentation, shallow burial diagenesis, and processes occurring due to the unroofing and weathering of the sediments are each considered.

5.3.1 Sources of organic matter in MF and SI sediments

A possible explanation for the observed opposite distribution and association of organic matter in Saanich Inlet and the Monterey Formation sediments could involve the input of organic matter from different sources. For example, in MF samples, large amounts of terrigenous organic carbon contemporaneously delivered with clay particles to the continental slope from seasonal runoff events, would result in the production of organic-rich detrital laminae, whereas in SI samples, the OM may be dominated by marine sources, resulting in organic carbon enrichment in the diatomaceous laminae.

Previous studies

The overwhelming consensus in the literature is that the organic matter in the biosiliceous unit of the Monterey Formation is of marine origin based on visual kerogen analyses (e.g. Graham and Williams, 1985), Rock-Eval and elemental composition kerogen typing (e.g. Kablanow and Surdam, 1983; Kruge, 1983), and biomarkers (e.g. King and Claypool, 1983). However, Isaacs (1986) reminds that a significant terrigenous OM input *should* be expected due to the proximity of the Miocene basins (or continental slope) to the shore. Support for this claim comes from Gilbert and Summerhayes (1981) who concluded that up to 20% of the OM in off-shore ODP Miocene sediments was terrestrially-derived, based on organic petrography. Furthermore, Isaacs and Magoon (1984) found approximately 35% terrigenous-sourced OM in samples from the onshore Santa Maria Basin.

Current study

To assess the possibility of a terrigenous source of the OM in MF samples from Lompoc, the geochemical proxies of OM source presented in Table 2 must be considered collectively. The data support a marine origin in both MF and SI sediments; however, consideration must be given to environmental variables which may have affected the organic matter during its formation as well as the potential alteration of these geochemical signals since the formation of the organic matter (DeLange et al., 1994).

C/N ratios and $\delta^{13}C$

The validity of the C/N ratios and $\delta^{13}C$ values indicating marine OM in SI sediments can be assessed with sediment trap data. The accumulation rates of TOC and opal in the surface traps are closely correlated (Figure 30), suggesting the coincident production of these biogenic materials, assumed to be related to diatom productivity.

The C/N ratios of MF samples are larger than what would be expected from organic matter sourced from diatoms (e.g. *Chaetoceros* C/N = 6.6; Parsons et al., 1961), but are lower than reported values for terrigenous OM (>20; Hedges et al., 1986). The possibility of organic matter of mixed

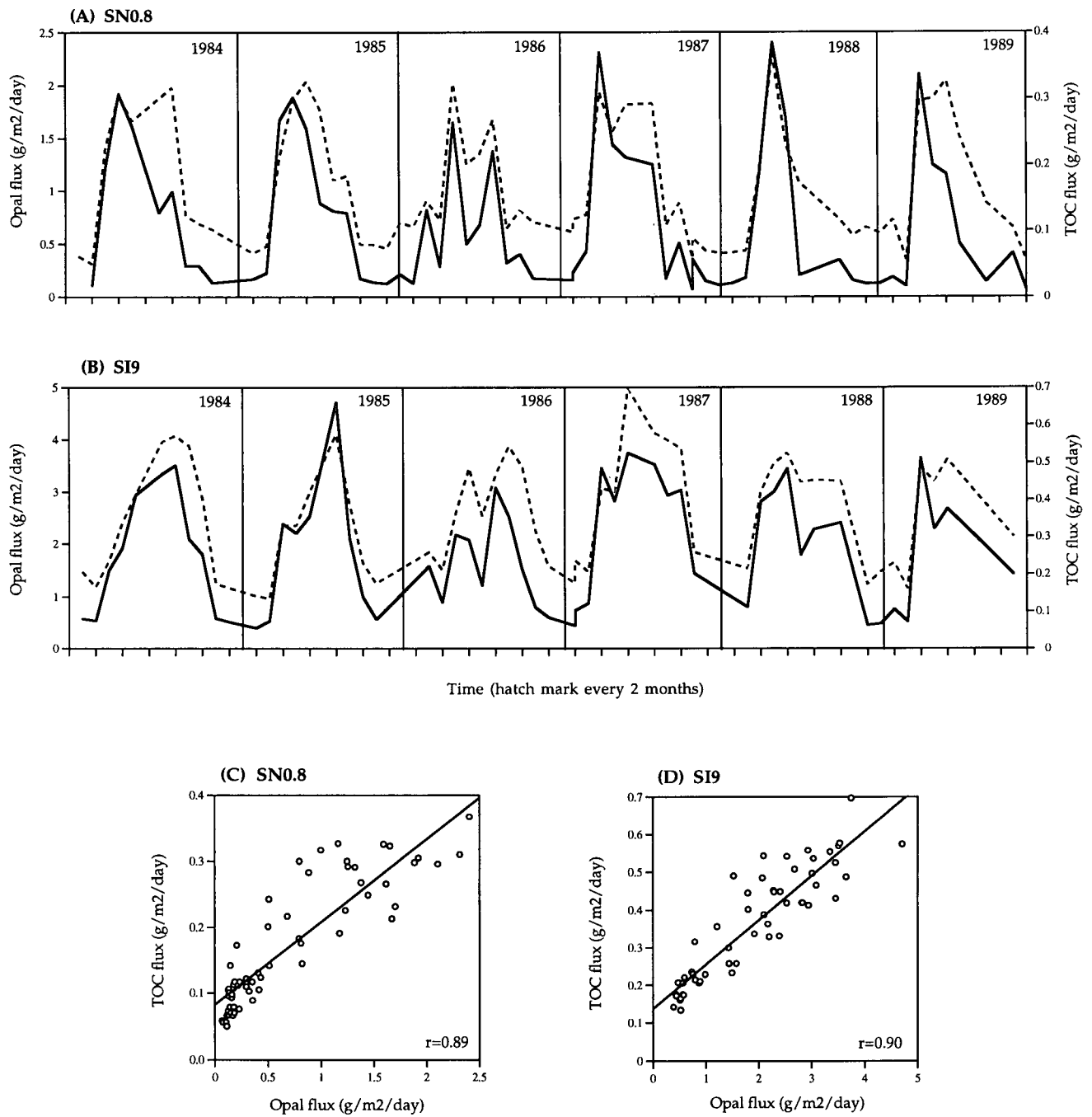


Figure 30. Accumulation rates of opal and TOC in shallow sediment traps. (A) and (B) are time series relationships showing production of opal (solid) and TOC (broken) in phase, whereas (C) and (D) are composite plots of the data in (A) and (B), also showing the parallel trajectories of TOC and opal flux.

marine and terrigenous sources can be assessed by plotting C/N ratios against $\delta^{13}\text{C}$ values (Jasper and Gagosian, 1990; Pedersen et al., 1992). A negative linear relationship between these two signals implies variable mixing (Figure 31a). The absence of a negative linear correlation in the MF samples (Figure 31b) suggests no mixing of marine and terrigenous organic matter.

The presence of inorganic nitrogen (i.e. nitrate) and/or organic nitrogen sorbed onto clays (Müller, 1977) or a significant addition of organic matter with a lower C/N ratio, like bacteria (Bordovskiy, 1965) are two processes that may lower the C/N ratios of organic matter. For either of these to be applicable to the MF samples, a C/N ratio initially high (>20) due to a predominant terrigenous source would be necessary to lower the ratios to those observed. Although there is a possibility for the presence of terrigenous OM, a *predominant* terrigenous source is unlikely (e.g. Garrison and Isaacs, 1981).

If the organic matter was entirely marine in origin, the C/N ratios may have been increased to those measured in MF samples by two processes: 1) reworking or winnowing of the sediments which re-exposes the organic matter to degradation processes (Pedersen et al., 1992) and 2) preferential degradation of nitrogen-rich compounds in the water column (Suess and Müller, 1980; Rosenfeld, 1981) and in the sediments (DeLange et al., 1994; Ganeshram, 1996). The first of these two possibilities can be dismissed due to the finely laminated nature of MF sediments, indicating minimal, if any, reworking. Also, sample 20 (see Appendix I), a speckled bed formed by a sediment gravity flow (Chang, 1998a) records reworking of the sediments, and yet does not have a C/N ratio any higher than the laminated samples. The second scenario, involving the degradation of marine organic matter, is the most likely explanation for the C/N ratios measured in the MF samples.

A marine source of MF organic matter is supported by the $\delta^{13}\text{C}$ data as well. Measured values between -20 and -21‰ are well within the marine OM window (-18 to -22‰; Deines, 1980). However, similar to the C/N ratios, factors occurring after the synthesis of organic matter can affect the original carbon isotopic signal. Most processes result in sedimentary OM that is isotopically lighter than the original. Preferential degradation of labile, marine organic matter (as opposed to terrestrial OM) produces lighter sedimentary OM (Craig, 1953) as does the degradation of organic

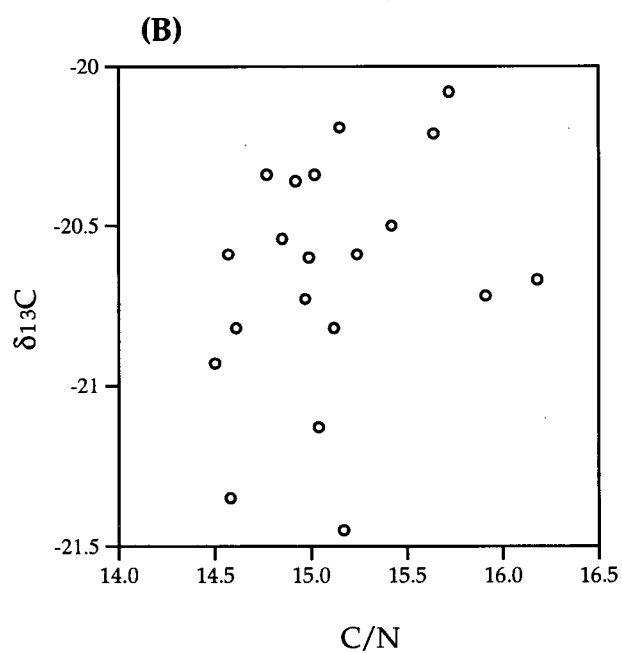
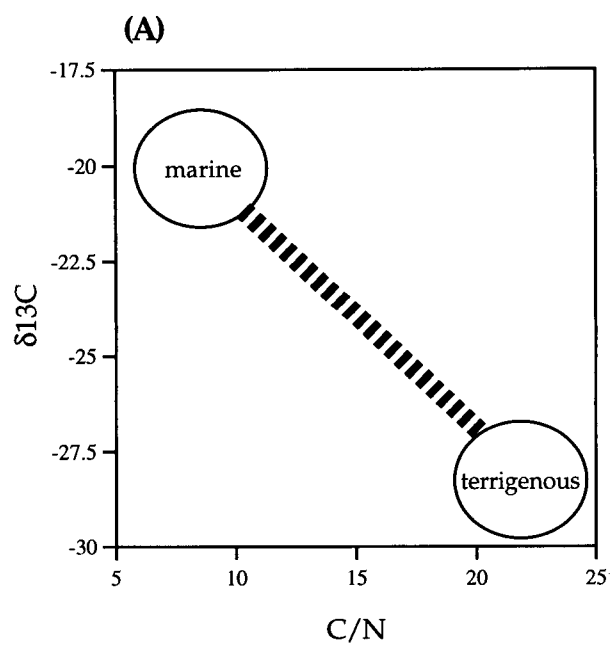


Figure 31. C/N ratios and $\delta^{13}\text{C}$ values. (A) Variable mixing of marine and terrigenous organic material results in data plotting along a regression joining the marine and terrigenous end-member values (Jasper and Gagosian, 1990). (B) MF data; negative linear trend is absent, suggesting that the organic matter is not a mixture of terrigenous and marine sources.

compounds that are isotopically heavy, e.g. proteins and carbohydrates (Degens et al., 1968). Other processes resulting in lighter sedimentary OM include the addition of biomass with a lighter composition (e.g. bacteria with $\delta^{13}\text{C} = -36\text{‰}$; Degens, 1969; Takigiku et al., 1991), oxic diagenesis (De Lange et al., 1994), and subaerial weathering (Van Os et al., 1996). Fontugne and Calvert (1992) concluded that these processes could result in a change no greater than $\sim 2.8\text{‰}$ in the original isotopic signal. If any of these processes affected the OM in MF sediments, the original OM would have had heavier isotopic values, i.e., at the heavy end of the marine window, and further from terrigenous OM values. A process which may increase the $^{13}\text{C}/^{12}\text{C}$ ratio of OM is bioturbation (Takigiku et al., 1991), but there is no evidence for burrowing in the finely-laminated sediments of this study.

The C/N ratios and $\delta^{13}\text{C}$ values of Monterey Formation and Saanich Inlet samples suggest a predominant marine source of organic matter, with no obvious mixing of marine OM with a significant amount of terrigenous OM. The differences in the C/N ratios at the two locations are most likely the result of a shorter water column in Saanich Inlet (200 m vs. 1000 m) as well as the younger age of the sediments which may have collectively contributed to decreased degradational effects. Sediment trap data record slight increases, if any, in the C/N ratios between the shallow and deep traps (Figure 32), and the SI ODP core samples have C/N ratios similar to those of the trapped material (6.1 to 8.9 versus 6.5 to 10.0, respectively).

Kerogen type

The marine nature of the OM present in MF sediments should be supported by the type of kerogen present. The modified van Krevelen diagram of the Rock-Eval pyrolysis results indicated a mixture of types II and III, suggesting marine (phytoplankton, zooplankton, and bacteria) and higher land plants as probable contributing sources (Tissot and Welte, 1984).

Some problems arise when using hydrogen and oxygen indices for characterizing kerogen types: organic matter may be adsorbed onto the rock matrix, altering the S2 peak and therefore the HI (Peters, 1986) and CO_2 may be evolved from carbonates, therefore altering the S3 peak and the OI (Katz, 1983). Because of these problems, kerogen types determined from a modified van Krevelen

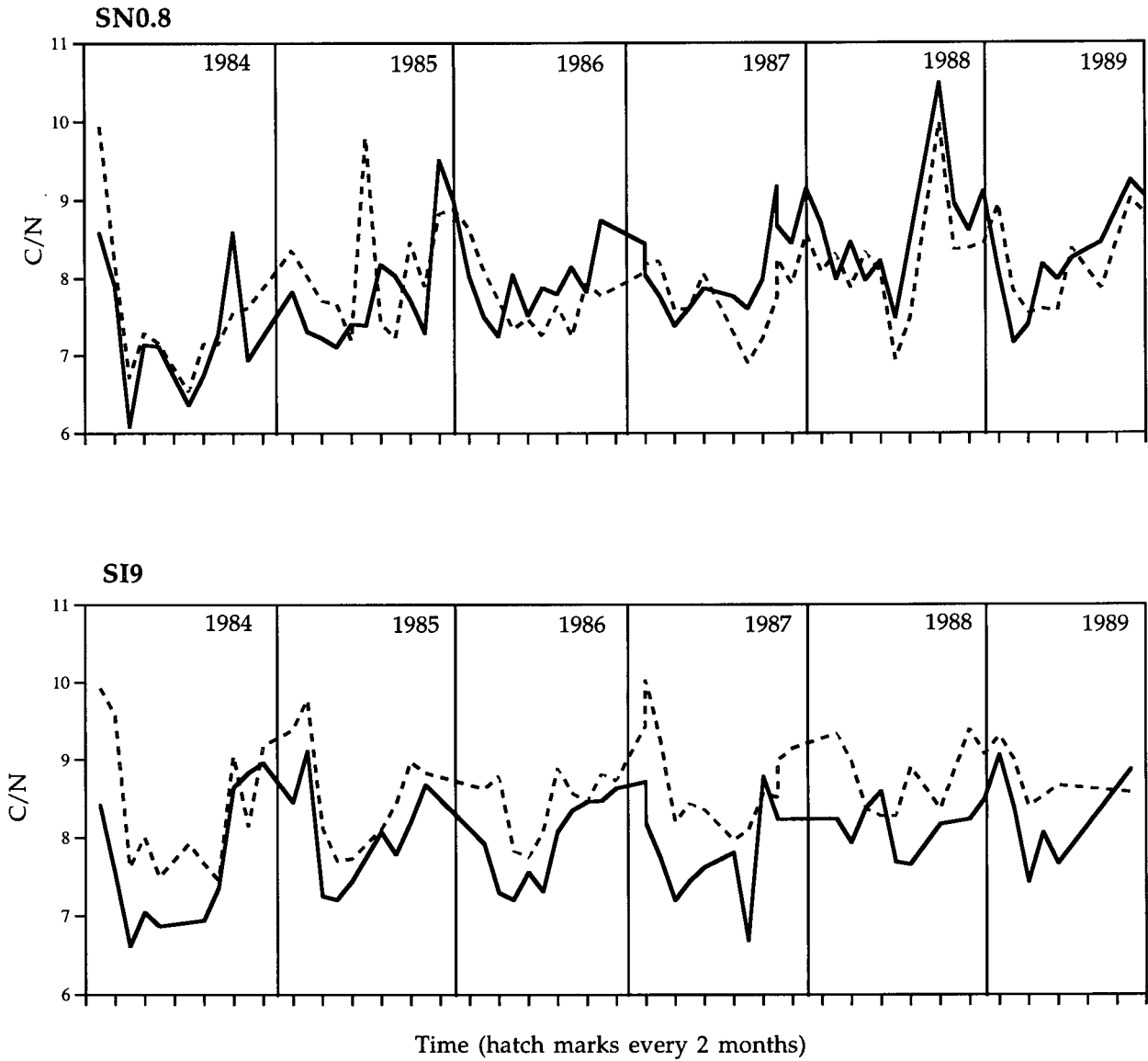


Figure 32. Comparison of C/N ratios in shallow (solid) and deep (broken) Saanich Inlet sediment traps. SN0.8 shows no consistent increase in ratio with depth, whereas SI9 does show a consistent increase in ratio from shallow to deep. These increases may be attributed to degradation of OM in the water column or to the addition of laterally-advected material with higher C/N ratios.

diagram (OI vs. HI) may be misleading. To assess and correct for adsorbed organic compounds and inorganic CO₂, a plot of %TOC versus S₂ can be made (Langford and Blanc-Valleron, 1990). The boundaries separating the kerogen types can be delineated on this plot, eliminating the need for S₃ and the possible associated problems, whereas adsorption by the rock matrix can be detected by a negative y-intercept.

Figure 33 shows this plot for MF samples. The MF data points fall within the type II field, indicating marine OM. The y-intercept is only slightly negative, indicating a small matrix effect (adsorption of pyrolytic organic compounds onto clay minerals), and therefore a potential alteration of the hydrogen index values. A single regression describing the MF data indicates that the OM present is of a similar type and quality. The average matrix-corrected HI value of these samples is calculated by multiplying the slope of the regression by 100. This results in a corrected average HI of 353, compared to the uncorrected average of 336 (<5% difference).

The different kerogen types obtained from the TOC/S₂ plot and the modified van Krevelen diagram (type II versus mixture of types II and III, respectively) are attributable to the way the kerogen type boundaries are determined, and not to any adsorption of pyrolytic organic compounds or inorganic CO₂. On the OI/HI plot, the lines separating types I, II and III represent maturation pathways of the different kerogen types; actual kerogen types may be more accurately represented by broad bands around the pathways (Peters, 1986).

5.3.2 Settling and sedimentation

The organic material found in both Saanich Inlet and Monterey Formation sediments appears to be of a marine origin. Therefore a fundamental difference in source cannot explain the opposite association of organic matter with opal at these two locations.

Four mechanisms occurring during settling and sedimentation may have contributed to the observed distribution of organic matter in Monterey Formation samples: (1) grain size and surface area may have influenced organic matter distribution; (2) OM may have been incorporated into fecal pellets; (3) marine OM may have been preferentially degraded in the water column and/or at the

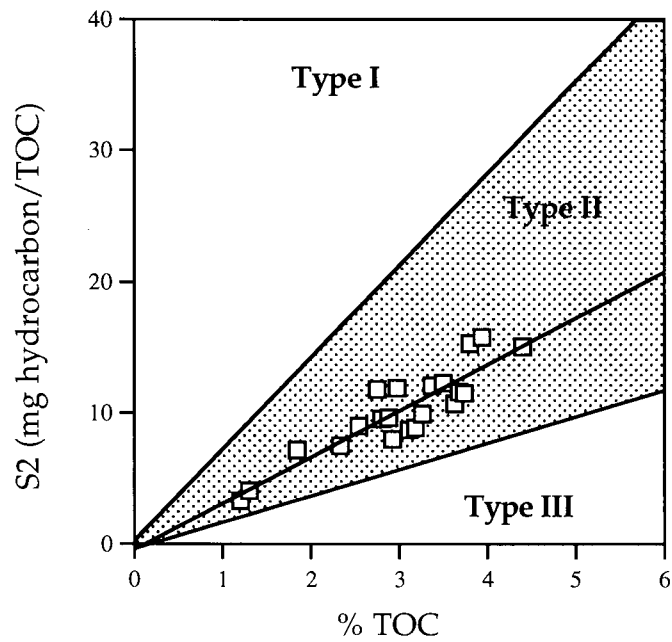


Figure 33. MF TOC versus S2. Kerogen type boundaries described by a slope of 7 for I/II and a slope of 2 for II/III (Langford and Blanc-Valleron, 1990). All points fall within the type II kerogen field, suggesting a marine OM source. The data can be described by a single regression, indicating a similar OM source in all samples analyzed. An intercept near the origin implies little matrix affect on the hydrogen index.

sediment-water interface; and (4) OM may have been diluted by opal.

Grain size and surface area

Trask (1955) observed twice as much organic matter in clays than silts, and a four-fold increase in TOC content in clays over that in fine sands. Similar associations of TOC with the finer sediment fraction have been observed in many coastal environments (e.g. Premuzic et al., 1982; Shimmiel et al., 1990; Calvert et al., 1995). One explanation that has been proposed for this relationship is the hydrodynamic equivalence of organic and clay particles (Tyson, 1987). The second explanation involves sorption of organic matter onto mineral surfaces where it becomes stabilized against microbial attack. Keil et al. (1994) showed that the irreversible sorption of OM to mineral surfaces slows remineralization rates by up to five orders of magnitude, and Mayer (1994) refined this model to show that sorption of OM into mineral mesopores (<10 nm wide) restricts the access of enzymes necessary for biodegradation.

Titanium is an element which is almost exclusively associated with the coarse fraction of a sediment and can therefore be used as a proxy of grain size (Calvert, 1976). In MF sediments, this can be shown in the relationship of Ti and opal (Figure 34a). Diatom frustules and fragments, abundant in the opal-rich laminae, are generally silt-sized, whereas the mud-rich laminae contain abundant clay-sized particles. Thus, the positive linear correlation ($r=0.84$) seen in Figure 34a is expected. Figure 34b shows the relationship between TOC and Ti; they are inversely and linearly correlated ($r=-0.79$). This suggests that TOC is preferentially associated with the finer fraction. Whether this association is depositional or diagenetic remains to be determined.

In SI sediments, the Ti/Al ratio is not significantly correlated with either opal or TOC (Figure 35), suggesting no grain-size control on the distribution of these materials.

Fecal pellets

Grazing by zooplankton is associated with respiration of some of the OM and maceration of diatom frustules (Grimm et al., 1996). Therefore, grazing activity and fecal pellet production could

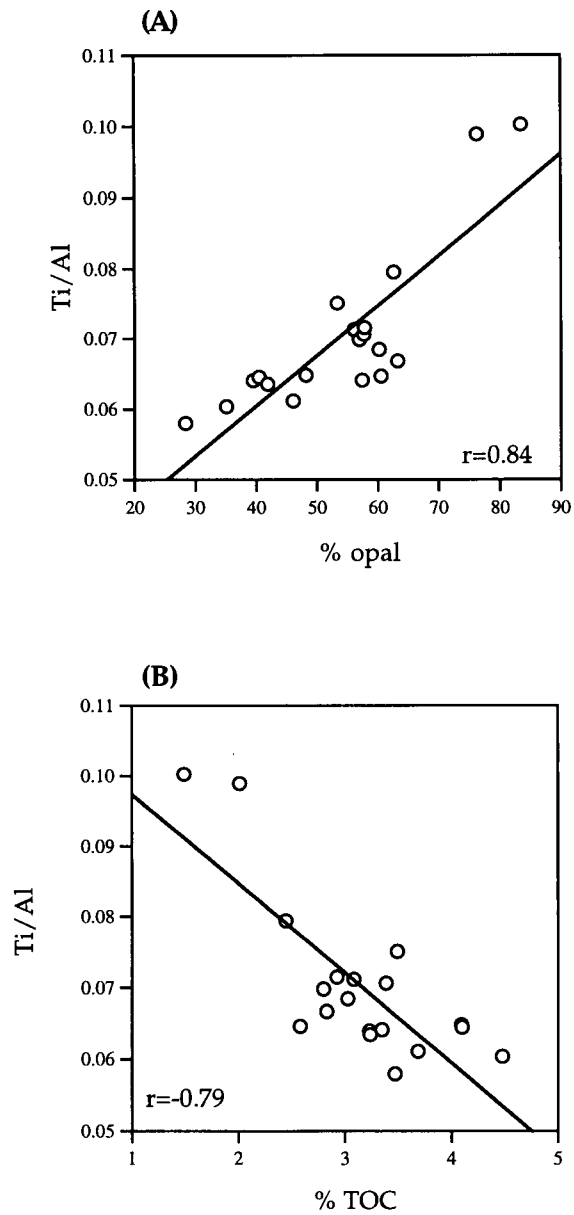


Figure 34. MF grain-size influences on the distribution of opal and organic matter. (A) MF opal versus Ti/Al ratio. Positive linear correlation indicates association of opal with the coarser sediment fraction. (B) MF TOC versus Ti/Al ratio. Negative linear correlation suggests that organic matter is associated with the finer fraction.

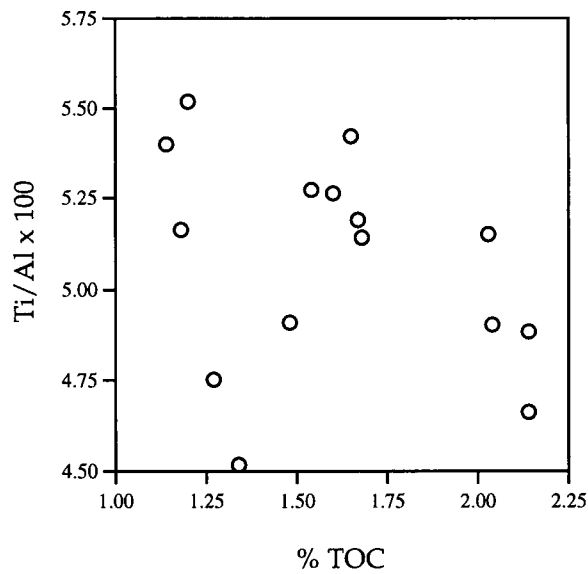
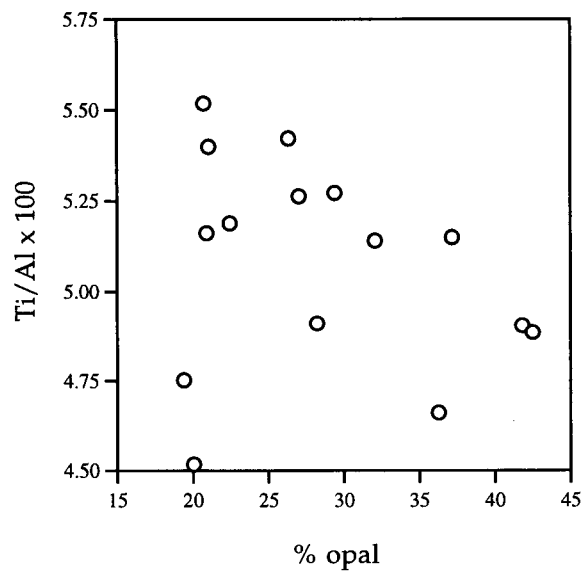


Figure 35. Saanich Inlet Ti/Al ratios ($\times 100$) versus weight percent opal and TOC. No correlations are evident, suggesting no grain-size control on the distribution of either opal or organic matter. This is in contrast to the MF results (see Figure 34).

potentially affect the OM and opal reaching the sediments. Fecal pellets of zooplankton and other grazers are large, fast-sinking particles that are important contributors to the sediment flux in some upwelling-influenced coastal regions (e.g. Santa Barbara Basin, Dunbar and Berger, 1981). Fecal pellets have a protective organic membrane that inhibits silica dissolution and organic matter degradation (Schrader, 1971) and hence are important vehicles for the delivery of these biogenic materials to the sea floor. Indeed, fecal pellets have been found to contain whole and fragmented calcareous and siliceous tests, organic matter, and detritus (e.g. Dunbar and Berger, 1981; Sancetta, 1989).

The effect of fecal pellets on OM distribution in MF sediments is difficult to estimate; no pellets were observed in the collected samples. Micro-scale analyses of lamina constituents did show more highly fragmented diatom debris in mud-rich intervals compared to opal-rich intervals (Chang, 1998b). This is most likely a grazing artifact although dissolution and/or mechanical breakage during settling and/or tractional movement might also play a role in the fragmentation of diatoms.

Preferential degradation of marine organic matter

The observed distribution of organic matter in the Monterey Formation could be explained if both marine and terrigenous organic matter were supplied to the depositional environment (marine in spring/summer, terrigenous in fall/winter), but the marine OM was preferentially degraded, producing a larger gradient between marine and terrigenous OM content. Marine organic matter is more labile than terrestrial organic matter; marine organisms are protein- and lipid-rich and therefore are of high energy value to heterotrophs, whereas terrestrial plants are rich in lignin and cellulose, compounds that possess lower nutritional value to heterotrophs and are less easily degraded (DeLange et al., 1994; Moore, 1969).

The formation of organic matter in the euphotic zone, accompanying the precipitation of siliceous tests during periods of diatom productivity in the spring and summer would presumably result in the deposition of an opal- and organic-rich lamina. However, microbial degradation of this marine-derived organic matter in either the water column or at the sediment-water interface would

produce an opal-rich lamina with low concentrations of TOC. The delivery of terrestrial organic matter via fluvial or eolian processes that are enhanced in the fall and winter, would result in the deposition of an organic-rich, detrital lamina. This OM is less labile than the marine OM, and could therefore be preferentially preserved.

In general terms, this scenario is consistent with the distribution of OM in Monterey Formation sediments. If this were the cause of the distribution however, OM in mud-rich laminae would have a strong terrigenous signal (light carbon isotopes, high C/N ratios, type III kerogen). As discussed above, such a strong terrigenous signal is absent. Also, if the preferential degradation of marine OM and the preferential preservation of terrigenous OM were responsible for the observed distribution and association of organic matter, the OM in the opal- and mud-rich intervals would possess different characteristics.

To assess this possibility, C/N ratios, $\delta^{13}\text{C}$ values, and HI values can be plotted versus percent opal or detritus; if the type of OM is different in the mud- and opal-rich intervals, trends will be evident. Figure 36 shows these relationships. Lack of significant trends suggests that the OM is similar in all the samples. Therefore, the preferential degradation of marine organic matter and preferential preservation of terrigenous OM cannot explain the observed distribution of OM in Monterey Formation samples.

Dilution of organic matter by opal

The concentration of organic matter in marine sediments is dependent on the amount of OM delivered to the sediments as well as the supply rates of other components such as carbonate, opal, and detritus (Calvert and Price, 1983; Tissot and Welte, 1984; Paropkari et al., 1992). A positive correlation between sedimentation rate and percent TOC has been shown in several marine settings (e.g. Müller and Suess, 1979), but at high sedimentation rates, this relationship deteriorates and actually causes an inverse correlation due to dilution (Ibach, 1982; Emerson, 1985). Dilution of organic matter by opal is complemented by the reduced dissolution of opal with higher opal accumulation rates; increased delivery of opal to the sediments saturates the pore waters with respect

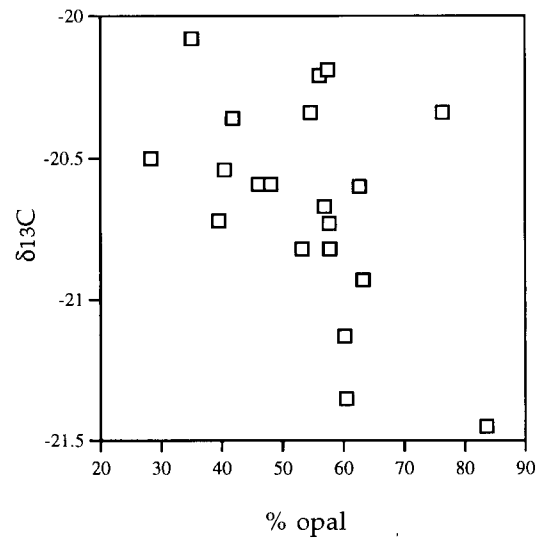
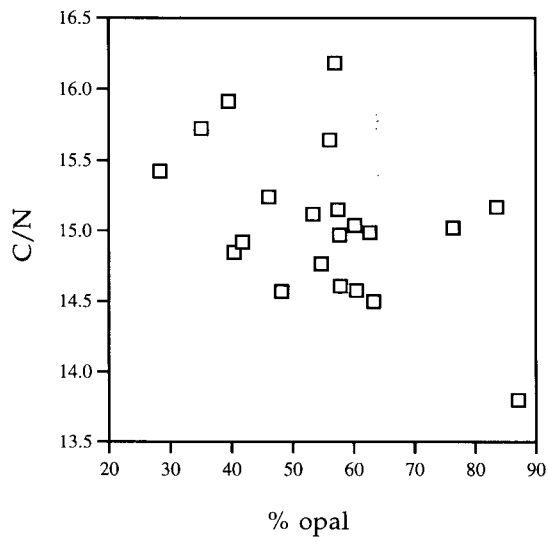


Figure 36. MF opal content versus C/N ratios and $\delta^{13}\text{C}$ values. No trends are evident, suggesting that the organic matter in all samples (mud-rich and opal-rich) are of a similar source.

to silica more quickly, resulting in increased opal burial (Archer et al., 1993).

Isaacs (1987) postulated dilution as a candidate for explaining the observed OM distribution in the Monterey Formation and supported it with the following data from two Monterey samples: sample 1 has 76% opal, 3.4% TOC, a silica accumulation rate (AR) of 11 mg/cm²/year, and an OM AR of 0.5 mg/cm²/year; sample 2 has 32% opal, 6.4% TOC, a silica AR of 1.6 mg/cm²/year, and an OM AR of 0.3 mg/cm²/year. Despite a slightly higher accumulation rate of organic matter in sample 1, the percent TOC is half that of sample 2 due to the seven-fold higher silica accumulation rate which diluted the organic matter in that sample.

McDonald (1997) similarly reported lower TOC in two bands of diatom ooze relative to the surrounding muddy sediments in the subarctic east Pacific. ²³⁰Th data show a quadrupling of the sedimentation rate in these diatomaceous bands. Although the OM was rapidly deposited, the concomitant rapid opal deposition diluted the OM content of the sediments.

Accumulation rates are required to assess the influence of dilution on controlling the OM concentration in the MF sediments. Although dilution cannot be determined definitively with the data on hand, the extremely high opal contents of some laminae and intervals (up to 86%) suggest that this process is a possible factor controlling the OM distribution in the MF.

5.3.3 Shallow burial diagenesis

It is possible that the coupling of opal and carbon, if in fact it was present in the euphotic zone and during settling and sedimentation, was destroyed during shallow burial diagenesis. Mud-rich and opal-rich laminae have inherently different porosities. Porosity and bulk density of MF diatomites are related to the composition; opal-rich intervals possess a higher porosity and lower density compared to mud-rich intervals (Isaacs, 1981). The relative bulk densities of individual laminae from these Monterey samples are known from x-radiograph prints which show that mud-rich laminae are more dense than opal-rich laminae. Porosity logs from a well drilled in the Monterey Formation show that muddy intervals are also less porous than diatomaceous intervals

(unpublished data from Nuevo Energy).

These differences in porosity may affect the distribution of organic matter during diagenesis via two processes: (1) organic matter may have migrated out of the more porous, diatomaceous laminae into the detritus-rich laminae where they were "trapped" either by adsorption onto clay minerals or by the low porosity; or (2) the greater porosity of the opal-rich laminae may have permitted enhanced respiration of the OM via enhanced circulation of oxidants (Moore, 1969; Schrader and Sorknes, 1991). These factors may have operated at very shallow burial depths, during burial diagenesis, or during unroofing and surface weathering.

The controls that post-depositional/diagenetic processes had on Monterey Formation OM distribution are difficult to determine with the available data. Examination of the organic carbon distribution in very shallowly-buried laminated diatomaceous sediments of modern environments can be employed to explore the pre-diagenetic signal.

The Guaymas Basin and slope in the Gulf of California is a region where laminated diatomaceous and organic-rich sediments are currently being deposited (Curry, Moore, et al., 1982). Laminae analyses from a shallow core sample (30 to 50 cm deep), by Donegan and Schrader (1981) revealed similar laminae compositions to MF samples; the light colored laminae contained 80-90% diatoms, 5-10% terrigenous detritus, and 5-10% organic matter, whereas the darker laminae contained 60-75% diatoms, 15-25% terrigenous detritus, and 10-15% organic matter. Sediment trap data from the Guaymas Basin does not corroborate the results of the lamina analyses by Donegan and Schrader (1981). Thunell et al. (1994) show that opal and organic carbon fluxes are coupled in deep traps in the Guaymas Basin (and therefore presumably upon delivery to the sediments). The decoupling of the opal and OM may therefore be attributed to dilution by high opal content or preferential degradation at the sediment/water interface.

These data suggest that shallow burial diagenesis was not responsible for the distribution of organic matter. However, Patience et al. (1990) attributed the higher organic carbon content of detritus-rich laminae relative to opal-rich laminae in sediments off Peru was attributed to the preferential bacterial oxidation of organic matter in the opal-rich laminae due to their higher porosity.

5.3.4 Unroofing

The Monterey Formation exposed at the Celite quarry has been emergent since the late Pleistocene (Ingle, 1981b). Active mining within the quarry further exposes the sediments to subaerial processes. Weathering and oxidation of the formation are enhanced under these conditions and many studies have shown that weathering can alter the quality and quantity of organic matter (e.g. Van Os et al., 1996; Clayton and Swetland, 1978; Littke et al., 1991; Leythaeuser, 1973), in some areas reducing TOC by up to 70%. If processes occurring after uplift and exposure are responsible for the OM distribution in the Monterey Formation, then weathering and oxidation must attack the OM in the opal-rich intervals at a faster rate than the OM in the mud-rich intervals. The differences in porosity and density of the opal- and mud-rich laminae mentioned previously could cause a redistribution or increased oxidation of OM via enhanced efficiency in the supply of oxidants.

If post-uplift alteration and outcrop exposure of the MF was responsible for the OM distribution, then non-exposed MF would show the opposite trend—TOC correlated with opal. This does not appear to be the case, however. More deeply buried MF stratigraphies record the association of OM with detrital-rich, not opal-rich, intervals (Isaacs, personal communication), similar to the surficial outcrop samples. Isaacs' assertion strongly suggests that unroofing and the subsequent weathering processes are not primarily responsible for the organic matter distribution in the Monterey Formation.

The data are insufficient to support a definitive conclusion regarding the fundamental problem of OM abundance and distribution in opal- and mud-rich laminae. To enable the resolution of the paradoxical distribution of organic matter in Saanich Inlet and Monterey Formation sediments, larger available sample sizes are needed to permit lamina-scale sampling. Also, analyses performed on unweathered diatomites would remove the possible effects of subaerial exposure on OM distribution. Furthermore, knowledge of accumulation rates may clear up uncertainties regarding flux verses weight percent and the resulting possibility of a dilution artifact.

6. CLOSING STATEMENTS

6.1 Summary and conclusions

Finely-laminated, organic- and opal-rich sediments from Saanich Inlet, British Columbia, the Santa Barbara Basin, California, and the Miocene Monterey Formation of Santa Barbara County, California were analyzed using multi-tracer geochemical analyses on individual laminae and groups of laminae. The goal of this study was to investigate the environmental controls on sediment composition and fabric and to explore the link between the biogeochemical cycling of organic carbon and opal. The results of this study are summarized below:

(1) The bulk compositions of the MF, SI and SBB are generally similar in that they each have significant amounts of opal, detritus, and organic matter; SBB sediments additionally contain appreciable carbonate. The TOC, opal, and detritus ranges overlap in SI and SBB samples, and contain significantly lower amounts of opal compared to the MF. The detrital content is much higher at these two locations compared to the MF due to their relative proximity to land and the presence of point-source, high discharge, fluvial events in these areas.

(2) The sediments at all three locations comprise relatively opal-rich and detrital-rich laminae. The formation of the laminae is controlled by episodic, likely seasonal, delivery of sediments. In Saanich Inlet, detritus is supplied nearly year-round, but seasonally pulsed production and sedimentation of opal produces a relatively opal-rich lamina in the spring and summer. The presence of diatom layers attributable to blooms and mats (Chang, 1998b) suggests that pulsed inputs of opal contributed to lamina formation in the Monterey Formation as well.

(3) Geochemical proxies of organic matter source (C/N ratios, $\delta^{13}\text{C}$ of organic matter, and kerogen type) indicate that marine organic matter predominates over terrigenous.

(4) In Saanich Inlet, TOC and opal have a positive, linear correlation whereas in Monterey Formation samples, there is a negative, linear relationship. In Santa Barbara Basin samples, there is no clear relationship between these variables. The contrasting trends in distribution observed in SI and MF samples are most likely due to the dilution of the organic matter in MF samples by high opal

flux, and/or by the redistribution and/or oxidation of the organic matter in diatomaceous laminae via diagenetic and/or weathering processes.

(5) Linking biogeochemical cycling of opal and organic carbon to discrete laminae could not be accomplished. In Saanich Inlet sediments, incongruities between geochemical data and x-radiograph representation of individual laminae suggest third-party sampling errors, compromising the reliability of the lamina-scale data set. In the Monterey Formation, the observed decoupling of opal and organic carbon contents renders this a problematic relationship to interpret.

6.2 Suggestions for future work

At the onset, geochemical analyses of individual laminae were intended to reveal a high-resolution geochemical record of discrete sedimentary events. The characteristic signatures of each lamina type would enable the reconstruction of changes in the biogeochemical cycling of organic carbon and opal. However, available sample volumes from ODP cores in Saanich Inlet were not sufficient to permit multi-tracer analyses. Monterey Formation laminae are extremely fine, making it difficult or impossible to extract uncontaminated, lamina-scale samples. Consequently, most samples spanned couplets, packets, and bundles, rather than individual laminae.

Other items that made this project difficult include uncertainties regarding the weathering history of outcrop samples, and potential third-party sampling errors. For others attempting similar projects, I make the following recommendations:

- (1) Select a location where weathering, and subsequent alteration, are not a problem. For example, core from the Monterey Formation deep within the opal-A zone that had not experienced hydrocarbon migration in or out the formation would be appropriate, as would the selection of another ODP site where diatomaceous, laminated sediments have been deposited and preserved. Resampling of selected intervals from the Saanich Inlet core might also be profitable, if larger volumes could be taken.
- (2) Collect a large enough sample to provide adequate mass of individual laminae for multi-tracer analyses, including: CNS, coulometry, opal, Rock-Eval, stable carbon isotopes, major

element abundances via XRF. At least 600 mg (preferably one gram) of sediment would be required for these analyses; an additional one gram of sediment would be needed if minor elements were to be determined. In this study, SI slab samples of the ODP core measured 20 x 1 x 2 cm. Individual laminae extracted from this slab provided masses between 200 and 400 mg (depending on relative opal versus detrital content). Therefore, two or three times more sample would be required to complete the necessary analyses. Slab samples taken in pairs or in triplicate that span the same stratigraphic interval would provide the required sample mass.

(3) Perform optical microscopy analyses on the entire section and note the locations of obvious blooms, highly fragmented diatom debris, and pure detrital laminae. Select laminae for geochemical analyses based on these results. This sequential, rather than coincident approach to coupling paleontological, sedimentological and geochemical analyses permits the identification of discrete genetic properties of lamina types prior to the selection of samples and the specific analyses to be used to test specific hypotheses involving those lamina types.

(4) Resolving the paradox of opal and organic carbon coupling/decoupling requires the determination of accumulation rates, to enable the comparison of opal and organic carbon fluxes. In ancient sediments, this could be accomplished by assuming the laminae are true varves (i.e. annual couplets) and coupling the varve counts with porosity, density, and compaction parameters. A more reliable approach to resolving the organic matter distribution patterns is the calculation of accumulation rates from two precisely-known age horizons in box cores—the sediment/water interface and a key horizon deeper within the sediments (e.g. a prominent shell layer (e.g. Schimmelmann et al., 1990) or an anthropogenic wood chip layer (e.g. Collins, 1997)).

REFERENCES

- Algeo, T.J., Phillips M., Jaminski, J., and Fenwick, M., 1994. High-resolution x-radiography of laminated sediment cores. *Journal of Sedimentary Research*, A64, p. 665.
- Archer, D., Lyle, M., Rodgers, K., and Froelich, P., 1993. What controls opal preservation in tropical deep-sea sediments? *Paleoceanography*, 8, p. 7-21.
- Barron, J.A., 1975. Marine diatom biostratigraphy of the upper Miocene-lower Pliocene strata of southern California, *J. Paleontol.*, 49, pp. 619-632.
- Barron, J.A. and Baldauf, J.G., 1989. Tertiary cooling steps and paleoproductivity as reflected by diatoms and biosiliceous sediments, *In: Productivity of the oceans: present and past*, (Berger, W.H., Smetacek, V.S., and Wefer, G., eds.). John Wiley and Sons, pp. 341-354.
- Behl, R. and Kennett, J.P., 1996. Brief interstadial events in the Santa Barbara Basin, NE Pacific, during the past 60kyr. *Nature*, 379, p. 243-246.
- Bordovskiy, O.K., 1965. Sources of organic matter in marine basins. *Marine Geology*, 3, p. 5-31.
- Bornhold, B.D., Firth, J.V. et al., 1997. Proceedings of the Ocean Drilling Program, Initial Reports, vol. 169S.
- Brodie, I. and Kemp, A.E.S., 1994. Variation in biogenic and detrital fluxes and formation of laminae in late Quaternary sediments from the Peruvian coastal upwelling zone, *Marine Geology*, 116, p. 385-398.
- Bull, D. and Kemp, A.E.S., 1996. Composition and origins of laminae in late Quaternary and Holocene sediments from the Santa Barbara Basin, *In: Palaeoclimatology and Palaeoceanography from Laminated Sediments*, (ed. A.E.S. Kemp), Geological Society Special Publication No. 116.
- Calvert, S.E., 1966. Origin of diatom-rich, varved sediments from the Gulf of California, *Journal of Geology*, 74, pp. 546-564.
- Calvert, S.E., 1990. Geochemistry and origin of the Holocene sapropel in the Black Sea, *In: Facets of modern biogeochemistry* (Ittekkot, V., Kempe, S., Michalis, W., and Spitzzy, A., eds.), Springer-Verlag, pp. 326-352.
- Calvert, S.E. and Price, N.B., 1983. Geochemistry of Namibian Shelf sediments, *In: Coastal Upwelling: Its sedimentary record*, Part A (Suess, E. and Thiede, J., eds.), Plenum, p. 337-375.
- Calvert, S.E., Pedersen, T.F., and Naidu, P.D., 1995. On the organic carbon maximum on the continental slope of the eastern Arabian Sea, *Journal of Marine Research*, 53, p. 269-296.
- Calvert, S.E., 1976. The mineralogy and geochemistry of near-shore sediments, *In: Chemical Oceanography* (Riley, J.P. and Chester, R., eds.), Academic Press, p.187-279.
- Chang, A.S., 1997. Sedimentary processes and paleoenvironmental significance of laminated diatomaceous sediments from the Miocene Monterey Formation, California, USA, unpublished M.Sc. thesis, University of British Columbia.
- Chang, A.S., 1998a. Speckled beds: Distinctive gravity-flow deposits in finely-laminated diatomaceous sediments, Miocene Monterey Formation, California, *Journal of Sedimentary Research*, in

review.

Chang, A.S., 1998b. Diatomaceous sediments from the Miocene Monterey Formation, California: A lamina-scale investigation of biological, ecological, and sedimentological processes, *Palaios*, in review.

Clayton, J.L. and Swetland, P.J., 1978. Subaerial weathering of sedimentary organic matter, *Geochimica et Cosmochimica Acta*, 42, p. 305-312.

Collins, A.D., 1997. Interannual variability of laminated sediment and its relationship to climate, Saanich Inlet, B.C., unpublished M.Sc. thesis, University of Victoria.

Craig, H., 1953. The geochemistry of the stable carbon isotopes. *Geochimica et Cosmochimica Acta*, 3, p.53.

Curry, J.R., Moore, D.G. et al., 1982. Initial Reports of the Deep Sea Drilling Project, 64: Washington (U.S. Gov't Printing Office).

Degens, E.T., 1969. Biogeochemistry of stable carbon isotopes. *In: Organic Geochemistry: Methods and Results* (Eglinton, G. and Murphy, M.T.J., eds.), Springer-Verlag.

Degens, E.T., Behrendt, M., Gotthardt, B., and Reppmann, E., 1968. Metabolic fractionation of carbon isotopes in marine plankton--II. data on samples collected off the coasts of Peru and Ecuador. *Deep-Sea Research*, 15, p.11.

Deines, P., 1980. The isotopic composition of reduced organic carbon, *In: Handbook of Environmental Isotope Geochemistry* (Fritz, P. and Fontes, J.Ch., eds), Elsevier, p.329-406.

DeLange, G.J., Van Os, B., Pruyssers, P.A., Middelburg, J.J., Castradori, D., Van Santvoort, P., Muller, P.J., Eggenkamp, H., and Prahl, F.G., 1994. Possible early diagenetic alteration of palaeo proxies, *In: Carbon cycling in the glacial ocean: constraints on the ocean's role in global change* (Zahn, R. et al., eds.), Springer-Verlag.

Donegan, D. and Schrader, H., 1981. Modern analogs of the Miocene diatomaceous Monterey shale of California: evidence from sedimentologic and micropaleontologic study, *In: The Monterey Formation and related siliceous rocks of California* (Garrison, R.E., Douglas, R.G., Pisciotto, K.E., Isaacs, C.M., and Ingle, J.C., eds.), Pacific Section SEPM, p. 149-157.

Dunbar, R.B. and Berger, W.H., 1981. Fecal pellet flux to modern bottom sediments of Santa Barbara Basin (California) based on sediment trapping, *GSA Bulletin*, part I, 92, p.212-218.

Emerson, S., 1985. Organic carbon preservation in marine sediments, *In: The carbon cycle and atmospheric CO₂: natural variations Archean to present* (Sundquist, E.T., and Broecker, W.S., eds.), Geophys. Monograph Series, vol. 32, AGU, p.78-87.

Emerson, S. and Hedges, J.I., 1988. Processes controlling the organic carbon content of open ocean sediments, *Paleoceanography*, 3, p. 621-634.

Engleman, E.E., Jackson, L.L., and Norton, D.R., 1985. Determination of carbonate carbon in geological materials by coulometric titration. *Chemical Geology*, 53, p. 125.

Espitalie, J., Madec, M., and Tissot, B., 1977. Source rock characterization method for petroleum exploration, *Proceedings of the Offshore Technology Conference*, pp. 439-442.

Farrell, J.W., Pedersen, T.F., Calvert, S.E., and Nielsen, B., 1995. Glacial-interglacial changes in

nutrient utilization in the equatorial Pacific Ocean, *Nature*, 377, pp. 514-517.

Fontugne, M.R. and Calvert, S.E., 1992. Late Pleistocene variability of the carbon isotopic composition of organic matter in the eastern Mediterranean: monitor of changes in carbon sources and atmospheric CO₂ concentrations, *Paleoceanography*, 7, p.1-20.

Fontugne, M.R. and Duplessy, J.-C., 1981. Organic carbon isotopic fractionation by marine plankton in the temperature range -1 to 31°C. *Oceanologica Acta*, 4, p.85-90/

Francois, R., 1987. Some aspects of the geochemistry of sulphur and iodine in marine humic substances and transition metal enrichment in anoxic sediments. Unpublished Ph.D. thesis, University of British Columbia.

Francois, R., 1988. A study on the regulation of the concentrations of some trace metals (Rb, Sr, Zn, Pb, Cu, V, Cr, Ni, Mn and Mo) in Saanich Inlet, British Columbia, Canada, *Marine Geology*, 83, pp. 285-308.

Freeman, K.H., and Hayes, J.M., 1992. Fractionation of carbon isotopes by phytoplankton and estimates of ancient CO₂ levels, *Global Biogeochemical Cycles*, 6, p.185-198.,

Ganeshram, R.S., 1996. On the glacial-interglacial variability of upwelling, carbon burial and denitrification on the northwestern Mexican continental margin, unpublished Ph.D. thesis, University of British Columbia.

Gardner, J.V., and Dartnell, P., 1995. Centennial-scale late Quaternary stratigraphies of carbonate and organic carbon from Santa Barbara Basin, hole 893A, and their paleoceanographic significance, *In: Proceedings of the Ocean Drilling Program, Scientific Results* (Kennett, J.P., Baldauf, J.G. and Lyle, M., eds.), vol. 146, part 2, pp. 103-124.

Gilbert, D. and Summerhayes, C.P., 1981. Distribution of organic matter in sediments along the Californian continental margin, *In: Initial Reports of the Deep Sea Drilling Program* (Yeats, R.S., Haq, B.U., et al., eds.), vol. 63, pp. 757-761.

Govean, F.M. and Garrison, R.E., 1981. Significance of laminated and massive diatomites in the upper part of the Monterey Formation, California. *In: The Monterey Formation and Related Siliceous Rocks of California* (eds. Garrison, R.E., Douglas, R.G., Pisciotto, K.E., Isaacs, C.M., and Ingle, J.C.), Pacific Section SEP, p.181-198.

Graham, S.A. and Williams, L.A., 1985. Tectonic, depositional, and diagenetic history of Monterey Formation (Miocene), central San Joaquin basin, California, *AAPG Bulletin*, 69, pp. 385-411.

Grimm, K.A., Lange, C.B., and Gill, A.S., 1996. Biological forcing of hemipelagic sedimentary laminae: evidence from ODP site 893, Santa Barbara Basin, California. *Journal of Sedimentary Research*, 66, p.613.

Grimm, K.A. and Orange, D.L., 1997. Synsedimentary fracturing, fluid migration, and subaqueous mass wasting: intrastratal microfractured zones in laminated diatomaceous sediment, Miocene Monterey Formation, California, USA, *Journal of Sedimentary Research*, 67, pp. 601-613.

Gross, M.G., Gucluer, S.M., Creager, J.S., and Dawson, W.A., 1963. Varved marine sediments in a stagnant fjord, *Science*, 141, p.918-919.

Gucluer, S.M. and Gross, M.G., 1964. Recent marine sediments in Saanich Inlet, a stagnant marine basin, *Limnology and Oceanography*, 9, pp. 359-376.

- Ibach, L.E.J., 1982. Relationship between sedimentation rate and total organic carbon content in ancient marine sediments, *AAPG Bulletin*, 66, p. 170-188.
- Ingle, J.C., 1981a. Origin of Neogene diatomites around the north Pacific Rim, In: *The Monterey Formation and Related Siliceous Rocks of California* (eds. Garrison, R.E., Douglas, R.G., Pisciotto, K.E., Isaacs, C.M., and Ingle, J.C.), Pacific Section SEPM, p.159-179.
- Ingle, J.C., 1981b. Cenozoic depositional history of the northern continental borderland of southern California and the origin of associated Miocene diatomites, In: *Guide to the Monterey Formation in the California coastal area, Ventura to San Luis Obispo* (ed. C.M. Isaacs), Pacific Section, AAPG, vol. 52, pp. 1-8.
- Isaacs, C.M., in press. Depositional framework of the Monterey Formation, California, In: *The Monterey Formation: from rocks to molecules* (eds. Isaacs, C.M. and Rullkötter, J.), Columbia University Press.
- Isaacs, C.M., 1987. Sources and deposition of organic matter in the Monterey Formation, South-Central coastal basins of California, In: *Exploration for heavy crude oil and natural bitumen* (Meyer, R.F., ed.), *AAPG Studies in Geology*, 25, p. 193-205.
- Isaacs, C.M., 1981. Field characterization of rocks in the Monterey Formation along the coast near Santa Barbara, California, In: *Field guide to the Monterey Formation in the California coastal area, Ventura to San Luis Obispo*, Pacific Section AAPG, v.52, p.39-54.
- Isaacs, C.M. and Magoon, L.B., 1984. Thermal indicators of organic matter in the Sisquoc and Monterey formations, Santa Maria Basin, California, *Abstracts - SEPM Midyear Meeting*, 1, p. 40.
- Isaacs, C.M., Keller, M.A., Gennai, V.A., Stewart, K.C., and Taggart, J.E. Jr., 1983. Preliminary evaluation of Miocene lithostratigraphy in the Point Conception COST well OCS-CAL 78-164 No. 1, off southern California, In: *Petroleum generation and occurrence in the Miocene Monterey Formation, California* (eds. Isaacs, C.M. and Garrison, R.E.), Pacific Section SEPM, p. 99-110.
- Jasper, J.P. and Gagosian, R.B., 1990. The sources and deposition of organic matter in the Late Quaternary Pigmy Basin, Gulf of Mexico, *Geochimica et Cosmochimica Acta*, 54, p.1117.
- Kablanow, R.I. and Surdam, R.C., 1983. Diagenesis and hydrocarbon generation in the Monterey Formation, Huasna Basin, California, In: *Petroleum generation and occurrence in the Miocene Monterey Formation, California* (eds. Isaacs, C.M. and Garrison, R.E.), Pacific Section SEPM, pp. 53-68.
- Katz, B.J., 1983. Limitations of 'Rock-Eval' pyrolysis for typing organic matter, *Organic Geochemistry*, 4, p.195-199.
- Keeling, R.F., 1993. Biogeochemical cycles; heavy carbon dioxide, *Nature*, 363, pp. 399-400..
- Keil, R.G., Montlucon, D.B., Prah, F.G., and Hedges, J.I., 1994. Sorptive preservation of labile organic matter in marine sediments, *Nature*, 370, p.549.
- Kemp, A.E.S., 1990. Sedimentary fabrics and variation in lamination style in Peru continental margin upwelling sediments, In: *Proceedings of the Ocean Drilling Program, Scientific Results* (Suess, E., von Huene, R., et al., eds.), vol. 112.
- Kemp, A.E.S. (ed.), 1996. "Palaeoclimatology and palaeoceanography from laminated sediments ",

Geological Society Special Publication No. 116, Geological Society, London, 258 p.

Kennett, J.P., Bauldauf, J.G. et al., 1994. Proceedings of the Ocean Drilling Program, Initial Reports, vol. 146 (part 2): College Station, TX (ODP).

Kennett, J.P. and Ingram, B.L., 1995. Paleoclimatic evolution of Santa Barbara Basin during the last 20 k.y.: marine evidence from Hole 893A. *In: Proceedings of the Ocean Drilling Program, Scientific Results*, vol. 146, part 2 (eds. Kennett, J.P., Baldauf, J.G., and Lyle, M.), College Station, Texas, Ocean Drilling Program, p. 309-325.

King, J.D. and Claypool, G.E., 1983. Biological marker compounds and implications for generation and migration of petroleum in rocks of the Point Conception deep-stratigraphic test well, OCS-CAL 78-164 No. 1, offshore California, *In: Petroleum generation and occurrence in the Miocene Monterey Formation, California* (eds. Isaacs, C.M. and Garrison, R.E.), Pacific Section SEPM, pp. 191-200.

Kroopnick, P.M., 1985. The distribution of ^{13}C of SCO_2 in the world oceans, *Deep-Sea Research*, 21, p.57-84.

Kruege, M.A., 1983. Diagenesis of Miocene biogenic sediments in Lost Hills oil field, San Joaquin Basin, California, *In: Petroleum generation and occurrence in the Miocene Monterey Formation, California* (eds. Isaacs, C.M. and Garrison, R.E.), Pacific Section SEPM, p. 39-51.

Lange, C.B. and Schimmelmann, A., 1995. X-radiography of selected, predominantly varved sedimentary intervals at Hole 893A, *In: Proceedings of the Ocean Drilling Program, Scientific Results*, vol. 146, part 2 (eds. Kennett, J.P., Baldauf, J.G., and Lyle, M.), College Station, Texas, Ocean Drilling Program, p.333.

Langford, F.F. and Blanc-Valleron, M.-M., 1990. Interpreting Rock-Eval pyrolysis data using graphs of pyrolyzable hydrocarbons vs. total organic carbon, *AAPG Bulletin*, 74, p.799-804.

Leythaeuser, D., 1973. Effects of weathering on organic matter in shales, *Geochimica et Cosmochimica Acta*, 37, p. 113-120.

Littke, R., Lkussmann, U., Krooss, B., and Leythaeuser, D., 1991. Quantification of loss of calcite, pyrite, and organic matter due to weathering of Toarcian black shales and effects on kerogen and bitumen characteristics, *Geochimica et Cosmochimica Acta*, 55, p. 3369-3378.

Mayer, L.M., 1994. Surface area control of organic carbon accumulation in continental shelf sediments, *Geochimica et Cosmochimica Acta*, 58, p. 1271-1284.

McDonald, D., 1997. The late Quaternary sedimentary history of primary productivity in the subarctic east Pacific, unpublished M.Sc. thesis, University of British Columbia.

Moore, L.R., 1969. Geomicrobiology and geomicrobiological attack on sedimented organic matter, *In: Organic Geochemistry: Methods and Results*, (Eglinton, G. and Murphy, M.T.J., eds.), Springer-Verlag, chapter 11.

Mortlock, R.A. and Froelich, P.N., 1989. A simple method for the rapid determination of biogenic opal in pelagic marine sediments. *Deep-Sea Research*, 36, p. 1415.

Müller, P.J., 1977. C/N ratios in Pacific deep-sea sediments: effect of inorganic ammonium and organic nitrogen compounds sorbed by clays, *Geochimica et Cosmochimica Acta*, 41, p.765-776.

Müller, P.J., and Suess, E., 1979. Productivity, sedimentation rate, and sedimentary organic matter in

the oceans--I. Organic carbon preservation, *Deep-Sea Research*, 26A, pp. 1347-1362.

Paropkari, A.L., Babu, C.P., and Mascarenhas, A., 1992. A critical evaluation of depositional parameters controlling the variability of organic carbon in Arabian Sea sediments, *Marine Geology*, 107, p.213-226.

Parsons, T.R., Stephens, K. and Strickland, J.D.H., 1961. On the chemical composition of eleven species of marine phytoplankters, *J. Fish. Res. Board Can.*, 18, pp. 1001-1016.

Parsons, T.R., Perry, R.I., Nutbrown, E.D., Hsieh, W., and Lalli, C.M., 1983. Frontal zone analysis at the mouth of Saanich Inlet, British Columbia, Canada, *Marine Biology*, 73, pp. 1-5.

Patience, R.L., Clayton, C.J., Kearsley, A.T., Rowland, S.J., Bishop, A.N., Rees, A.W.G., Bibby, K.G., and Hopper, A.C., 1990. An integrated biochemical, geochemical, and sedimentological study of organic diagenesis in sediments from Leg 112, *In: Proceedings of the Ocean Drilling Program, Scientific Results* (Suess, E., von Huene, R., et al., eds.), vol. 112, p. 135-153.

Pedersen, T.F., Nielsen, B., and Pickering, M., 1991. The timing of late Quaternary productivity pulses in the Panama Basin and implications for atmospheric CO₂, *Paleoceanography*, 6, pp. 657-677.

Pedersen, T.F., Shimmield, G.B., and Price, N.B., 1992. Lack of enhanced preservation of organic matter in sediments under the oxygen minimum on the Oman Margin, *Geochimica et Cosmochimica Acta*, 56, p.545-551.

Peters, K.E., 1986. Guidelines for evaluating petroleum source rock using programmed analysis, *AAPG Bulletin*, 70, p.318.

Pike, J. and Kemp, A.E.S., 1996. Records of seasonal flux in Holocene laminated sediments, Gulf of California, *In: "Palaeoclimatology and palaeoceanography from laminated sediments"* (ed. Kemp, A.E.S.), Geological Society Special Publication No. 116, Geological Society, London, p. 157-170.

Piper, D.Z. and Isaacs, C.M., 1995. Geochemistry of minor elements in the Monterey Formation, California: seawater chemistry of deposition, USGS Professional Paper 1566, 41pp.

Pisciotta, K.A. and Garrison, R.E., 1981. Lithofacies and depositional environments of the Monterey Formation, California, *In: The Monterey Formation and Related Rocks of California* (eds. Garrison, R.E., Douglas, R.G., Pisciotta, K.E., Isaacs, C.M., and Ingle, J.C.). Pacific Section SEPM, p.97-122.

Premuzic, E.T., Benkovitz, C.M., Gaffney, J.S., and Walsh, J.J., 1982. The nature and distribution of organic matter in the surface sediments of the world oceans and seas, *Organic Geochemistry*, 4, p.63-77.

Rau, G.H., Takahashi, T., and Des marais, D.J., 1989. Latitudinal variations in plankton d13C: implications for CO₂ and productivity in past oceans, *Nature*, 341, p.516-518.

Reineking, A., Langel, R., and Schikowski, J., 1993. 15N, 13C-on-line measurements with an elemental analyser (Carlo-Erba, NA 1500), a modified trapping box and a gas isotope mass spectrometer (Finnigan, MAT 251), *Isotopenpraxis Environ. Health Stud.*, 29, p. 169-174.

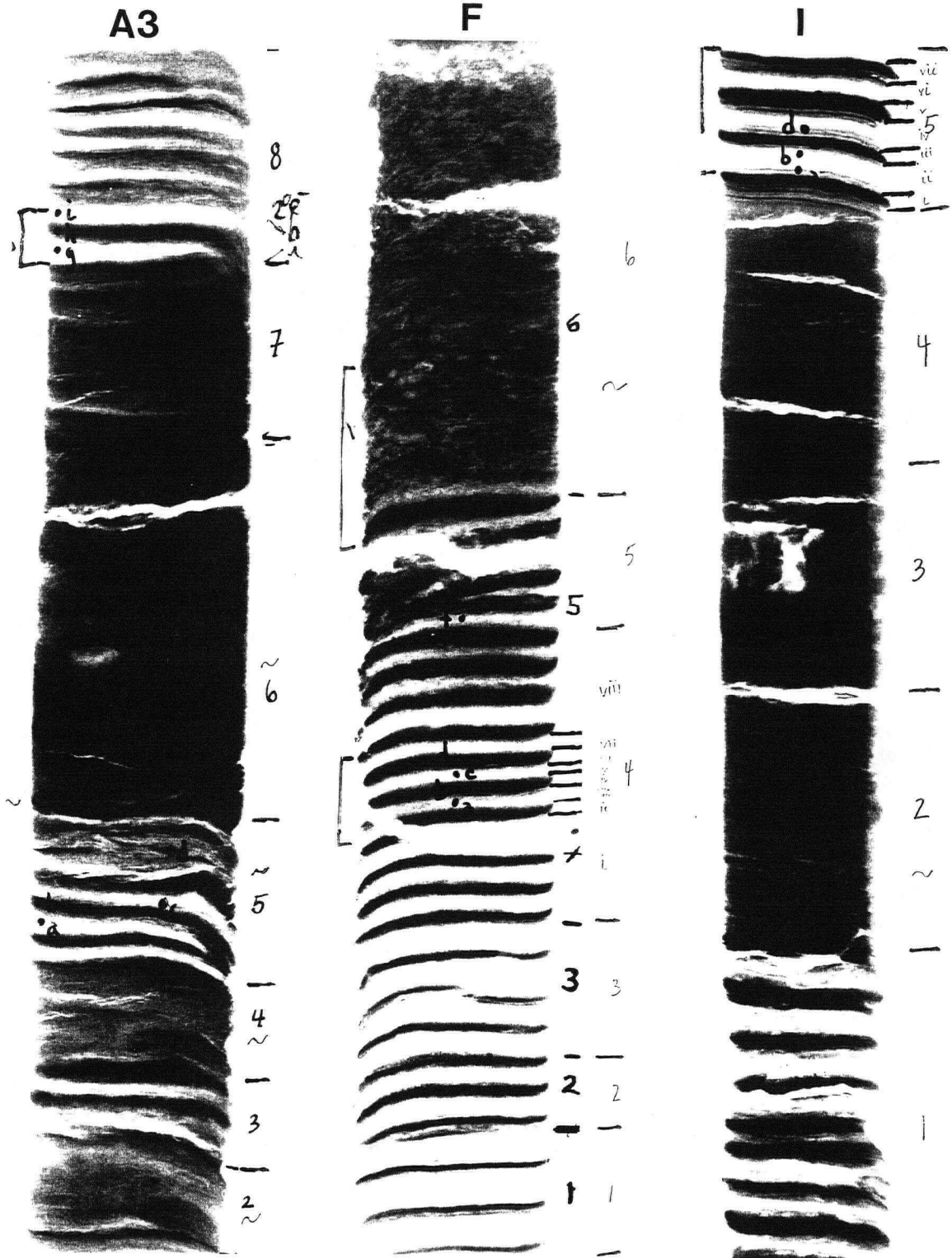
Rosenfeld, J.K., 1981. Nitrogen diagenesis in Long Island Sound sediments, *American Journal of Science*, 281, p. 436-462.

Sancetta, C., 1989. Sediment transport by fecal pellets in British Columbian fjords, *Marine Geology*, 849, p. 331-346.

- Sancetta, C. and Calvert, S.E., 1988. The annual cycle of sedimentation in Saanich Inlet, British Columbia: implications for the interpretation of diatom fossil assemblages, *Deep-Sea Research*, 35, p.71-90.
- Sancetta, C., 1996. Laminated diatomaceous sediments: controls on formation and strategies for analysis. In: "Palaeoclimatology and palaeoceanography from laminated sediments" (ed. A.E.S. Kemp), Geological Society Special Publication No. 116, Geological Society, London, p.17-22.
- Sarmiento, J.L. and Bender, M., 1994. Carbon biogeochemistry and climate change, *Photosynthesis Research*, 39, p. 209-234.
- Schimmelmann, A., Lange, C.B., and Berger, W.H., 1990. Climatically controlled marker layers in Santa Barbara Basin sediments, and fine-scale core-to-core correlation. *Limnology and Oceanography*, 35, p. 165.
- Schimmelmann, A. and Lange, C.B., 1996. Tales of 1001 varves: a review of Santa Barbara Basin sediment studies, In: Palaeoclimatology and Palaeoceanography from Laminated Sediments, (ed. A.E.S. Kemp), Geological Society Special Publication No. 116, p.121-142.
- Schrader, H., 1971. Fecal pellets: role in sedimentation in pelagic diatoms, *Science*, 174, p.55-57.
- Schrader, H. and Sorknes, R., 1991. Peruvian coastal upwelling: late Quaternary productivity changes revealed by diatoms, *Marine Geology*, 97, p. 233-246.
- Shimmield, G.B., Price, N.B., and Pedersen, T.F., 1990. The influence of hydrography, bathymetry, and productivity on sediment type and composition of the Oman Margin and in the northwest Arabian Sea, In: The geology and tectonics of the Oman Region (Robertson, A.H.F., Searle, M.P., and Ries, A.C., eds.), p. 759-769.
- Soutar, A., Johnson, S.R., and Baumgartner, T.R., 1981. In search of modern depositional analogs to the Monterey Formation, In: The Monterey Formation and related siliceous rocks of California (Garrison, R.E., Douglas, R.G., Pisciotto, K.E., Isaacs, C.M., and Ingle, J.C., eds.), Pacific Section SEPM, p.123-147.
- Stein, R., 1995. Clay and bulk mineralogy of late Quaternary sediments at Site 893, Santa Barbara Basin, In: Proceedings of the Ocean Drilling Program, Scientific Results (Kennett, J.P., Baldauf, J.G. and Lyle, M., eds.), vol. 146, part 2, pp. 89-102.
- Stucchi, C. and Whitney, F., 1997. Circulation and nitrogen transport in Saanich Inlet, B.C.
- Suess, E. and Müller, P.J., 1980. Productivity, sedimentation rate and sedimentary organic matter in the oceans: II--Elemental fractionation, In: Biogéochimie de la matière Organique à l'interface eau-sédiment marin, Colloques Internationaux du CNRS, no. 294, pp. 17-26.
- Takigijū, R., Popp, B.N., Johnson, M.W., Hayes, J.M., Albrecht, P., Callot, H.J., and Ocampo, R., 1991. Primary and secondary controls on carbon-isotopic compositions of sedimentary organic matter, In: Diversity of environmental biogeochemistry (Berthelin, J., ed.), Elsevier, pp. 3-14.
- Thunell, R., Pride, C., Tappa, E., and Muller-Karger, F., 1994. Varve formation in the Gulf of California: insights from time series sediment trap sampling and remote sensing, *Quaternary Science Reviews*, 12, p. 451-464.
- Tissot, B.P., and Welte, D.H., 1984. Petroleum formation and occurrence. Springer-Verlag.

- Trask, P.D., 1955. Organic content of recent marine sediments, *In: Recent marine sediments, A symposium* (Trask, P.D., ed.), AAPG.
- Tyson, R.V., 1987. The genesis and palynofacies characteristics of marine petroleum source rocks, *In: Marine petroleum source rocks*, (eds. Brooks, J and Fleet, A.J.), Geological Society Special Publications, 26, pp. 47-67.
- Van Os, B., Middelburg, J.J., and De Lange, G.J., 1996. Extensive degradation and fractionation of organic matter during subsurface weathering, *Aquatic Geochemistry*, 1, p.303-312.
- Verardo, D.J., Froelich, P.N., and McIntyre, A., 1990. Determination of organic carbon and nitrogen in marine sediments using the Carlo Erba NA-1500 Analyzer. *Deep-Sea Research*, 37, p. 157.
- Wedepohl, K.H. (ed.), 1969. Handbook of Geochemistry, Springer-Verlag.
- White, L.D., Garrison, R.E., and Barron, J.A., 1992. Miocene intensification of upwelling along the California margin as recorded in siliceous facies of the Monterey Formation and offshore DSDP sites. *In: Upwelling systems: evolution since the early Miocene* (Summerhayes, C.P., Prell, W.L., and Emeis, K.C., eds.). Geological Society Special Publication No. 64, pp. 429-442.
- Whitney, F., 1995. Chemical oceanography, *In: Saanich Inlet study; synthesis workshop summary* (Calder, A.A., and Mann, G.S., eds.). Water Quality Branch, B.C. Ministry of Environment, Lands, and Parks, Victoria, pp. 23-35.

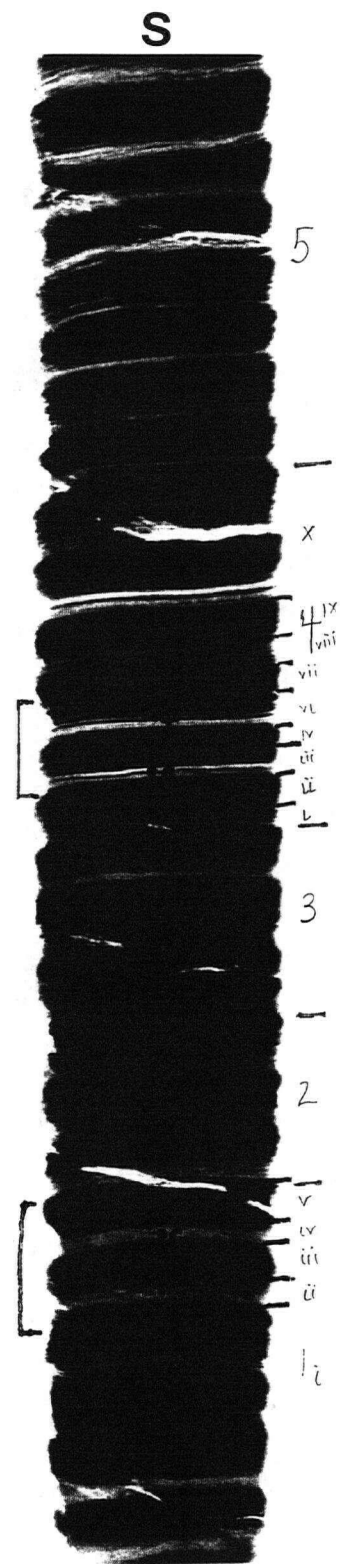
APPENDIX I. X-RADIOGRAPH CONTACT PRINTS OF SAANICH INLET AND MONTEREY FORMATION SEDIMENT SLABS WITH LOCATIONS OF SUBSAMPLES FOR GEOCHEMISTRY.



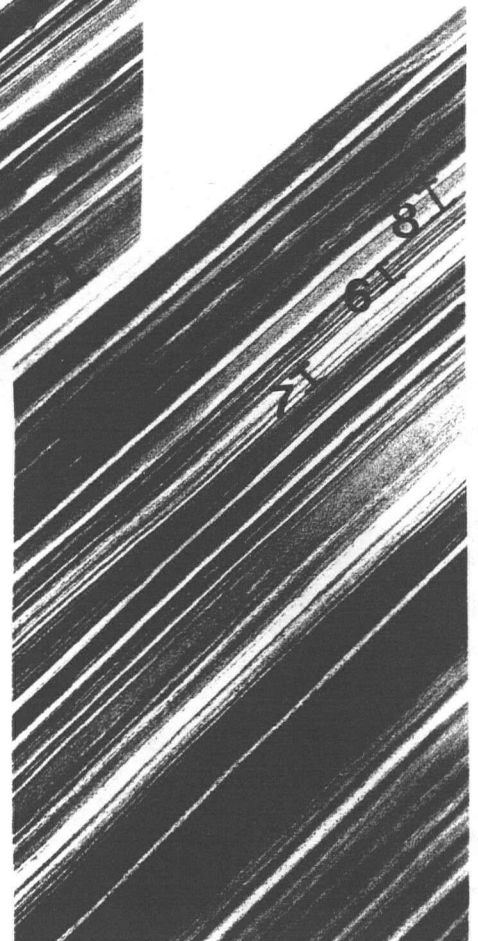
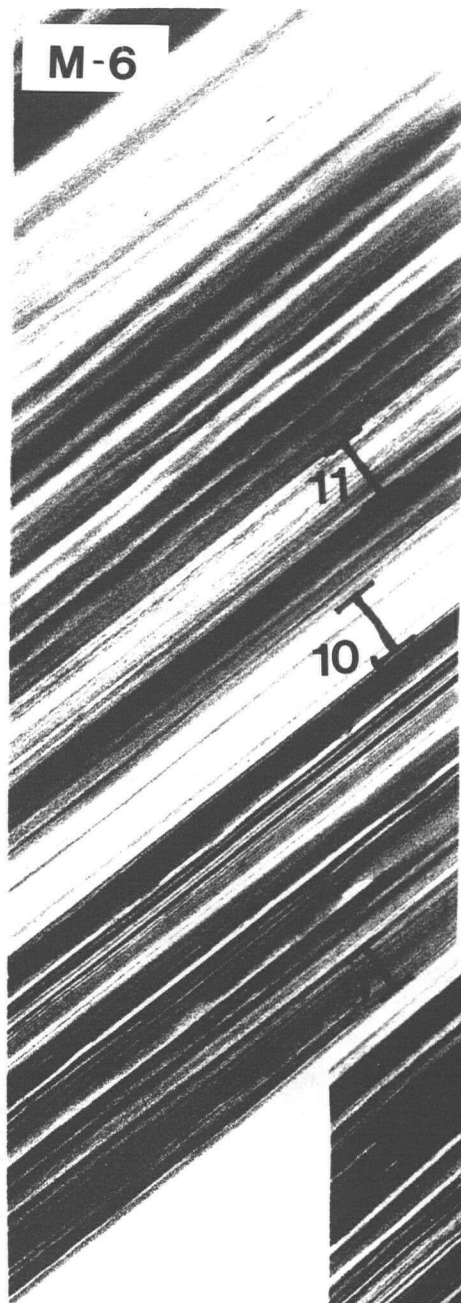
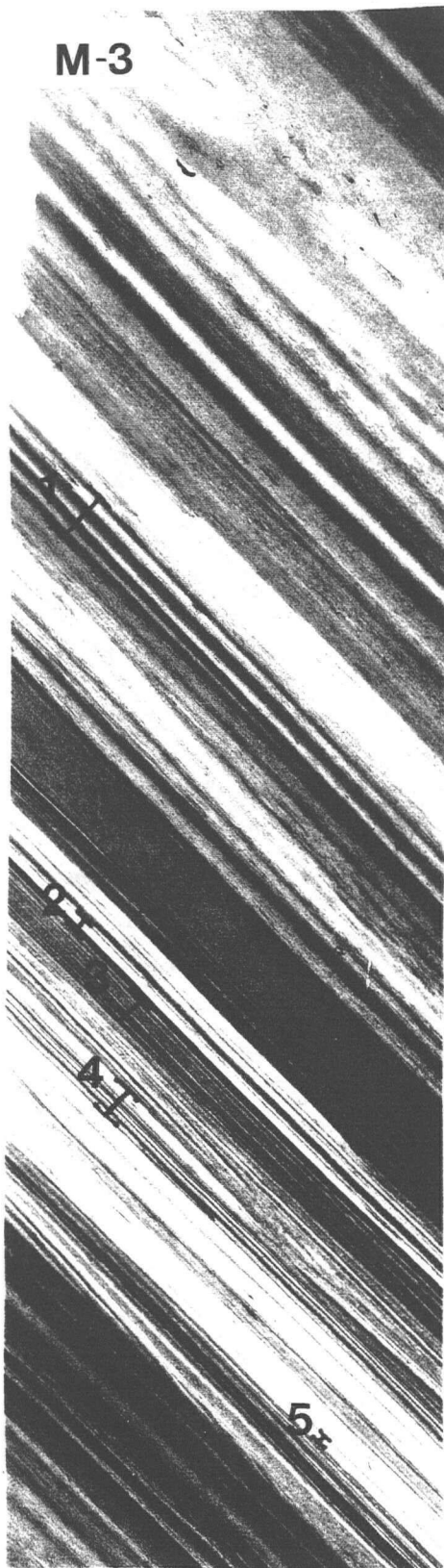
Appendix I-A. X-radiograph contact prints of Saanich Inlet sediment slabs: A3, F, I, M, N, P, Q, and S. Geochemistry subsample location are indicated by the numbers (Arabic and Roman) to the right of the print. Other notations on the print indicate samples used for other analyses.



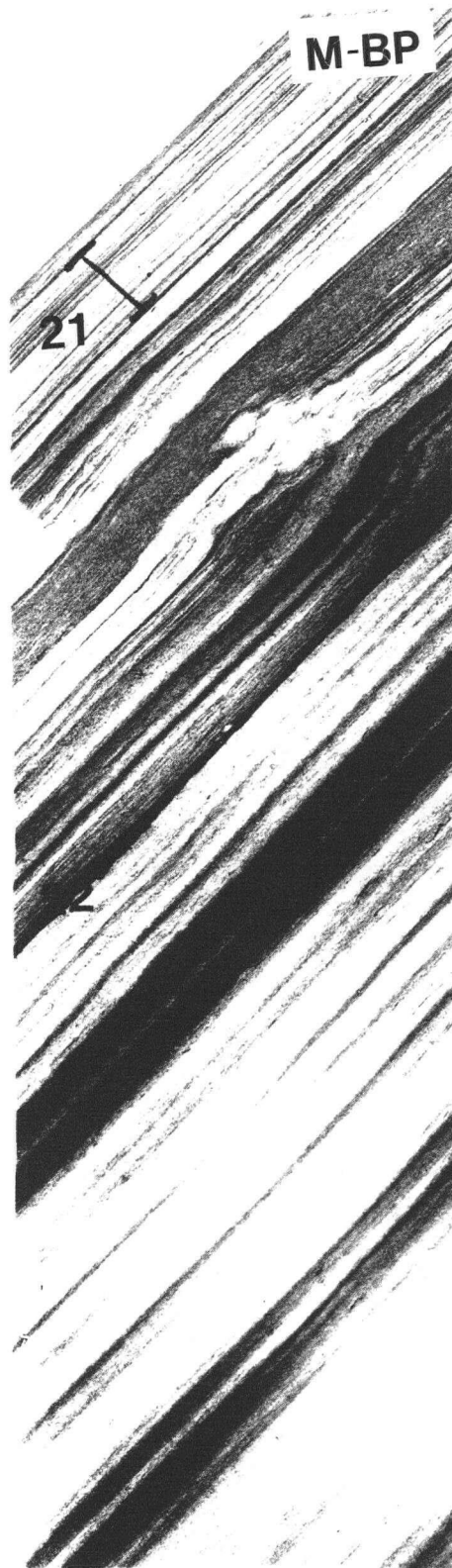
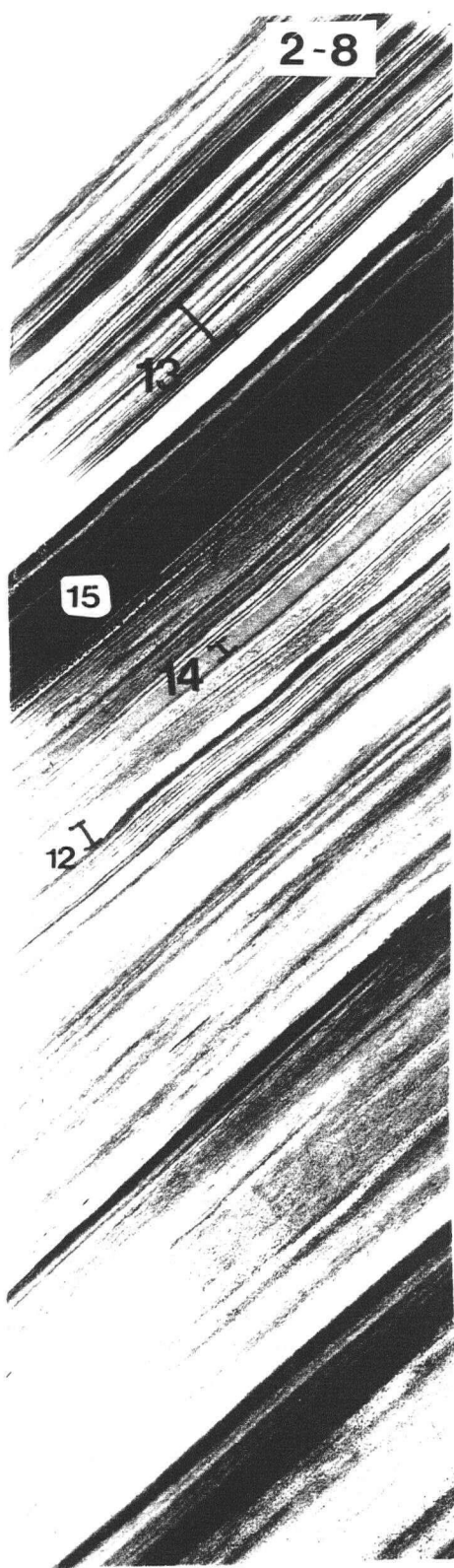
Appendix I-A continued.



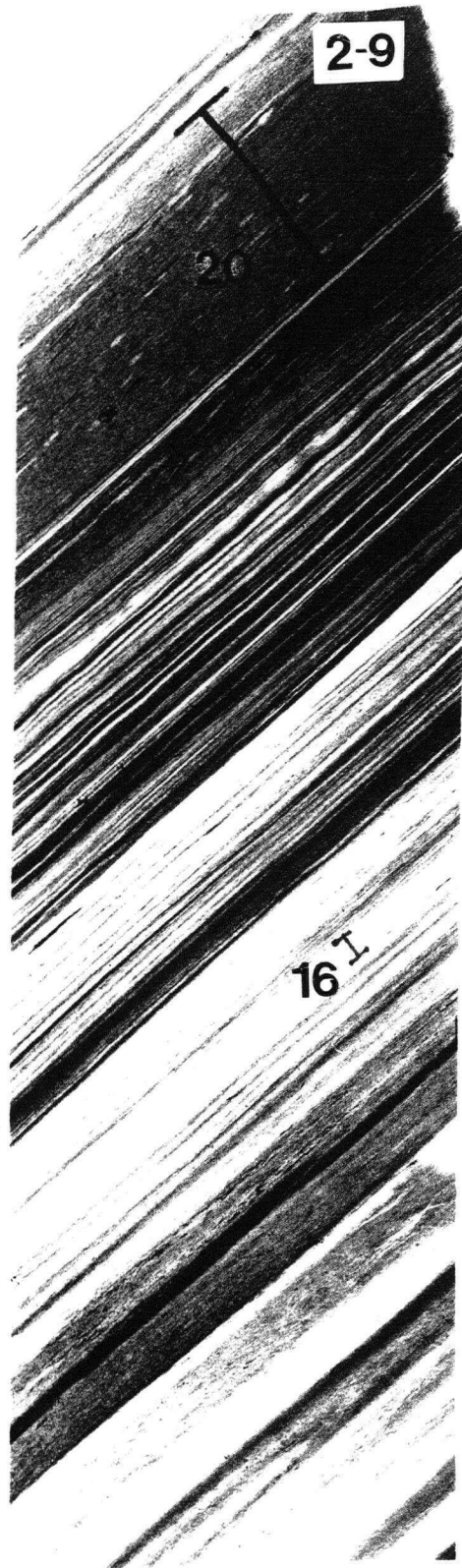
Appendix I-A continued.



Appendix I-B. X-radiograph contact prints of Monterey Formation sediment slabs: M-3, M-6, M-BP, 2-8, and 2-9. Sub-samples used for geochemistry are indicated on the prints.



Appendix I-B continued.



Appendix I-B continued.

APPENDIX II. DESCRIPTIONS OF SAANICH AND MONTEREY SAMPLES

Table II-1. Descriptions of Saanich Inlet ODP samples.

SAMPLE	DESCRIPTION
A31	mud-dominated; low/moderate bimodality
A32	massive; bioturbated
A33	sub-equal; moderate bimodality
A34	massive; bioturbated
A35	opal-dominated; high bimodality; bioturbated
A36	massive; bioturbated
A37	massive
A38	mud-dominated; low/moderate bimodality; 12 laminae
F1	opal-dominated; high bimodality; 6 laminae
F2	sub-equal; high bimodality; 3 mud, 2 opal laminae
F3	opal-dominated; high bimodality; 8 laminae
F4i	opal-dominated; moderate/high bimodality; 4 laminae
F4ii	mud lamina
F4iii	opal-rich lamina
F4iv	mud lamina
F4v	opal-rich lamina
F4vi	mud lamina
F4vii	opal-rich lamina
F4viii	sub-equal; moderate bimodality; 4 mud, 3 opal laminae
F5	sub-equal; moderate bimodality; 8 laminae
F6	massive; bioturbated
I1	opal-dominated; amalgamated opal laminae; moderate/high bimodality; 18 laminae
I2	massive; bioturbated
I3	massive
I4	massive
I5i	mud lamina
I5ii	amalgamated opal laminae; low/moderate bimodality
I5iii	mud lamina
I5iv	amalgamated opal laminae; low/moderate bimodality
I5v	mud lamina

Table II-1 continued.

SAMPLE	DESCRIPTION
I5vi	amalgamated opal laminae; low bimodality
I5vii	mud lamina
M7i	break in slab; cannot be described
M7ii	muddy opal lamina
M7iii	mud lamina
M7iv	amalgamated opal laminae; low bimodality
M7v	mud-dominated; low bimodality
M7vi	sub-equal; moderate/high bimodality; couplet
M7vii	sub-equal; moderate bimodality; bioturbated; 4 mud, 3 opal laminae
M8	massive; bioturbated
M9	opal-dominated; moderate bimodality; 4 laminae
N1	sub-equal; moderate bimodality
N2	massive; bioturbated
N3	massive; bioturbated
N4	massive; bioturbated
N5	mud-dominated; low/moderate bimodality
N6	mud-dominated; moderate bimodality
N7	massive; bioturbated
N8	massive; bioturbated
N9	massive
P3	sub-equal; amalgamated opal laminae; low/moderate bimodality; 8 laminae
Q1	sub-equal; moderate bimodality; 8 laminae
Q2	opal-dominated; amalgamated opal laminae; moderate bimodality; 8 laminae
Q3i	opal-dominated; amalgamated opal laminae; moderate bimodality; 6 laminae
Q3ii	sub-equal; amalgamated opal laminae; moderate bimodality
Q3iii	mud lamina
Q3iv	amalgamated opal laminae; low bimodality
Q3ix	amalgamated opal lamiane; moderate bimodality
Q3v	mud lamina
Q3vi	amalgamated opal lamiane; moderate bimodality
Q3vii	mud lamina
Q3x	mud lamina
Q3xi	sub-equal; amalgamated opal laminae; low/moderate bimodality; 8 laminae

Table II-1 continued.

SAMPLE	DESCRIPTION
Q4	opal-dominated; amalgamated opal laminae; moderate bimodality; 6 laminae
Q5	opal-dominated; moderate bimodality
S1i	mud-dominated; low bimodality; 5 mud, 4 opal laminae
S1ii	fuzzy opal-rich lamina
S1iii	mud lamina
S1iv	fuzzy opal-rich lamina
S1v	mud lamina
S2	sub-equal; amalgamated opal laminae; low bimodality; 6 laminae
S3	mud-dominated; low bimodality; 6 laminae
S4i	amalgamated opal laminae; low bimodality
S4ii	mud lamina
S4iii	amalgamated opal laminae; low/moderate bimodality
S4iv	mud lamina
S4ix	mud lamina
S4vi	amalgamated opal lamiane; moderate bimodality
S4vii	mud lamina
S4viii	amalgamated opal lamiane; low bimodality
S4x	sub-equal; amalgamated opal laminae; low/moderate bimodality; 4 laminae
S5	mud-dominated; low/moderate bimodality; amalgamated opal laminae

Table II-2. Descriptions of Monterey Formation samples.

SAMPLE	DESCRIPTION
1	mud-dominated; moderate bimodality; widely-spaced; chalk stripes
2	sub-equal; high bimodality; pinstripes; couplet
3	mud-dominated; low bimodality; closely-spaced; pin/chalk stripes
4	mud-dominated; moderate/high bimodality; closely-spaced; pin stripes
5	diatom bloom lamina
6	mud-dominated; low bimodality; closely-spaced; pin stripes
7	opal-dominated; low/moderate bimodality; closely-spaced; pin stripes
8	2 diatom bloom laminae separated by a speckle bed
9	mud-dominated; low bimodality; pin stripes
10	opal-dominated; moderate/high bimodality; moderately-spaced; pin/chalk stripes
11	sub-equal; low/moderate bimodality; closely-spaced; razor stripes
12	closely packed diatom blebs
13	sub-equal; moderate/high bimodality; closely-spaced; razor/pin stripes
14	light grey structureless lamina
15	mud-dominated; low-bimodality; moderately-spaced
16	2 laminae similar to 14
17	3 laminae similar to 14, 16; chalk stripes
18	mud-dominated; high bimodality; widely-spaced; pin stripes
19	sub-equal; high bimodality; closely-spaced; pin stripes
20	speckle bed
21	sub-equal; moderate bimodality; razor stripes
22	black waxy lamina

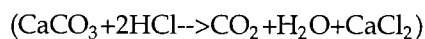
APPENDIX III. ANALYTICAL METHODS

Opal

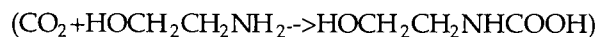
Weight percent biogenic opal was determined using a method modified from Mortlock and Froelich (1989) involving extraction of biosilica with sodium carbonate and subsequent analysis via molybdate-blue spectrophotometry. 8-50 mg of powdered sample were treated with 3 ml each of 10% HCl and 10% H₂O₂. 20 ml of 2M Na₂CO₃ were then added to the decarbonated and organic-free samples and the samples were placed in an 85°C water bath for 5 hours to permit extraction of opal. Following extraction, oxidizing molybdate solution and reducing solution were added, and after standing overnight, absorbances were read on a spectrophotometer at a wavelength of 812nm. Two blanks and two sediment standards were run with each batch of 36 samples. The precision of this method was ±2.56% (1s).

Carbonate Carbon

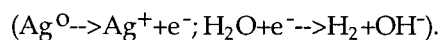
Weight percent carbonate carbon was determined via coulometric titration. The method is similar to that of Engleman et al. (1985). A test tube containing 50 mg of powdered sample was attached to a Coulometrics Inc. model 5010 coulometer with a 5030 carbonate carbon apparatus. 10% HCl was added to the sample and decomposition proceeded for 8 minutes in a heated environment. Evolved CO₂



was carried by a CO₂-free stream into a titration cell containing ethanolamine and thymolphthalein indicator. The ethanolamine reacts with the CO₂ forming a strong titratable acid



causing the blue indicator to fade and the percent transmittance to increase. This triggers a titration current which produces OH⁻ ions at a silver electrode



The OH⁻ ions neutralize the acid, the ethanolamine solution returns to its original blue color, transmittance decreases, and the current switches off. The total current required to titrate the produced acid is integrated and displayed on the instrument as μg carbon. Weight percent carbonate carbon is calculated using the equation:

$$\% \text{carbonate carbon} = [C_{\text{CO}_2}(\mu\text{g}) - C_{\text{blank}}(\mu\text{g}) / \text{sample weight}(\mu\text{g})] \times 100.$$

CaCO₃ standards and blanks were run with each batch of 12 samples.

Total carbon and nitrogen

Instrument components, parameters, and operation are similar to that described in Verardo et al. (1990). 25-35 mg of powdered sample were weighed into 8x5mm tin capsules which were loaded into the autosampler of the Carlo Erba NA-1500 Analyzer. Samples were flash-combusted in an O₂- and He-rich reactor at a temperature of 1050°C. The combustion products were oxidized in a column containing Cr₂O₃ and Co₃O₄ + Ag granules. The resultant CO₂, NO_x, and H₂O were carried into a reduction reactor with metallic copper where nitrous oxides were reduced to N₂, and any excess oxygen was removed. N₂, CO₂, and H₂O were then swept through a water-absorbing magnesium perchlorate filter. N₂ and CO₂ were separated chromatographically with a Poropak QS chromatographic column and the gases were measured via thermal conductivity detection. Acetanilide, bulk sediment standards, and blanks were run with each batch of 38 samples.

Major and minor element abundances

Both major and minor elements were measured using x-ray fluorescence spectrometry. Major element (Al, Fe, Mn, Ti, Ca, K, Na, Si, Mg, P) sample preparation is similar to that of Calvert (1990). 0.4 g of powdered sample and 3.6 g of Spectroflux 105 (Li₂B₄O₇, LiCO₃, La₂O₃) were weighed into Au-Pt crucibles and placed in an 1100°C muffle furnace for 30 minutes. Weight lost during fusion (volatiles) was compensated for by the addition of Spectroflux 100 (Li₂B₄O₇). This mixture was re-heated over a Meeker burner, the resultant melt poured into an aluminum mold at 400°C, and pressed into a flat disc using a brass plunger also at 400°C. Samples to be analyzed for minor

elements (As, Ba, Co, Cr, Cu, Mn, Nb, Ni, Pb, Rb, Sr, V, Y, Zn, Zr) were prepared by pressing one gram of powdered sample into a rigid disc backed with borax in a hydraulic press at 10 tons of pressure. Discs and pellets were analyzed by a Philips PW 1400 wavelength-dispersive sequential automatic spectrometer fitted with a Rh-target x-ray tube.

Rock-Eval Pyrolysis

Ground, whole rock samples were analyzed via Rock-Eval pyrolysis following the methods of Espitalie et al. (1977) and Peters (1986). Samples are subjected to step-wise programmed heating to 550°C, in an inert (helium) atmosphere. The evolved pyrolyzates are measured via a flame ionization detector. Results are reported as S1, S2, and S3. S1 and S2 represent the evolved hydrocarbons (HC) and have units of mg HC/g rock. S3 represents the generated CO₂ and has units of mg CO₂/g rock.

Carbon and nitrogen stable isotopes

Carbon isotopes of organic matter were determined in a manner described in Pedersen et al. (1991). Carbonate carbon was removed from a portion of ground sample by the addition of 10% HCl. The decarbonated sample was placed into a tin cup and introduced into a Carlo-Erba 1106 CHN elemental analyzer coupled to a VG Isotech Prism mass spectrometer. The combusted CO₂ product was separated and introduced into the mass spectrometer. The ¹³C and ¹²C were measured and reported relative to the PDB.

Nitrogen isotopes of bulk samples were determined as described in Farrell et al. (1995). Ground samples were combusted in a Fisons NA 1500 element analyser and the evolved N₂ was introduced to a VG PRISM mass spectrometer in He.

APPENDIX IV. GEOCHEMICAL DATA OF SAANICH INLET, MONTEREY FORMATION,
AND SANTA BARBARA BASIN SAMPLES

Table IV-1. Geochemistry of Saanich Inlet samples; weight percent total organic carbon and opal, C/N ratios, and stable isotope values.

SAMPLE	% TOC	% OPAL	C/N	$\delta^{13}\text{C}$	$\delta^{15}\text{N}$
A31	1.27	19.41	7.06	-21.84	8.77
A32	1.21	17.75	6.72	-21.98	8.51
A33	1.30	23.38	6.84	-21.87	8.71
A34	1.18	20.93	6.94	-22.18	8.10
A35	1.20	20.75	6.67	-22.03	8.08
A36	1.22	14.52	6.78	-21.91	8.35
A37	1.20	14.65	7.06	-22.08	8.01
A38	1.14	21.06	6.71	-22.12	8.53
F1	2.14	42.51	8.23	-21.06	9.64
F2	1.88	36.70	7.83	-21.29	9.08
F3	2.04	41.85	7.56	-21.04	9.54
F4i	2.03	36.80	8.12	-21.30	9.87
F4ii	2.22	34.58	8.22	-21.20	9.03
F4iii	1.77	34.23	7.70	-21.83	9.98
F4iv	2.30	37.46	7.93	-21.30	9.82
F4v	1.73	41.77	7.52	-21.68	9.55
F4vi	2.40	44.93	8.89	-20.91	9.33
F4vii	2.13	30.33	8.19	-21.63	9.83
F4viii	2.14	36.27	7.64	-21.53	9.32
F5	2.03	37.18	7.81	-21.47	9.30
F6	1.89	35.55	7.27	-21.43	8.54
I1	1.85	31.40	7.12	-21.30	6.43
I2	2.03	24.90	7.25	-21.23	7.06
I3	1.90	24.36	7.04	-21.30	6.35
I4	1.85	28.18	6.85	-21.26	7.11
I5i	1.70	32.19	6.80	-21.55	8.38
I5ii	1.66	38.89	6.92	-21.64	10.07
I5iii	1.89	31.84	7.00	-21.45	9.85
I5iv	1.54	32.78	6.70	-22.03	9.04
I5v	1.85	25.71	6.85	-21.58	9.52
I5vi	1.54	24.55	7.00	-22.09	9.28
I5vii	1.77	33.61	6.81	-21.52	9.26
M7i	1.52	35.83	6.08	-21.29	6.46
M7ii	1.90	29.62	7.92	-21.31	10.16
M7iii	1.63	23.79	7.09	-21.54	7.93
M7iv	1.42	31.64	6.45	-21.51	7.87
M7v	1.64	27.58	6.83	-21.69	7.80
M7vi	1.37	26.99	6.85	-21.37	6.50
M7vii	1.52	32.35	6.91	-21.40	6.21
M8	1.66	33.07	6.92	-21.25	7.22
M9	1.62	29.15	6.48	-21.24	7.21
N1	1.34	22.98	7.05	-21.94	7.37
N2	1.46	23.26	6.95	-21.86	8.12
N3	1.46	23.64	7.30	-21.93	8.09

Table IV-1 continued.

SAMPLE	% TOC	% OPAL	C/N	$\delta^{13}\text{C}$	$\delta^{15}\text{N}$
N4	1.31	18.42	7.28	-21.93	7.15
N5	1.38	25.41	7.26	-21.89	7.93
N6	1.50	21.34	7.14	-21.77	7.53
N7	1.43	18.38	7.15	-21.91	7.88
N8	1.38	20.06	6.90	-21.98	6.99
N9	1.34	20.05	6.70	-21.79	6.95
P3	1.69	33.08	7.35	-21.45	9.70
Q1	1.65	26.34	6.88	-21.70	9.43
Q2	1.68	32.08	7.00	-21.49	9.36
Q3i	1.69	29.27	7.04	-21.56	10.47
Q3ii	1.56	23.95	7.43	-21.95	10.48
Q3iii	1.74	26.82	7.57	-21.72	10.61
Q3iv	1.60	32.56	7.62	-21.77	9.10
Q3ix	1.94	28.80	8.43	-21.77	8.67
Q3v	1.81	26.62	7.87	-21.71	9.69
Q3vi	1.52	31.37	8.00	-21.82	7.98
Q3vii	1.82	28.27	8.27	-21.39	9.11
Q3x	1.84	34.04	8.00	-21.21	8.43
Q3xi	1.67	22.45	6.96	-21.64	8.95
Q4	1.69	30.81	6.76	-21.53	10.00
Q5	1.60	27.03	6.67	-21.71	9.65
S1i	1.48	28.22	7.05	-21.57	9.66
S1ii	1.43	27.74	7.15	-21.67	9.14
S1iii	1.67	37.49	7.59	-21.14	10.46
S1iv	1.53	28.76	7.29	-21.67	9.25
S1v	1.54	30.69	7.33	-21.48	9.21
S2	1.48	29.39	6.73	-21.51	8.87
S3	1.54	29.42	7.33	-21.56	9.32
S4i	1.45	21.43	7.25	-21.79	10.39
S4ii	1.63	31.67	7.09	-21.35	10.22
S4iii	1.37	21.21	7.21	-21.99	9.79
S4iv	1.60	28.48	7.62	-21.40	8.08
S4ix	1.60	26.28	7.27	-21.69	8.84
S4vi	1.50	27.51	7.14	-21.63	10.09
S4vii	1.51	26.03	7.19	-21.48	9.71
S4viii	1.41	29.80	7.05	-21.62	10.31
S4x	1.47	27.61	7.00	-21.64	8.43
S5	1.49	28.68	6.77	-21.52	8.90

Table IV-2. Geochemistry of Monterey Formation samples; weight percent total organic carbon and opal, C/N ratios, and stable carbon isotopes values of organic matter.

SAMPLE	% TOC	% OPAL	C/N	$\delta^{13}\text{C}$
1	4.10	40.47	14.85	-20.54
2	2.92	57.73	14.61	-20.82
3	3.38	57.65	14.97	-20.73
4	3.49	53.26	15.12	-20.82
5	1.41	87.07	13.80	-
6	3.24	41.82	14.92	-20.36
7	2.83	63.23	14.50	-20.93
8	2.69	54.60	14.77	-20.34
9	3.47	28.36	15.42	-20.5
10	2.58	60.47	14.58	-21.35
11	3.69	46.09	15.24	-20.59
12	1.49	83.52	15.17	-21.45
13	3.35	57.43	15.15	-20.19
14	3.02	60.21	15.04	-21.13
15	4.48	35.06	15.72	-20.08
16	2.01	76.29	15.02	-20.34
17	2.44	62.62	14.99	-20.6
18	3.23	39.50	15.91	-20.72
19	2.80	56.89	16.18	-20.67
20	3.08	56.07	15.64	-20.21
21	4.09	48.14	14.57	-20.59
22	1.80	17.80	13.02	-

Table IV-3. Geochemistry of Santa Barbara Basin samples; weight percent total organic carbon, opal, calcite, and C_{org}/N_{total} weight ratios.

SAMPLE	%TOC	%OPAL	%CALCITE	C/N
AA	1.654	6.236	4.25	7.32
AB	1.730	8.749	5.07	7.42
AC	1.710	14.033	4.49	7.43
AD	1.869	12.367	4.96	7.76
AE	1.839	8.590	6.00	7.83
AF	1.718	10.652	4.91	7.81
AG	1.727	7.663	5.19	7.48
AH	1.763	7.421	6.38	7.77
EA	4.718	11.579	6.42	9.87
EB	-	21.966	-	-
EC	2.690	11.184	5.11	8.88
ED	2.424	21.166	5.01	8.78
EE	2.533	16.196	5.49	8.89
EF	2.759	17.171	5.11	8.76
GA	1.946	10.272	6.54	8.65
GB	1.699	13.236	5.26	7.83
GC	1.669	9.842	12.80	8.52
GD	1.698	15.522	22.06	8.41
GE	1.743	11.917	13.35	8.54
GF	1.744	17.947	4.76	7.39
GG	1.739	10.268	4.05	8.20
GH	1.884	13.266	12.31	8.45
GI	2.007	16.873	10.35	9.42
HA	1.879	12.035	5.10	8.21
HB	1.974	9.755	6.02	8.97
HC	2.021	19.543	4.98	8.64
HD	-	7.733	-	-
HE	2.041	14.807	5.16	8.54
HF	-	15.117	-	-
HG	1.643	11.257	3.63	8.21
JA	1.867	8.011	9.23	8.37
JB	1.919	8.290	8.38	8.31

Table IV-3 continued.

SAMPLE	%TOC	%OPAL	%CALCITE	C/N
JC	1.969	7.821	7.02	8.31
JD	1.189	5.733	2.85	7.82
JE	1.723	8.098	6.05	8.36
MA	-	5.616	-	-
MB	1.609	13.306	4.73	7.45
MC	1.620	16.691	4.04	7.11
MD	1.664	18.816	4.95	7.40
ME	1.731	21.141	4.41	7.56
MF	1.806	34.395	3.91	7.53
MG	1.881	17.178	5.97	8.21

Table IV-4. Major element abundances of Saanich Inlet samples. Values are reported as weight percent oxides.

SAMPLE	Al ₂ O ₃	CaO	Fe ₂ O ₃	K ₂ O	MgO	MnO	Na ₂ O	P ₂ O ₅	SiO ₂	TiO ₂
A31	13.47	2.36	5.60	1.57	3.40	0.08	4.04	0.16	60.13	0.64
A34	13.75	2.27	5.92	1.55	3.28	0.09	4.27	0.17	60.02	0.71
A35	11.96	2.18	5.64	1.42	3.22	0.08	4.12	0.16	54.78	0.66
A38	13.15	2.34	6.43	1.73	3.33	0.10	3.97	0.16	60.64	0.71
F1	8.60	1.60	3.90	0.93	2.83	0.05	6.18	0.16	61.58	0.42
F3	9.38	1.76	4.20	1.15	3.12	0.06	5.88	0.18	64.09	0.46
F4viii	10.94	2.07	4.61	1.24	2.92	0.07	5.55	0.28	68.51	0.51
F5	9.32	2.72	4.11	1.09	2.86	0.07	5.37	0.96	61.32	0.48
N9	15.05	2.49	6.81	1.48	3.56	0.17	4.85	0.25	67.21	0.68
Q1	11.25	1.88	4.87	1.35	3.03	0.06	4.33	0.16	60.30	0.61
Q2	10.89	1.87	4.69	1.35	3.05	0.06	4.77	0.15	62.03	0.56
Q3xi	11.56	1.85	4.90	1.31	2.94	0.06	4.83	0.17	60.85	0.60
Q5	11.21	1.77	4.90	1.21	2.91	0.06	4.86	0.16	58.06	0.59
S1i	12.22	1.86	4.99	1.40	2.98	0.08	4.51	0.17	62.74	0.60
S3	11.19	1.84	4.70	1.25	2.73	0.07	4.72	0.17	60.27	0.59

Table IV-5. Major element abundances of Monterey Formation samples. Values are reported as weight percent oxides.

SAMPLE	Al ₂ O ₃	CaO	Fe ₂ O ₃	K ₂ O	MgO	MnO	Na ₂ O	P ₂ O ₅	SiO ₂	TiO ₂
1	4.39	0.82	1.74	0.74	0.76	0.02	1.54	0.30	71.00	0.25
2	4.12	0.80	1.89	0.72	0.66	0.01	1.36	0.33	72.02	0.26
3	3.85	0.75	1.55	0.70	0.71	0.02	1.35	0.25	70.79	0.24
4	3.32	0.66	1.45	0.59	0.55	0.01	1.30	0.30	73.49	0.22
6	5.53	1.01	2.09	0.94	0.90	0.02	1.69	0.34	69.56	0.31
7	4.58	0.96	1.78	0.77	0.53	0.01	1.45	0.33	75.94	0.27
9	7.23	1.37	2.27	1.27	0.99	0.02	2.02	0.46	65.42	0.37
10	4.38	0.97	1.61	0.82	0.59	0.01	1.57	0.34	73.12	0.25
11	5.56	1.10	1.95	0.97	0.85	0.02	1.73	0.38	69.30	0.30
12	1.13	0.71	0.74	0.22	0.20	0.01	1.14	0.16	81.24	0.10
13	4.24	1.33	2.16	0.70	0.67	0.02	1.20	0.40	73.36	0.24
14	3.31	0.69	1.29	0.63	0.59	0.02	1.24	0.30	75.33	0.20
15	6.94	1.13	2.67	1.22	1.36	0.05	1.91	0.50	63.02	0.37
16	1.26	0.74	0.90	0.26	0.38	0.02	1.03	0.20	78.71	0.11
17	2.28	2.92	1.15	0.44	1.89	0.03	1.20	0.33	70.95	0.16
18	4.60	5.86	1.85	0.90	3.68	0.04	1.56	0.59	59.90	0.26
19	2.92	4.84	1.46	0.53	3.10	0.04	1.22	0.43	65.72	0.18
20	3.18	1.46	1.59	0.57	0.82	0.04	1.17	0.39	76.43	0.20
21	5.59	1.10	2.09	0.99	1.27	0.02	1.59	0.24	68.13	0.32

Table IV-6. Major element abundances of Santa Barbara Basin samples. Values are reported as weight percent oxides.

SAMPLE	Al ₂ O ₃	CaO	Fe ₂ O ₃	K ₂ O	MgO	MnO	Na ₂ O	P ₂ O ₅	SiO ₂	TiO ₂
AC	13.72	3.74	5.90	2.59	3.18	0.04	3.16	0.22	56.28	0.62
AD	13.75	2.27	5.92	1.55	3.28	0.09	4.27	0.17	60.02	0.71
AE	15.08	4.13	5.40	2.62	3.23	0.04	3.61	0.24	54.99	0.67
EC	14.66	4.13	5.32	2.60	3.00	0.04	3.13	0.22	57.75	0.64
EF	13.00	4.10	5.11	2.47	2.76	0.03	3.14	0.21	59.37	0.61
GB	13.04	3.94	6.21	2.35	2.92	0.04	3.31	0.21	53.44	0.65
GH	11.88	8.05	5.23	2.42	3.15	0.04	2.72	0.29	53.72	0.59
HA	13.13	4.60	5.72	2.68	3.00	0.04	2.95	0.22	54.69	0.65
HE	13.50	4.35	5.79	2.18	2.72	0.04	3.38	0.21	56.42	0.62
JB	14.41	5.64	6.33	2.24	3.64	0.05	3.70	0.26	50.01	0.63
JD	17.33	2.59	5.61	3.34	3.48	0.04	3.10	0.22	56.41	0.81
MB	13.00	3.77	5.74	2.72	3.26	0.04	3.44	0.21	53.89	0.63
MH	16.69	4.39	7.36	2.98	2.88	0.05	3.11	0.26	64.89	0.73

Table IV-7. Minor element abundances of Saanich Inlet samples. Values are reported as ppm.

SAMPLE	V	Cr	Mn	Co	Ni	Cu	Zn	Rb	Sr	Y	Zr	Ba	Pb
A31	170.4	95.3	842.8	18.5	52.8	36.0	87.7	39.4	150.1	15.9	98.6	433.4	17.6
A34	155.0	84.3	785.0	21.8	56.2	33.2	93.3	43.6	135.8	24.1	105.4	451.5	11.7
A35	175.4	104.6	819.5	17.1	37.4	35.7	73.9	48.4	147.0	16.2	100.8	369.9	49.4
A38	233.5	137.9	1189.9	23.3	66.6	47.4	105.3	51.6	179.3	13.8	114.6	642.6	38.9
F1	133.5	61.0	578.1	8.2	35.0	21.4	63.0	42.5	88.2	20.0	69.8	350.3	13.8
F3	113.3	51.5	497.9	17.1	36.9	12.6	66.2	47.7	78.3	12.3	65.4	233.1	17.2
F4viii	137.4	67.1	615.4	20.3	33.0	32.6	83.7	43.3	101.2	13.8	77.4	237.1	19.7
F5	132.2	61.3	633.5	0.4	46.5	22.3	65.4	43.9	196.2	10.4	84.0	396.1	41.0
N9	188.1	94.1	1417.3	24.2	57.7	42.1	74.1	42.9	141.0	17.9	88.4	466.7	43.3
Q1	113.5	67.3	531.1	11.8	42.8	25.4	65.0	47.2	116.1	20.2	87.7	292.1	8.6
Q2	132.0	76.3	641.3	20.7	34.9	18.9	67.0	47.1	123.0	21.3	91.7	341.5	23.7
Q3xi	137.8	82.3	662.0	24.9	19.8	12.3	70.8	48.2	119.5	16.9	90.4	434.5	29.6
Q5	140.4	83.0	624.9	2.5	50.3	19.0	72.0	49.1	125.0	15.2	97.0	399.4	45.2
S1i	139.9	97.1	760.8	24.4	26.5	21.1	73.5	43.8	126.6	17.0	103.9	408.6	4.2
S3	147.1	104.1	727.3	10.5	42.7	22.3	78.7	49.3	139.2	18.4	104.7	376.5	32.7

Table IV-8. Minor element abundances of Santa Barbara Basin samples. Values are reported as ppm.

SAMPLE	V	Cr	Mn	Ni	Cu	Zn	Rb	Sr	Y	Zr	Nb	Ba	Pb
AC	168.8	128.8	496.5	49.1	33.8	113.4	102.6	241.9	33.8	115.1	10.5	609.9	17.8
AD	160.7	113.3	433.6	63.8	30.6	114.1	110.9	248.9	30.5	124.3	6.9	513.0	26.5
AE	171.0	142.6	529.9	65.3	29.7	120.3	117.9	300.4	31.0	129.7	15.4	727.3	16.9
EB	167.5	105.6	417.9	69.0	28.4	108.6	102.7	249.8	13.4	123.5	10.5	611.5	29.6
EC	204.7	142.7	467.4	86.1	31.4	119.8	101.6	273.7	19.9	119.3	12.0	700.8	25.6
EF	172.6	141.5	425.8	81.3	23.7	116.3	106.4	253.0	22.1	135.5	8.2	646.5	28.3
GB	178.8	109.4	448.3	74.4	40.7	106.8	104.2	244.9	25.8	117.6	16.0	640.5	15.0
GH	128.8	93.1	350.2	37.6	21.6	67.5	81.9	332.9	23.5	121.6	16.3	631.8	36.5
HE	129.3	88.0	363.5	63.0	36.5	78.1	82.9	281.0	25.3	111.5	5.8	503.9	20.6
HF	151.4	106.7	409.0	53.6	31.2	98.4	102.0	299.1	17.2	123.7	10.4	664.7	13.0
JB	189.1	117.9	438.5	57.8	30.6	112.2	103.0	318.1	23.5	97.7	10.6	583.7	33.3
JC	185.7	111.3	469.4	57.9	27.2	115.2	98.7	287.3	30.6	95.6	12.9	590.2	40.2
JD	207.1	126.2	506.5	69.4	48.1	140.7	139.9	176.1	28.5	118.5	13.2	584.0	22.1
MB	151.0	100.8	404.1	47.3	19.4	102.5	101.1	241.5	24.3	105.2	5.8	444.3	16.8
MD	147.9	93.7	385.4	51.1	26.5	99.6	94.4	242.7	23.0	106.7	4.9	493.8	27.5
MH	161.3	102.4	456.9	76.7	38.1	105.4	101.6	243.6	21.5	97.3	0.5	536.2	24.5

Table IV-9. Rock-Eval data from Monterey Formation samples.

SAMPLE	% TOC	HI	OI	SI	S2	S3	T max
1	4.40	342	28	2.79	15.06	1.26	391
2	3.18	278	43	1.59	8.86	1.38	387
3	3.50	351	36	2.24	12.30	1.26	393
4	3.37	359	32	2.27	12.12	1.09	392
6	3.26	304	33	2.16	9.92	1.09	384
7	3.11	279	29	1.91	8.70	0.93	393
8	2.92	273	34	1.69	8.00	1.01	393
9	3.68	315	30	2.23	11.61	1.13	387
10	2.33	321	40	1.50	7.50	0.94	385
11	3.74	308	31	2.16	11.54	1.17	375
12	1.20	275	46	1.32	3.31	0.56	374
12	1.30	315	52	1.61	4.10	0.68	373
13	3.63	294	39	1.87	10.69	1.43	391
14	2.80	341	50	2.20	9.55	1.41	390
15	3.80	402	33	2.71	15.28	1.29	391
16	1.84	390	63	1.43	7.18	1.17	389
17	2.54	355	50	1.45	9.03	1.28	384
18	2.97	401	36	1.48	11.92	1.08	401
19	2.88	335	41	1.35	9.66	1.20	392
20	2.75	429	44	1.84	11.80	1.23	390
21	3.94	400	34	1.99	15.78	1.36	401